NASA/TM—2002–104606, Vol. 23

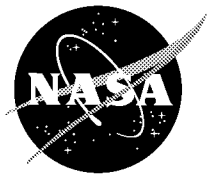

Technical Report Series on Global Modeling and Data Assimilation

Volume 23

Prospects for Improved Forecasts of Weather and Short-Term Climate Variability on Subseasonal (2-Week to 2-Month) Time Scales

S. Schubert, R. Dole, H. van den Dool, M. Suarez, and D. Waliser

Proceedings from a Workshop Sponsored by the Earth Sciences Directorate at NASA's Goddard Space Flight Center, Co-sponsored by NASA Seasonal-to-Interannual Prediction Project and NASA Data Assimilation Office

April 16-18, 2002

November 2002

The NASA STI Program Office ... in Profile

Since its founding, NASA has been dedicated to the advancement of aeronautics and space science. The NASA Scientific and Technical Information (STI) Program Office plays a key part in helping NASA maintain this important role.

The NASA STI Program Office is operated by Langley Research Center, the lead center for NASA's scientific and technical information. The NASA STI Program Office provides access to the NASA STI Database, the largest collection of aeronautical and space science STI in the world. The Program Office is also NASA's institutional mechanism for disseminating the results of its research and development activities. These results are published by NASA in the NASA STI Report Series, which includes the following report types:

- TECHNICAL PUBLICATION. Reports of completed research or a major significant phase of research that present the results of NASA programs and include extensive data or theoretical analysis. Includes compilations of significant scientific and technical data and information deemed to be of continuing reference value. NASA's counterpart of peer-reviewed formal professional papers but has less stringent limitations on manuscript length and extent of graphic presentations.
- TECHNICAL MEMORANDUM. Scientific and technical findings that are preliminary or of specialized interest, e.g., quick release reports, working papers, and bibliographies that contain minimal annotation. Does not contain extensive analysis.
- CONTRACTOR REPORT. Scientific and technical findings by NASA-sponsored contractors and grantees.
- CONFERENCE PUBLICATION. Collected papers from scientific and technical conferences, symposia, seminars, or other meetings sponsored or cosponsored by NASA.
- SPECIAL PUBLICATION. Scientific, technical, or historical information from NASA programs, projects, and mission, often concerned with subjects having substantial public interest.
- TECHNICAL TRANSLATION. English-language translations of foreign scientific and technical material pertinent to NASA's mission.

Specialized services that complement the STI Program Office's diverse offerings include creating custom thesauri, building customized databases, organizing and publishing research results . . . even providing videos.

For more information about the NASA STI Program Office, see the following:

- Access the NASA STI Program Home Page at http://www.sti.nasa.gov/STI-homepage.html
- E-mail your question via the Internet to help@sti.nasa.gov
- Fax your question to the NASA Access Help Desk at (301) 621-0134
- Telephone the NASA Access Help Desk at (301) 621-0390
- Write to:
  NASA Access Help Desk
  NASA Center for AeroSpace Information
  7121 Standard Drive
  Hanover, MD 21076–1320

NASA/TM—2002–104606, Vol. 23

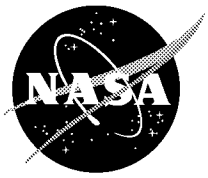

Technical Report Series on Global Modeling and Data Assimilation

Volume 23

Prospects for Improved Forecasts of Weather and Short-Term Climate Variability on Subseasonal (2-Week to 2-Month) Time Scales

Siegfried Schubert, Goddard Space Flight Center, Greenbelt, MD

Randall Dole, NOAA- Cooperative Institute for Research in Environmental Sciences
Climate Diagnostics Center, Boulder, CO

Huug van den Dool, NOAA- Climate Prediction Center, Camp Springs, MD

Max Suarez, Goddard Space Flight Center, Greenbelt, MD

Duane Waliser, Institute for Terrestrial and Planetary Atmospheres
State University of New York, Stony Brook, NY

National Aeronautics and
Space Administration

Goddard Space Flight Center
Greenbelt, Maryland 20771

November 2002

Available from:

NASA Center for AeroSpace Information
7121 Standard Drive
Hanover, MD 21076–1320
Price Code: A17

National Technical Information Service
5285 Port Royal Road
Springfield, VA 22161
Price Code: A10

Table of Contents

Abstract

A workshop was held in April of 2002 that brought together various experts in the Earth Sciences to focus on the subseasonal prediction problem. While substantial advances have occurred over the last few decades in both weather and seasonal prediction, progress in improving predictions on these intermediate time scales (time scales ranging from about two weeks to two months) has been slow. The goals of the workshop were to get an assessment of the "state of the art" in predictive skill on these time scales, to determine the potential sources of "untapped" predictive skill, and to make recommendations for a course of action that will accelerate progress in this area. A remarkable aspect of the workshop was the multi-disciplinary nature of the attendees, consisting of about 100 scientists with specialties in areas that included stratospheric dynamics, hydrology and land surface modeling, the monsoons, the Madden-Julian Oscillation (MJO) and other tropical variability, extratropical variability including extratropical-tropical interactions, coupled atmosphere-ocean-land modeling, weather prediction, seasonal prediction, and various aspects of statistical modeling, analysis, and prediction. This broad range of expertise reflected the wide array of physical processes that are deemed potentially important sources of predictive skill on subseasonal time scales.

One of the key conclusions of the workshop was that there is compelling evidence for predictability at forecast lead times substantially longer than two weeks. Tropical diabatic heating and soil wetness were singled out as particularly important processes affecting predictability on these time scales. Predictability was also linked to various low-frequency atmospheric phenomena such as the annular modes in high latitudes (including their connections to the stratosphere), the Pacific/North American pattern (PNA), and the MJO. The latter, in particular, was highlighted as a key source of untapped predictability in the tropics and subtropics, including the Asian and Australian monsoon regions.

The key recommendations of the workshop are:

a) That a coordinated and systematic analysis of current subseasonal forecast skill be conducted by generating ensembles of 30-day hindcasts for the past 30-50 years with several "frozen" AGCMs. Specific goals include, sampling all seasons, and generating sufficiently large ensembles to estimate the evolution of the probability density function.

b) That a series of workshops be convened focused on modeling the MJO, and that a coordinated multi-nation/multi-model experimental prediction program be developed focused on the MJO.

c) That new satellite observations and new long-term consistent reanalysis data sets be developed for initialization and verification, with high priority given to improvements in estimates of tropical diabatic heating and cloud processes, soil moisture, and surface fluxes (including evaporation over land).

d) That NASA and NOAA develop a collaborative program to coordinate, focus, and support research on predicting subseasonal variability.

Specific steps to implement the above recommendations are: 1) to begin immediately to develop a framework for an experimental MJO prediction program, 2) to convene a follow-up workshop in the spring of 2003 to organize the AGCM hindcast project, and conduct initial meetings on modeling the MJO, and 3) for NASA and NOAA to put out a joint announcement of opportunity within the next year to focus research, modeling and data development efforts on the subseasonal prediction problem.

I. Introduction

"It seems quite plausible from general experience that in any mathematical problem it is easiest to determine the solution for shorter periods, over which the extrapolation parameter is small. The next most difficult problem to solve is that of determining the asymptotic conditions - that is, the conditions that exist over periods for which the extrapolation parameter is very large, say near infinity. Finally, the most difficult is the intermediate range problem, for which the extrapolation parameter is neither very small nor very large. In this case the neglect of either extreme is forbidden. On the basis of these considerations, it follows that there is a perfectly logical approach to any computational treatment of the problem of weather prediction. The approach is to try first short-range forecasts, then long range forecasts of those properties of the circulation that can perpetuate themselves over arbitrarily long periods of time (other things being equal), and only finally to attempt forecast for medium-long time periods which are too long to treat by simple hydrodynamic theory and too short to treat by the general principles of equilibrium theory".

John von Neumann (1955)

Almost a half century after the eminent mathematician, John von Neumann, spoke those words it appears that we are finally ready to tackle the "medium-long" time scale prediction problem. In fact we have, over the last few decades, made important strides in both weather (short time scale) and seasonal/climate (very long time scale) prediction. The critical roles of initial atmospheric conditions in the former, and boundary conditions in the latter, have helped to guide and prioritize research and development, as well as to establish new observing systems targeting these prediction problems.

As surmised by von Neuman, progress in predicting time scales between those of weather and short-term climate (time scales roughly between 15 and 60 days) has been at best modest. The variability on these time scales is rich with well known phenomena such as blocking, the PNA, and the MJO, yet the important mechanisms involved, their predictability, and the ability of current models to simulate them are still in question. Improvements made in predicting these time scales are in many ways an important step in making further progress in weather and climate prediction. For weather, these time scales offer the hope for extending (at least occasionally) the range of useful forecasts of weather and/or weather statistics, while for the seasonal and longer term climate prediction problem they are a key component of the atmospheric "noise" that is a limiting factor in the climate prediction problem.

How predictable is the PNA? How predictable is the MJO? What is the connection between the variations in predictability of weather and the PNA, blocking, the MJO, or various other subseasonal modes? What is the role of the stratosphere? What is the link between subseasonal variability and the

El Nino/Southern Oscillation (ENSO)? Is intraseasonal variability the key to understanding and predicting the interannual variability of the Indian monsoon? How important is ocean coupling to subseasonal prediction? What is the relative contribution of SST and atmospheric initial conditions to the predictability of subseasonal variability on weekly to monthly time scales? Are our models good enough to capture the dominant modes of variability? Are the uncertainties in the predictions dominated by errors in the initial conditions (e.g. the tropics or soil moisture) or deficiencies in the models? These are some of the key issues that need to be addressed for achieving useful long range weather predictions, and for improving and determining the limits of seasonal and longer predictions.

This document summarizes the proceedings of a workshop that was organized to bring together various experts in the field to focus on the subseasonal prediction problem. The basic goal of the workshop was to get an assessment of our current understanding of the above issues, and to determine what we can do to help make progress on the subseasonal prediction problem: this includes necessary advances in models, analysis, theory, and observations.

The workshop was held at the Newton White Mansion in Mitchellville, Maryland on April 16-18, 2002. There were about 100 attendees (see Appendix), with 43 presentations (see extended abstracts), including six invited talks. The workshop was jointly sponsored by the NASA Seasonal to Interannual Prediction Project (NSIPP) and the Data Assimilation Office (DAO), with support and funding from the Goddard Earth Sciences Directorate. Additional funding was provided by the Earth Sciences Enterprise at NASA headquarters. The workshop organizing committee consisted of Siegfried Schubert (chair, NASA/DAO and NSIPP), Max Suarez (NSIPP), Randall Dole (NOAA-CIRES Climate Diagnostics Center), Huug van den Dool (NOAA/Climate Prediction Center), and Duane Waliser (SUNY/Institute for Terrestrial and Planetary Atmospheres).

In the following section we present summaries of each session. The overall summary is given in section III, and the recommendations are presented in section IV. The final sections of the document include the list of participants, the agenda of the workshop, and the abstracts (some of them extended) of the talks.

II. Summary of sessions

The workshop was opened with welcoming remarks from Franco Einaudi, the Chief of the Goddard Earth Sciences Directorate. The keynote talk was given by Eugenia Kalnay, Chair of the Department of Meteorology at the University of Maryland, and a leading expert on dynamical extended range prediction. The rest of the workshop was organized into six sessions. Each session began with a 45 minute invited talk, followed by a number of 20 minute contributed presentations. In the following we provide summaries of each session.

The keynote talk by Eugenia Kalnay (see extended abstract) reviewed some of the key areas that provide opportunities for making progress on the subseasonal prediction problem. These opportunities include the use of coupled atmosphere-ocean models to more realistically simulate extratropical atmosphere-ocean feedbacks, improved simulations of the MJO including "interim" empirical/statistical approaches that nudge the GCMs to produce more realistic MJO characteristics, taking better advantage of the history of 15-day ensemble forecasts routinely made by the U.S. National Weather Service, and improved initialization and ensemble methodologies with coupled models. These basic ideas were, in fact, at the core of many of the presentations that followed.

i) Current operational methods and their skill (Chair: Randy Dole)

The session opened with an invited presentation by Huug van den Dool on "Climate Prediction Center (CPC) Operational Methods and Skill in the Day 15 – Day 60 Forecast Range" (see extended abstract). Van den Dool emphasized the great challenges posed by forecasts in the 15-60 day time range. This time scale is intermediate between short-range and long-range forecasts, with the former predominantly determined by initial conditions and the latter by boundary forcing. Forecasting in this time range therefore constitutes a mixed problem in which both initial and boundary conditions are likely to play important roles. Van den Dool described current CPC operational practice, which is to provide a 30-day forecast for U.S. precipitation and temperatures for the U.S. at a lead-time of two weeks; i.e., effectively a forecast for mean conditions over days 15-45. The forecasts are developed through subjective procedures that effectively combine output from both statistical-empirical and numerical model

predictions. Predictors include Optimal Climate Normals, Canonical Correlation Analysis, and National Centers for Environmental Prediction (NCEP) model forecasts. When applicable, El Nino – Southern Oscillation composites, soil-moisture state, and potential impacts from the MJO are also considered. Comparisons between monthly and seasonal forecasts show that at present the spatial pattern of the monthly forecast is usually similar to that of the seasonal forecast, with modest positive skill but a somewhat lower signal to noise ratio.

Following the presentation by van den Dool, Frederic Vitart provided an overview of monthly forecasting at the European Center for Medium Range Weather Forecasts (ECMWF, see extended abstract). He described a new monthly forecasting project at ECMWF designed to fill the gap between medium-range forecasting (out to 10 days) and seasonal forecasts. The ECMWF system is based on a 51-member ensemble of coupled ocean-atmosphere model integrations, with the atmospheric component being run at T159L40 resolution, and the oceanic component at a zonal resolution of 1.4 degrees and 29 vertical levels. So far, several monthly forecasts have been performed. Preliminary results suggest that the monthly forecasting system may produce useful forecasts out to week 4, although the model is deficient in simulating a realistic MJO more than 10 days in advance. Plans are to run the experimental system every two weeks for the next few years in order to assess the skill of this coupled model.

Zoltan Toth then described the NCEP Global Ensemble Forecast System and discussed approaches to extending forecasts beyond 16 days. Toth emphasized four issues: 1) This is a combined initial condition-boundary condition problem, as stated previously; 2) that potential predictability in this range is relatively low, but variable in time and space; 3) that a key issue is predicting regime changes; and 4) that the models being used are far from perfect. With regard to each of these issues, he suggested: 1) we need to employ coupled models as part of the prediction strategy; 2) that ensemble prediction methods are essential for enhancing the predictable signal, detecting variations in predictability, and providing probabilistic forecasts; 3) that major regime changes are sometimes well predicted, but case-to-case variations are great, and the extent to which these variations are intrinsic or due to model errors or observational deficiencies is unknown; and 4) that new approaches are needed to correct for the effects of model errors, including biases in both the first and second moments. A critical issue is the lack of adequate variability in the models, which leads to "overconfident" forecasts. It is vital to adjust for this bias in order to improve forecast estimates of probability distributions.

Steve Colucci provided an overview of recent results on ensemble predictions of blocking (see extended abstract). He discussed results of research with the NCEP MRF model, and unpublished work by J. L. Pelly and B.J. Hoskins with the ECMWF model. These studies examined the climatology of blocking over 3-5 year periods. Preliminary results suggest that blocking frequency is underpredicted in both the NCEP and ECMWF model, but that this bias can be at least partially corrected to produce calibrated probabilistic forecasts that extend the range of skillful blocking forecasts.

Arun Kumar discussed the impact of atmospheric initial conditions on monthly-mean model hindcasts with an atmospheric general circulation model (AGCM). The AGCMs were run from atmospheric conditions starting at lead times from 1-4 months in advance. The results suggest that January simulations with a shorter (1 month) lead time have a higher signal-to-noise ratio, especially at higher latitudes, and therefore consideration should be given to using observed initial conditions in this time of year.

The final presentation of the session, given by Thomas Reichler, also examined the role of atmospheric initial conditions on long-range predictability. The study design consisted of running ensemble AGCM predictability experiments with the NCEP seasonal forecasting model at T42L28 resolution from a variety of initial condition (IC) and boundary condition (BC) states, including ENSO and non-ENSO (neutral) years. The basic conclusions were that initial conditions have a noticeable influence on weekly hindcast skill in winter out to weeks 2 to 6, with the effects most pronounced at high latitudes, the middle atmosphere, at lower levels over the Indian Ocean, during active phases of the Antarctic Oscillation (AAO), and when ENSO is weak.

ii) Predictability of extra-tropical "modes" (Chair: Max Suarez)

This session dealt with various aspects of a number of coherent atmospheric teleconnection patterns that have time scales sufficiently long to afford predictability on weekly and longer time scales.

The session began with an invited talk by Mike Wallace about a study on the impact of the Arctic Oscillation (AO) and the PNA on subseasonal variability, carried out by Roberta Quadrelli and Mike

Wallace (see extended abstract). The analysis was based on NCEP/NCAR reanalysis data for DJFM for the period 1958-1999. They examined the variability of 10-day means of sea level pressure, 500mb height and 1000-500mb thickness fields during the extremes in the two polarities of both the AO and PNA. They found that both the AO and the PNA have a substantial impact on the frequency of occurrence of weather often associated with cold air outbreaks in middle latitudes. For the AO, this is characterized by enhanced variability during the low index state (weak sub-polar westerlies).

Mark Baldwin reported on work with Tim Dunkerton that examined the ability to predict the AO using statistical techniques (see extended abstract). They note that the AO is the surface expression of the Northern Annular Mode (NAM): the latter is most persistent at stratospheric levels, peaking in the lowermost stratosphere, where the DJF e-folding time scale exceeds 30 days. They further showed that the persistence of the AO has a strong seasonality with substantially more persistence (e-folding time of 15-20 days) during the winter season when the planetary wave coupling to the stratosphere is strongest. They found a linear relationship between the lower stratospheric NAM and the average AO 10–40 days later, that should make possible predictions of the AO at the 10-40 day range.

Steven Feldstein examined the dynamical mechanisms of the growth and decay of the North Atlantic Oscillation (NAO). The study involved a diagnostic analysis using NCEP/NCAR reanalysis data as well as calculations with a forced, barotropic model. The results showed a life cycle of about two weeks. Both high-frequency (period <10 days) and low-frequency (period >10 days) transient eddy fluxes were found to drive the NAO growth, while the decay of the NAO occurs through both the divergence term and the low-frequency transient eddy fluxes. The results further showed an important difference between the NAO and PNA patterns, in that the NAO lifecycle is dominated by nonlinear processes, whereas the PNA evolution is primarily linear.

Grant Branstator showed examples from the observations and two different model simulations (the NSIPP-1 and NCAR models) of wavetrains that are meridionally confined and zonally-elongated as a result of being trapped within the waveguide of the mean winter Northern Hemisphere jets (see extended abstract). He discussed how these wavetrains are important for the subseasonal prediction problem because they act to connect widely spaced locations around the globe within about a week, they impact

the time mean and bandpass eddy statistics, and they effect various other teleconnection patterns such as the NAO and the ENSO response.

Sumant Nigam examined the mature-phase dynamics of PNA variability. He noted that the PNA represents circulation and precipitation variability on both intraseasonal and seasonal time-scales, and that the PNA has sometimes been erroneously associated with ENSO variability as it can be excited during ENSO winters as well. The pattern was simulated with forcing (diagnosed from reanalysis data) using a steady linear primitive equation model. The model results indicated that zonal/eddy coupling and sub- monthly vorticity transients are important in the pattern's generation.

Tim Delsole introduced the concept of an optimal persistence pattern (OPP) as a component of a time-varying field that remains auto-correlated for the longest time lags. He showed how OPPs can be used for isolating persistent patterns in stationary time series, and for detecting trends, discontinuities, and other low-frequency signals in non-stationary time series. The results of his analysis showed, among other things, that the PNA is the most predictable (in a linear sense) atmospheric pattern.

Wilbur Chen examined subseasonal variability and teleconnectivity for various time scales associated with the PNA, NAO and AO using NCEP/NCAR reanalyses for the period 1971-2001 (see extended abstract). He showed that as the timescale increases (7-day, 31-day and 61-day means), the teleconnections not only become stronger and better established, but also much more organized and located in certain preferred regions. He furthered illustrated the sensitivity of the January-March teleconnection patterns to the based point used to define the correlation patterns.

Hyun-Kyung Kim presented work carried out with Wayne Higgins to monitor the PNA, the Arctic Oscillation (AO), the North Atlantic Oscillation (NAO), and the Antarctic Oscillation (AAO). Indices of these patterns were developed for the period January 1950 to the present, using the NCEP/NCAR CDAS/Reanalysis. Forecasts of the indices are made by projecting the loading pattern of each mode onto the MRF and ensemble forecast data. The indices and forecasts for the most recent 120 days are posted on the monitoring weather and climate web site of NCEP/CPC and updated daily. (http://www.cpc.ncep.noaa.gov/products/precip/CWlink).

iii-iv) Predictability of the ISO/MJO (Chair: Cecile Penland) and **Tropical/ extra-tropical interactions** (Chair: Duane Waliser)

In view of the strong connections between the topics on the ISO/MJO and tropical-extratropical interactions, this section is a synthesis of both sessions III and IV. While the names intraseasonal oscillation (ISO) and MJO are often used interchangeably, it is now becoming common practice to refer to the boreal summer variability as the ISO, while the MJO is a boreal winter or cold season phenomena. For convenience we have chosen not make that distinction here, so that in the following we refer to both phenomena as simply the MJO. Note also that in this section, the references to the speakers appear in parenthesis and usually at the end of the sentence. Invited presentations were made by Duane Waliser (session iii, see extended abstract), and Prashant Sardeshmukh (session iv, see extended abstract).

Tropical intraseasonal variability was shown to interact with and/or influence a wide range of phenomena including local weather in the tropical Indo-Pacific region, onsets and breaks of the Asian-Australian monsoons, persistence extra-tropical circulation anomalies in the Pacific-America sectors, extreme precipitation events along the western United States, the development of tropical storms/hurricanes in the Pacific/Atlantic sectors, and even the initiation of El Nino / La Nina events (Duane Waliser). This latter aspect was even extended to the point that the MJO may help characterize the intrinsic time scale, at least its biennial character of ENSO (William Lau, see extended abstract). Additional influences from the MJO include the modulation of N. Pacific cyclone activity (Mike Chen) and the persistence of the S. America convergence zone (Leila Carvahlo). There is also the indication that an independent intraseasonal oscillation may exist over S. America (Jiayu Zhou, see extended abstract).

A number of presentations (e.g., Prashant Sardeshmukh, Duane Waliser, Ken Sperber) showed that improvements in tropical diabatic heating variability (e.g., MJO, ENSO, other equatorial "waves") will/should result in enhanced (long-lead and seasonal) forecasting skill in the Tropics as well as mid-latitudes via tropical/extra-tropical teleconnections. For example, one idealized dynamical predictability study showed that with a reasonable GCM representation of the tropical MJO, the expected limit of useful predictability for the MJO might be about 25 days (Duane Waliser). Unfortunately, GCMs in both climate simulation and prediction or numerical weather forecasting settings still exhibit rather poor

simulations of MJO variability except for a few isolated cases (Duane Waliser, Ken Sperber, Suranjana Saha). In fact, even the interannual variability of features such as the Asian monsoon appear to be poorly simulated due to the poor representation of intraseasonal variability and its (albeit) only weak dependence on boundary conditions (Ken Sperber). Apart from tropical diabatic heating, one presentation (Klaus Weickmann) noted that atmospheric intraseasonal variability can arise due to the effect of mountain and frictional torques on the adjustment of the atmosphere to stochastically-varying flow over mountains. Thus, to properly account for tropical – extratropical interactions on intraseasonal time scales, it may be important to understand the separate roles and influences from the above stochastically-forced process and from the more deterministic tropical diabatic heating process (i.e. MJO).

One presentation (Prashant Sardeshmukh) showed that forecasts based on a multivariate linear inverse model (LIM) could predict seven-day averages of northern hemisphere stream function at lead times of about three weeks at skills superior to the NCEP Medium-Range Forecast model (MRF). This presentation, along with another (Newman), showed how the above predictability came in large part from an ability to describe the evolution of tropical heating, a phenomenon which is not described well by the MRF. Both presentations emphasized how LIM's prediction skill was tied to the identification of three optimal structures for growth: one dominated by tropical heating, one which combined tropical heating and midlatitude dynamics, and a third dominated by midlatitude dynamics. In addition, it was noted that while the LIM can likely provide useful subseasonal predictions of midlatitude variability, it may be necessary to use non-linear models to provide better estimates of uncertainty – i.e. forecasting forecast skill. Of course, these non-linear models need to represent the strength and variability of tropical heating properly.

Monitoring and forecasting of MJO was discussed in a number of contexts. For example, at least two empirical real-time forecasting schemes appear to be forthcoming (Matthew Wheeler – see extended abstract, Charles Jones, Yan Xue- see extended abstract), in addition to the one that already exists via shallow-water model wave filtering (Matthew Wheeler). These activities can be expected to provide useful real-time MJO forecasts out to 10-20 days lead-time, particularly in the current environment in which no operational model has been shown to do well at simulating/forecasting the MJO. One research group has built an empirical mid-latitude forecasting model based on the canonical relationship between

the MJO and mid-latitude anomalies over the Pacific – North American sector (Yan Xue). Such a model (and associated website) is designed to provide an aid for extended range weather and/or short-term climate forecasts. Additional presentations examined the structural variability as well as frequency and propagation characteristics of MJO events (Jones) to better understand the different types MJO events and their associated probabilities for occurrence, including for example how ENSO influences these probabilities (or vice versa). Along these same lines, it was pointed out (Duane Waliser, William Lau) that a number of recent analyses have shown that there is no obvious relation between interannual SST variability in the tropics and the overall activity of the MJO, except that MJO events typically propagate further east during El Nino conditions. However, the analysis from one presentation (William Lau) suggested that the biennial tendency of ENSO may in part be derived from the coupling between the interannual and intraseasonal time scales.

Two presentations (Suranjana Saha, Hilary Spencer – see extended abstract) pointed out specific instances of the extreme sensitivity that the MJO simulation character has on even subtle changes in model parameterization. One of these presentations stressed the need to simulate a correct basic state in a numerical weather prediction model, for both the sake of obtaining an accurate climatology and thus less drift with lead time but also to obtain a better representation of transients that depend on the mean state (Suranjana Saha). In fact, very recent studies have shown that the simulation quality of the MJO can be particularly sensitive to the basic (e.g., low-level zonal wind direction in the Indian/western Pacific Oceans). The other presentation (Hilary Spencer) highlighted the rather significant change in the simulation quality of the MJO simply due to an increase in the vertical resolution (namely in the mid-troposphere). Along somewhat similar lines, it was shown that assimilation of total column water vapor content into the GEOS AGCM can significantly influence the model's representation of the MJO (Man Li Wu – see extended abstract), furthering the suggesting that correct treatment of moist convection and the hydrological cycle are vital to the simulation of the MJO. Another study extended this notion to a completely general framework, pointing out that our analyses and re-analyses data sets are severely hampered by not only a lack of data but also due to incorrect moist physical parameterizations (Arthur Hou – see extended abstract). This study highlighted the improvements that can be gained in these sorts of validating data sets via the assimilation of satellite-based precipitation estimates.

A number of talks stressed the importance of what might have previously been thought of as unimportant details as actually being significant to the subseasonal prediction problem. In one case study, it was shown that the evolution of the seasonal mean circulation over the Pacific North American region was deterministically influenced by subseasonal SST variability (Ben Kirtman). In another case, it was shown that proper simulation of the detailed characteristics of a tropical atmospheric heat anomaly associated with a given El Nino, including the correct partition between basic state and anomaly, were crucial to obtaining a proper mid-latitude teleconnection properties for that given event (Hilary Spencer). Along similar lines, it was shown that distinct sub-seasonal (i.e. monthly) extra-tropical atmospheric signals do occur in response to ENSO and that seasonal averages not only can smear these out but can obscure them entirely (Marty Hoerling).

v) **Role of land surface processes** (Chair: Huug van den Dool)

Randy Koster gave the invited presentation for this session (see extended abstract). There were four additional papers, by Masao Kanamitsu et al. (see extended abstract), Adam Schlosser et al., Paul Dirmeyer and Mike Bosilovich et al. (see extended abstract). To this I will add some comments made by Huug van den Dool in his invited talk about operational methods that relate to the land surface. To paraphrase (and extend slightly) on Koster's list of requirements:

1) Soil moisture needs to have an effect on the atmosphere. This effect has to be quantifiable.
2) Soil moisture needs to have a memory, either through a long autocorrelation (lifetime "on the spot") or in a more Lagrangian sense as prediction skill where soil moisture anomalies are allowed to evolve and move around.
3) Finally, does realistic soil moisture actually help in the prediction?

Koster et al made several shortcuts and studied "potential predictability" in a model to find "where" soil moisture could make a difference. Different models give, unfortunately, very different estimates of where soil moisture could make a difference. Kanamitsu et al have gone ahead and made a fairly realistic soil moisture data set for 1979-present by manipulating the precipitation that enters the land scheme of the so-called Reanalysis-2. A large focus here is on verification, which leads to a focus on DATA. Model forecasts with and without realistic soil moisture show improved skill in temperature.

The impact on precipitation is unclear. Kanamitsu doubts that we need dynamical models if all we can harvest is the impact on temperature. Van den Dool showed extensively by empirical means how dry (wet) antecedent soil leads to warmer (colder) conditions for the next several months. Such tools are already in place for use in CPC's monthly forecasts and are being relied upon for the warm season. Schlosser showed that the autocorrelation of soil moisture varies from weeks to seasons. He also argued that the beneficial impact of realistic initial soil moisture in a model becomes impossible to find when the model biases overwhelm any small effects we are looking for. The focus here is on a-priori removal of systematic errors. Dirmeyer delineated that the model drift consists of three parts, each with their own time scale. The first is caused by precipitation bias, the second by radiation biases, and the third would be coupling effects. Dirmeyer also raised the question as to whether we should be using model consistent soil moisture or realistic soil moisture. Nearly everybody wanted to know why models have precipitation biases, and what it would take to reduce them. The tracer study by Bosilovich added another perspective to the question about the origin of precipitation in a given area.

Closing comments:

A) Although the effect of soil moisture is expected in "the warm season" it is important year round for a number of reasons: i) There is a warm season somewhere on the planet all the time, and by teleconnection the impacts could be far away, especially when trends in land use over large areas (South East Asia) are considered. ii) Soil moisture calculations need to be done year round and iii) There may be carry over effect from snow cover/depth to soil moisture anomalies.

B) GCMs appear to overdo the impact of soil moisture on for instance the near surface temperature.

C) We need data at the most basic level to verify model results. There appears to be an almost complete lack of evaporation data. Need bright minds to think of measuring (surface) evaporation on a scale larger than a tower here and there.

D) We need to find non-local impacts of soil moisture for this field of scientific endeavor to be really important (over and above simple empirical methods) for forecasts in day15-60 range.

E) What are the causes of large precipitation biases in GCMs, and how to improve the situation?

vi) Link between low frequency and weather/regional phenomena

(Chair: Siegfried Schubert)

This session consisted of a number of talks dealing with various aspects of weather and climate variability and predictability, including diagnostic studies of the errors (both random and systematic) that affect AGCM simulations and forecasts.

The invited presentation was made by Jeff Whitaker on the subject of "Storm Track Prediction" by Jeff Whitaker and Tom Hamill (see extended abstract). The transition between weather and climate prediction was defined to occur at the forecast lead time at which all skill is lost in predicting individual storms. Prediction of weather beyond that transition is based on the assumption that the large scales organize weather to allow predicting the statistics of weather, in particular the short waves that are the major precipitation producers during the cold season.

A number of results were presented from 23 years of three week "reforecasts" for JFM with the MRF model (T62L28) that was operation during the first half of 1998. They found that in the extratropics, the short waves lose skill after 5 days, while the long waves have skill well into week two. The results of a CCA analysis showed that the most predictable pattern for day 10 forecasts is the PNA. A regression analysis further showed a time evolution in which an initial broad anomaly develops in the North Pacific, followed by rapid intensification in the eastern Pacific of a baroclinic wave, followed by downstream propagation. Results for week 2 were quite similar, while the three week averages showed a link to the west Pacific pattern. The above evolution is associated with well-defined storm track shifts. Furthermore, the storm track shifts were more coherent for longer averaging periods (more individual storms). In the second part of the talk, Jeff examined week two quantitative precipitation forecasts (QPFs) with the above forecast model, and based on his analysis of the storm track shifts. The results were based on near real time 15 member ensemble runs at CDC since 1 Dec 2001. The results showed that skillful QPFs in week 2 are possible, but that ensemble bias correction is crucial.

The next talk was given by Yehui Chang on "Extreme weather events and their relationship to low frequency teleconnections" by Y. Chang and S. Schubert (see extended abstract). The presentation described a method for characterizing extremes in daily precipitation over the continental United States

using a combination of compositing and linear regression. The results showed that the extremes have both regional and seasonal dependencies. For example, during the cold season, the extremes in precipitation tend to be associated with well-known "large-scale" weather systems, while during the warm season they are associated with more localized convective systems. The results were applied to both the observations and the results from simulations with the NASA/NCAR AGCM run with idealized warm, neutral and cold ENSO SST. The AGCM results and to a lesser extent the observations (1963-1999) showed evidence for a substantial impact of ENSO on the statistics of the extremes events. Preliminary evidence was also presented for impacts of subseasonal modes of variability (e.g. the PNA and the NAO) on the statistics of the extreme events.

J. Shukla presented the results of a study on the "Relationship between the PNA internal pattern and the ENSO-forced pattern: time scales from daily to seasonal", by David Straus and J. Shukla. The study involved the separation of seasonal mean variability during boreal winter into that forced by SST and that generated internally. The study was based on 30 winters of ensembles of simulations with the COLA AGCM forced with observed SST as well as, long simulations with climatologically varying SST. They distinguish between the ENSO-forced response (or external pattern of variability) and the 'PNA"-like pattern of internal variability. They found that when these patterns are projected onto pentad data, the probability density function (pdf) obtained for the ENSO pattern is distinct from that of the PNA pattern. They further found that during warm events the PNA pattern has greater chance of having both polarities, while during cold events the ENSO pdf is wider than that of the PNA, and there is enhanced intraseasonal variability.

Rob Black presented a talk on an "Assessment of midlatitude subseasonal variability in NASA/GSFC general circulation models", by Black, Robinson and McDaniel (see extended abstract). They performed a preliminary assessment of the storm tracks and anomalous weather regimes in AMIP-style integrations of two different models. These consist of the NASA/NCAR AGCM used by the DAO for data assimilation, and the NASA Seasonal-to-Interannual Prediction Project (NSIPP)-1 AGCM used by NSIPP to assess predictability and to carry out predictions on seasonal-to-interannual time scales. The results showed that the models regional patterns of upper tropospheric eddy kinetic energy (EKE) are well represented for both the synoptic and low frequency eddies, and represent an improvement over earlier models. Both models, however, have weaker than observed low frequency and synoptic EKE (by

20-30%). The NSIPP model in particular, has synoptic EKE that is only 64% of the observed values. The authors present a number of diagnostics to attempt to explain the model discrepancies. A diagnosis of the baroclinic and barotropic aspects of the model dynamics shows that the NSIPP model synoptic eddies are experiencing enhanced barotropic energy losses to the mean flow in the jet exit region, while the background baroclinic forcing is closer to the observed values. The authors speculate that the existing deficiencies in the low frequency EKE of both models may be related to the scale interaction between the synoptic and low frequency eddies.

Ming Cai presented a talk on "Diagnostics of Climate Variability and Trend Using Potential Vorticity Maps" by Ming Cai and Eugenia Kalnay. They examined the strong warming trend in high latitudes of the NH during the last 2 decades, and conjectured that changes in extratropical frontal activity may explain part of the much-amplified warming trend in high latitudes. Their diagnostic technique centered on an analysis of potential vorticity surfaces in which they define PV folding zones. The interannual variability of an extratropical PV Folding Index (PVFI) and extreme surface cold and warm events were both shown to have a strong QBO signal. They further showed that the interannual variability of the PVFI is correlated with interannual variability of warm and cold events. An advantage of using the PVFI, over say the AO index is that it measures both mobile and standing parts of polar vortex variability, and is not constrained by "inactive" periods or warmer seasons.

Glen White's talk focused on the systematic errors of the NCEP operational 0-15 day forecasts (see extended abstract). He showed that the systematic errors are similar to the bias in long (multi-year) model simulations, and suggested that improvements in the short-range systematic errors should help to improve the 2 week to two month forecasts. An advantage of focusing on the short-range forecasts is that they should be easier to diagnose, since they occur before nonlinearity dominates the forecast evolution. The analysis addressed, in particular, the systematic errors in the surface fluxes. Glen showed that considerable differences exist between different estimates of air-sea fluxes. Current global forecast systems have problems with cloudiness that produce inaccurate short wave fluxes and problems with moisture that affect long wave fluxes. A key deficiency of current models appears to be in the representation of low-level oceanic stratus clouds.

Mark Helfand presented results from a study of the interannual variability of the United States Great Plains Low-Level Jet (GPLLJ) during May through August (see extended abstract). The results, base on 17 years of GEOS-1 reanalysis data showed that the GPLLJ is one of the most persistent and stable features of the low-level continental flow. The interannual variance was found to have 3 maxima with one over the upper Great Plains, another over Texas, and a third over the western Gulf of Mexico. Mark showed evidence for an intermittent biennial oscillation in the maxima over Texas. Of particular relevance to the subseasonal prediction problem is the finding that the typical duration of the interannual anomalies is on the order of several weeks, with the more southerly maxima having the longest time scales. Further analysis is required to better understand the nature of the biennial oscillation and robustness of the week-to-week coherence of these anomalies.

III. Discussion and Summary

The final discussion session, chaired by J. Shukla, summarized the main findings of the workshop and outline steps that should be taken to make progress on the subseasonal prediction problem. J. Shukla highlighted some of the lessons learned from the numerical weather prediction (NWP) problem. In particular, it was pointed out that much of the improvement in weather forecast skill over the last 30 years has come about because of improvements to the models. It remains to be seen whether this will also be true for the subseasonal prediction problem, though it is already clear that models will have to do many things right (e.g., land, weather, MJO, stratosphere, etc.) to make substantial progress towards the prediction problem throughout the globe. He also outlined a set of baseline forecast experiments that could serve to better assess the status of our current subseasonal prediction capabilities (see below).

The following is a synthesis of the summary session and includes further (post-workshop) summaries and analysis provided by members of the organizing committee. Specific recommendations are given in section IV.

Forecasting on time scales longer than weather but shorter than one season (about 2 weeks to 2 months) is perhaps the most challenging weather/climate forecasting problem we will face in the coming years. This workshop was held in order to take stock of current capabilities, and to examine recent progress in

a number of different areas of weather and climate research that offer potentially substantial gains in forecast skill on 2 week to 2 month time scales. The workshop participants, therefore, included scientists from traditionally disparate communities, including researchers with specialties in stratospheric dynamics, hydrology and land surface modeling, the monsoons, the MJO and other tropical variability, extratropical variability including extratropical-tropical interactions, coupled atmosphere-ocean-land modeling, weather prediction, seasonal prediction, and various aspects of statistical modeling, analysis, and prediction.

The key finding of the workshop is that there is compelling evidence for predictive skill at lead times substantially beyond two weeks. It is understood that at these times scales the predictions are largely probabilistic (e.g., phase information about individual storm systems is lost), and that the ultimate goal should be the prediction of the evolution of the probability density function (PDF), thereby bridging both the weather and seasonal forecast problems. The various presentations suggested that we should not expect to find a single dominant source of predictive skill on these time scales. In fact predictive skill will likely come from a host of different phenomena depending on region, season, and time scales of interest. For example, during the boreal winter there is evidence for enhanced predictability in the middle and high latitudes associated with the Arctic Oscillation, the stratosphere, the PNA pattern, and tropical forcing. Evidence for analogous sources of predictability exist in the Southern Hemisphere (e.g., the Antarctic oscillation). The MJO offers the potential for improved forecast skill, especially of the Asian-Australian monsoon. Memory of the soil moisture (and snow melt) offers hope for skillful warm season predictions at lead times beyond two weeks in a number of different continental regions, primarily of surface temperature and to a lesser extent precipitation.

In the following we summarize some of the key unresolved issues and outline specific steps that should help translate the various potential sources of predictability into measurable improvements in forecast skill.

i. Role of tropical heating and the MJO

This is one of the most promising sources of predictability and represents a major opportunity for improvements. Current GCMs do poorly in simulating many aspects of tropical convection and the

links to the extratropics, especially the heating associated with the MJO. Simpler (compared with GCMs) linear inverse models (LIMs) show skill at 3 weeks in the extratropics associated with tropical heating, a skill not realized in current GCMs. Statistical and other modeling studies suggest that deficiencies in the ability of GCMs to simulate MJOs are a serious impediment to improving forecasts of subseasonal variability of the Asian-Australian monsoons, the predilection for hurricane formation, and other subseasonal variability including that over the southwestern United States. It was also pointed out that improving the representation of tropical transients in GCMs will likely have a much greater impact on forecasts than improvements in the extratropics, and this will have major impacts on a larger portion of the world's population.

While modeling deficiencies are a major problem in this area, deficiencies in the estimates of tropical heating (both for initial conditions and for model verification) are also important. It is clear that we will need better estimates of tropical heating. Little work has been done to date to address predictability associated with tropical heating on subseasonal time scales using GCMs. How important are the details of the heating fields (how accurately must these be observed) and can we expect to predict these beyond two weeks. LIMs of GCMs offer an important diagnostic tool to address these issues.

Considerable work is needed to better understand the nature and predictability of the tropically forced modes. For example, issues specific to the MJO include, the sensitive of MJO predictability estimates to the GCM, season, ENSO, SST coupling, and mid-latitude variability. How does MJO predictability influence mid-latitude circulation and extreme event predictability? Can we use empirical forecasts of MJO heating and assimilate that into forecast models as a short-term means to improve medium to extended range predictions? The role of subseasonal SST variations not directly coupled to the MJO also requires further study.

ii. Extratropical modes of variability

Annular "modes" provide one of the most promising prospects for skill beyond two weeks in the middle and high latitudes. These modes appear to have long enough time scales and strong enough influences on the surface that memory of the initial conditions can produce useful forecasts at long lead times. For example, the Arctic Oscillation has a strong influence on middle and high latitude surface temperatures.

There is intriguing evidence of stratospheric influence: strength of wintertime stratospheric vortex influences the subsequent tropospheric circulation. Another low frequency pattern that has a substantial impact on the Northern Hemisphere extratropical climate is the PNA pattern. In fact, the PNA was identified as the most predictable of all the extratropical modes examined. Blocking episodes represent another source of predictability, though this is yet-to-be-realized since current models tend to under predict blocking frequency. Still other low frequency teleconnection patterns have been recently discovered in which the tropospheric jets act as wave guides, resulting in zonally elongated wave patterns that link distant parts of the globe. The predictability associated with those modes is yet to be determined.

Key issues that need to be further addressed include the nature of the link of the annular modes to the stratosphere and the signal to noise ratio (i.e. how large is the predictable signal from the stratosphere compared with the total variability). There is a need to better understand the sources of predictability associated with blocking and the PNA (e.g. tropical heating, weather, ENSO). How do the variations in the jets affect predictability associated with the wave guiding mechanism. How well do models reproduce these and other low frequency modes, the interactions with the stratosphere, and interactions with weather/extremes? Does the signal get lost beyond two weeks due to model drift? What is the sensitivity to horizontal and vertical resolution?

iii. Soil moisture and snow

Soil moisture may be very important on subseasonal time scales (perhaps more so even than for the seasonal problem) – consistent with intrinsic time scales of soil moisture anomalies (weeks to one month).

Among the outstanding issues is the fact that LSMs currently do not agree on the strength of interactions between land and atmosphere. Little has been done to address the predictability of snow in current GCMs. Results from current studies suggest strong regional and seasonal dependence (need to pick the right season and the right region).

The availability of land surface data is poor, yet the need is great (especially soil moisture, snow and estimates of evaporation). Can we get evaporation from satellites? We need to consider in predictability studies that soil moisture anomalies move around – this relates to the difference between the predictability time scale and the autocorrelation. Model bias is an issue, especially for rainfall. While soil moisture sensitivity is a summer phenomenon, we need to get the right seasonal cycle, so that snow is important (how that impacts soil moisture in spring). Current results suggest that 80% of the soil moisture effect is on temperature, while the impact on precipitation is still uncertain.

iv. Links with weather and other regional phenomena

Numerous studies have demonstrated that weather or synoptic variability is influenced by (and influences) low frequency variations such as the MJO, the PNA pattern, and blocking. For the subseasonal prediction problem we need to better understand how these interactions affect predictability, and determine those properties (or statistics) of weather that are predictable at lead times beyond which individual storm systems can be predicted. Examples of weather properties that are potentially predictable include changes in storm tracks, changes in regions of preferred hurricane formation, and changes in extreme events. A key issue in addressing these problems concerns the ability of climate models to simulate weather systems. For example, are detailed high-resolution simulations of individual hurricanes needed? Or, is it sufficient to only predict large-scale changes in the factors influencing hurricane formation?

A related issue concerns the resolution that is necessary in climate models to make them useful for addressing predictability on regional scales? Various local climatological features, such as the United States Great Plains Low Level Jet (LLJ), have a profound impact on regional climates, making it unlikely that climate models that do not adequately resolve such phenomena can provide useful predictions on regional scales.

In general, we need to begin to define more stringent quality measures to assess the veracity of model simulations that directly link errors in the models to uncertainties and errors in predictions at longer time scales. Clearly, climate drift plays an important role in that it often exceeds the signal that we are trying to predict. The diurnal cycle is a key example of large systematic errors that are common to most

climate models and that likely impact our ability to make useful regional predictions - especially over continents during the warm season.

In addition to reducing systematic errors, useful and reliable regional predictions (and for that matter predictions at all scales) require that models produce realistic variability and show sensitivity to initial conditions. This is necessary so that the spread of ensemble members will provide realistic assessments of forecast uncertainties (more on this below).

v. Methodology and data

A number of suggestions for improving forecast skill at the subseasonal time scale dealt with the application and development of new forecast methodologies. These included the use of atmosphere-ocean coupled models to better simulate the interactions between the atmosphere and ocean, especially in the extratropics. The key argument here is that this should provide more realistic time scales of the atmospheric anomalies. There is also evidence that ocean feedbacks can produce more realistic simulations of the MJO. Another suggestion was to use ocean mixed-layer models: these might provide most of the benefits of a full ocean model, but their use avoids the problems of spin-up and other shocks to the system that often occur when starting up a fully-coupled atmosphere ocean model forecast.

There is a clear need to improve the initialization of coupled atmosphere/land/ocean models in a way that minimizes model shocks and retains the information in the initial conditions. This includes improvements in how one samples from the initial PDF, including uncertainties in the tropical heating and other important forcing mechanisms. Simpler models should be used where possible to help diagnose the full AGCMs. Other uses of simpler (e.g. linear and/or lower order) models include more economical estimates of higher order statistics that could be used, for example, for forecasting forecast skill.

New data sets are needed for both initialization and verification of model forecasts, and for validating models. These include long term comprehensive and consistent reanalysis data sets of the atmosphere, land, surface fluxes, and sea surface temperatures for a host of studies, including hindcast experiments that address issue of model forecast skill and predictability. The reanalysis data sets also need to

provide improved diabatic (latent and radiative) heating, precipitation, and clouds to allow better tropical analyses for initialization, as well as to help validate convection schemes. Long term soil moisture, snow and, if possible, evaporation observations are needed for reanalysis, for initializing the land, and improving land surface models. There is also a need for better observations of the diurnal cycle over warm season continents to improve the diurnal cycle of precipitation/convection in GCMs.

IV. Recommendations

The results presented at the workshop suggest that substantial progress on the subseasonal prediction problem will likely be the result of progress in a number of disparate lines of research and development. As such, we believe that it will be crucial that the major climate and weather centers (in particular NASA and NOAA) work together to help coordinate and focus these various efforts. In the following we outline areas of high priority research and make specific recommendations on near term "action items" that we believe are most likely to lead to substantial improvements of predictions on subseasonal time scales.

i. High priority research and development

Tropical heating

- Improvements in the ability of GCMs to simulate the MJO
- Improved satellite estimates of subseasonal variability in tropical heating, especially vertical profiles, and related phenomena such as precipitation and clouds.
- Development of long-term consistent reanalysis data sets with improved representation of the tropics
- Improved initialization and ensemble methodologies
- Determine the role of subseasonal SST variability, and assess the gains in forecast skill from employing coupled atmosphere-ocean models, including models with only mixed layer components
- Develop and exploit simplified models to help diagnose and benchmark the skill of full GCMs
- Improve our understanding of tropical/extratropical interactions

Soil moisture and snow

- Improved model simulations of soil moisture and snow – determine realism of the simulated soil memory
- Improved satellite observations of soil moisture and snow
- Development of long term consistent data sets of soil moisture, evaporation, and snow, including those from global reanalysis systems
- Improve understanding of the coupling between the land surface and atmospheric processes

Extratropical modes of variability

- Improved understanding and simulation of annular modes, and their impact on the surface climate
- Improved understanding of the link to the stratosphere and associated potential predictability in the troposphere
- Improved long-term reanalysis datasets with a well-resolved stratosphere
- Improved understanding of the nature and predictability of various other modes of subseasonal variability such as the PNA, as well as an assessment of how well models are able to capture these modes
- Improved understanding of how subseasonal variability impacts weather and how predictable the impacts are

ii. High priority action items:

a) That a coordinated and systematic analysis of current subseasonal forecast skill be conducted by generating ensembles of 30-day hindcasts for the past 30-50 years with several "frozen" AGCMs. Specific goals include, sampling all seasons, and generating sufficiently large ensembles to estimate the evolution of the probability density function.

b) That a series of workshops be convened focused on modeling the MJO, and that a coordinated multi-nation/multi-model experimental prediction program be developed focused on the MJO.

c) That new satellite observations and new long-term consistent reanalysis data sets be developed for initialization and verification, with high priority given to improvements in estimates of tropical diabatic heating and cloud processes, soil moisture, and surface fluxes (including evaporation over land).

d) That NASA and NOAA develop a collaborative program to coordinate, focus, and support research on predicting subseasonal variability.

Specific steps to implement the above recommendations are: 1) to begin immediately to develop a framework for an experimental MJO prediction program, 2) to convene a follow-up workshop in the spring of 2003 to organize the AGCM hindcast project, and conduct initial meetings on modeling the MJO, and 3) for NASA and NOAA to put out a joint announcement of opportunity within the next year to focus research, modeling and data development efforts on the subseasonal prediction problem.

Acknowledgments

This workshop was supported by the Goddard Earth Sciences Directorate as part of a cross-cutting program to coordinate activities on weather and climate prediction. Additional funding was provided by NASA headquarters through the Global Modeling and Analysis Program, and by the NASA Seasonal-to-interannual Prediction Program (NSIPP).

We wish to thank Nefertari Johnson for her invaluable and tireless effort in putting the various disparate pieces of this document together.

References

Von Neuman, John, 1955: Some remarks on the problem of forecasting climate fluctuations. In "Dynamics of Climate": The Proceedings of a Conference on the Application of Numerical Integration Techniques to the Problem of the General Circulation held October 26-28, 1955. Richard L. Pfeffer, Ed, published in 1960 by Pergamon Press, pp 137.

Appendix – List of Participants

Jordan	Alpert	NWS/ NCEP/ EMC
Phil	Arkin	Earth System Sciences Interdisciplinary Center
Bob	Atlas	DAO/NASA/ Goddard Space Flight Center
Julio	Bacmeistar	UMBC/GEST NSIPP
Mark	Baldwin	Northwest Research Associates
Anjuli	Bamzai	NOAA OGP
Anthony	Barnston	International Research Institute (IRI)
Lennart	Bengtsson	Max Planck Institute fur Meteorologie / COLA
Robert	Black	Georgia Tech, School of EAS
Michael	Bosilovich	NASA/ Goddard Space Flight Center
Grant	Branstator	NCAR
Antonio	Busalacchi	Earth System Sciences Interdisciplinary Center
Ming	Cai	The University of Maryland
Kenneth	Campana	NOAA/NCEP
Peter	Caplan	NCEP
Juan Carlos	Jusem	SAIC/NASA/GSFC
Marco	Carrera	NOAA/Climate Prediction Center
Leila	Carvalho	University of California, Santa Barbara
Arun	Chakraborty	Florida State University
Simon	Chang	Office of Naval Research
Yehui	Chang	DAO/NASA/ Goddard Space Flight Center
Winston	Chao	NASA/ Goddard Space Flight Center
Muthnbel	Chelliah	CPC/ NCEP/ NWS
Mike	Chen	Iowa State University
Wilbur	Chen	NOAA/ NWS/ NCEP/ CPC
Ngar	Cheung Lau	GFDL/NOAA
Stephen	Colucci	Cornell University
Timothy	Delsole	Center for Ocean-Land-Atmosphere Studies
Paul	Dirmeyer	Center for Ocean-Land-Atmosphere Studies
Randall	Dole	NOAA-CIRES Climate Diagnostics Center
Timothy	Dunkerton	Northwest Research Associates
Franco	Einaudi	NASA Goddard Space Flight Center
Steven	Feldstein	The Pennsylvania State University
Rosana	Ferreira	GEST/NSIPP/NASA Goddard Space Flight Center
Mary	Floyd	Westover Consultants, Inc.
Christian	Franzke	EMS Environmental Institute, Penn State
Ron	Gelaro	DAO/NASA/ Goddard Space Flight Center
Lisa	Goddard	International Research Institute (IRI)
Milt	Halem	NASA/ Goddard Space Flight Center
Jongli	Han	NCEP/RSIS
Mark	Helfand	DAO/NASA/ Goddard Space Flight Center
Wayne	Higgins	Climate Prediction Center / NCEP/ NWS/ NOAA

Marty	Hoerling	NOAA-CIRES Climate Diagnostics Center
Fiona	Horsfall	NOAA
Arthur	Hou	NASA/ Goddard Space Flight Center
Jin	Huang	NOAA/OGP
Ming	Ji	NOAA/OGP
Charles	Jones	ICESS
Hann-Ming	Juang	NCEP/NOAA
Eugenia	Kalnay	University of Maryland
Masao	Kanamitsu	ECPC/ SIOI/ UCSD
Richard	Kerr	Science
Hyun-Kyung	Kim	NCEP/CPC
Kyu-Myong	Kim	NASA/ Goddard Space Flight Center
Jim	Kinter	COLA
Ben	Kirtman	COLA
Michael	Kistler	NASA Seasonal to Inter. Prediction Project
Randall	Koster	NASA/ Goddard Space Flight Center
Vernon	Kousky	NOAA
V.	Krishnamurthy	COLA, IGES
Arun	Kumar	NCEP/NOAA
Bill	Lau	NASA/ Goddard Space Flight Center
Jim	Laver	NOAA/NWS/CPC
Tsengdar	Lee	NASA Headquarters
Stefan	Liess	Max Planck Institute fur Meteorologie
Larry	Marx	COLA
Michiko	Masutani	NOAA/EMC
David	Melendes	NOAA
Kingtse	Mo	NOAA/Climate Prediction Center
Shrinivas	Moorthi	NOAA/NCEP
Steven	Mullen	University of Arizona
William	Neff	NOAA
Matt	Newman	NOAA-CIRES Climate Diagnostics Center
Sumant	Nigam	University of Maryland
Warwick	Norton	University of Oxford, UK
Ed	Olenic	NOAA/CPC
Hua-Lu	Pan	NOAA/NCEP
Michael	Patterson	NOAA/OGP
Philip	Pegion	NASA - NSIPP/ SAIC
Malaquias	Pena	University of Maryland
Peitao	Peng	CPC/NCEP/NOAA
Cecilie	Penland	NOAA-CIRES Climate Diagnostics Center
Roberta	Quadrelli	University of Washington/JISAO
Michael	Rabinowitz	University of Maryland and NASA/GSFC
Oreste	Reale	GEST/DAO
Thomas	Reichler	Scripps - UCSD
Michele	Reinecker	NASA/ Goddard Space Flight Center
John	Roads	University of California, San Diego

Andrew	Robertson	International Research Institute
Suranjana	Saha	EMC/NCEP/NWS/NOAA
Prashant	Sardeshmukh	University Colorado
Jae-Kyung	Schemm	CPC/ NCEPINWS / NOAA
Adam	Schlosser	COLA
Siegfried	Schubert	NASA/ Goddard Space Flight Center
J.	Shukla	GMU/COLA
Hilary	Spencer	University of Reading
Ken	Sperber	PCMDI, Lawrence Livermore National Laboratory
David	Starr	NASA/ Goddard Space Flight Center
Bill	Stern	GFDL / NOAA
David	Straus	COLA
Max	Suarez	NASA/ Goddard Space Flight Center
Liqiang	Sun	International Research
Naomi	Surgi	Environmental Modeling Center, NCEP
Marina	Timofeyeva	NOAA
Zoltan	Toth	SAIC-NCEP/EMC
Steve	Tracton	NOAA/NCEP
Alberto	Troccoli	NASA/UMBC
Huug	van den Dool	NOAA/Climate Prediction Center
Frederic	Vitart	ECMWF
Duane	Waliser	SUNY, Stony Brook
Mike	Wallace	University of Washington/JISAO
Wanqiu	Wang	NOAA
Klaus	Weickmann	NOAA-CIRES Climate Diagnostics Center
Matthew	Wheeler	Bureau of Meteorology Research Centre
Jeff	Whitaker	NOAA-CIRES Climate Diagnostics Center
Glenn	White	NOAA/EMC
Man Li	Wu	NASA/ Goddard Space Flight Center
Yan	Xue	NCEP/Climate Prediction Center
Song	Yang	Climate Prediction Center / NOAA / NCEP
Soo-Hyun	Yoo	CPC/NOAA
Jiayu	Zhou	GEST/NASA Goddard Space Flight Center
Yaping	Zhou	RSIS/CPC/NCEP
Yuejian	Zhu	EMC/ NCEP/ NOAA

Agenda

Tuesday, April 16

01:40	The Relationship Between the Classic PNA Pattern and the ENSO-Forced Pattern on Time Scales from Daily to Seasonal David M. Straus and J. Shukla	158
02:00	Assessment of midlatitude subseasonal variability in NASA/GSFC General Circulation Models. Robert X. Black and Dennis P. Robinson	159
02:20	Diagnostics of Climate Variability and Trend Using Potential Vorticity Maps. Ming Cai and Eugenia Kalnay	163
02:40	Systematic Errors and Surface Fluxes In the NCEP global model Glenn White	164
3:00	Configuration and intraseasonal duration of interannual anomalies of the Great Plains Low Level Jet. Mark Helfand	170
3:20	BREAK	
3:50	**DISCUSSION (Chair: Shukla)**	
5:30	END OF WORKSHOP	

Some Opportunities in Dynamic Extended Range Forecasting

Eugenia Kalnay, Ming Cai, and Malaquias Pena
University of Maryland
College Park, MD 20742

Extracting useful predictability from the Dynamic Extended Range Forecasting (DERF) time range, two weeks to two months, is not easy. D. Burridge (pers. comm.) referred to this forecast range as the "dry patch of predictability", meaning that it is too long for weather forecasting from information in the initial conditions, and too short for influences such as ENSO forcing to set in and provide predictability from boundary conditions. Nevertheless, it should be both economically very important and scientifically possible to advance significantly beyond what we are doing today.

In this talk we review some of the opportunities that we believe have not yet been exploited within the DERF "dry patch".

Extratropical ocean-atmosphere coupling. It is common to see AMIP runs referred to as "the upper limit on the skill that one can possibly obtain, since the SSTs are perfect". This statement is not really true, since in AMIP (perfect SST) runs the interaction between the ocean and atmosphere in the extratropics is seriously flawed. Away from the deep tropics the atmosphere is mostly forcing the ocean, and AMIP runs are set up so that instead, the ocean always forces the atmosphere, and the atmosphere provides no feedback. Pena et al (2002) have shown that a) locally coupled anomalies last much longer than locally uncoupled anomalies, b) in the extratropics, atmosphere-driving anomalies last longer than ocean-driving anomalies, and the opposite is true in the tropics. As could be expected from these results, they also found that c) the AMIP runs have shorter persistent anomalies than the reanalysis. This indicates that "perfect" coupled ocean-atmosphere models should be able to predict persistent anomalies much better than AMIP models. Another result obtained by Pena et al (2002) is that in AMIP runs, high skill in the extratropics is correlated with ocean-driving situations in the reanalysis and vice versa, indicating that it may be possible to identify a priori expected skill.

Intraseasonal variability. The Madden-Julian Oscillation (MJO) is a large amplitude, strong organizing influence in the atmosphere, with time scales of several weeks. Waliser and others have shown that few models are able to reproduce it realistically (one exception is the GLA 4^{th} order model developed at NASA/GSFC in the early 1980's!). Until the models become good enough to predict the MJO with the right frequency and amplitude, it should be possible to use the robust statistical characteristics of the MJO to nudge or otherwise force forecast models to reproduce in a statistically optimal way the MJO during a forecast. This would increase the skill of both the tropical and extratropical forecasts during the first few weeks.

15-day ensemble forecasts. The 2-weeks daily ensembles of the NWS contain a treasure of information on potential predictability that is not being exploited to its full potential. For example, during the Oklahoma-Texas drought of the summer of 1998, it was

apparent that the ensemble captured well the persistent nature of the drought, maintained by a large extent by the local soil moisture feedback (Hong and Kalnay, 2000, 2002). However, this was not being conveyed to the public in real time.

Improved initial conditions and coupled ensembles. Improving the initial conditions of coupled models could enhance predictability from initial conditions in the DERF time scales. One approach for doing this is the use of breeding to determine the subspace of dominant errors in the forecasts used as background or first guess for the analysis (Kalnay and Toth, 1994, Patil et al, 2001, Corazza et al, 2002, Ott et al, 2002). Cai et al (2002) have shown promising results for improved data assimilation and ensemble forecasting using the Zebiak-Cane model. Cai and Kalnay (2002) have experimented with breeding in the NSIPP coupled atmospheric-ocean system, and their preliminary results indicate that by performing breeding based on ocean rescaling, it is possible to capture the dominant instability of the coupled system even if the atmospheric noise saturates. This should allow using the observations in a more effective way, by minimizing the errors in the initial conditions that project on this and other coupled growing modes. It should also allow the creation of more effective initial perturbations for ensemble forecasting.

References:

Cai, Ming, E. Kalnay and Z. Toth, 2002: Bred Vectors of the Zebiak-Cane Model and Their Application to ENSO Predictions. Accepted in J. of Climate.

Cai, Ming and Eugenia Kalnay, 2002: Coupled ENSO instabilities derived with breeding. WMO, Research activities in atmospheric and oceanic modeling. Report #23, [Available from WMO, C.P. No 2300, CH1211, Geneva, Switzerland].

Corazza, M., E. Kalnay, D. J. Patil, R. Morss, I. Szunyogh, B. R. Hunt, E. Ott, and M. Cai, 2001: Use of the breeding technique to estimate the structure of the analysis "errors of the day". Submitted to Nonlinear Processes in Geophysics, European Geophysical Society.

Hong, Song-you and E. Kalnay, 2000: Origin and maintenance of the Oklahoma-Texas drought of 1998. Nature, 842-845.

Hong, Song-you and Eugenia Kalnay, 2002: The 1998 Oklahoma-Texas Drought: Mechanistic Experiments with NCEP Global and Regional Models. J. of Climate, in press.

Kalnay, E., and Z. Toth, 1994: Removing growing errors in the analysis cycle. Preprints of the Tenth Conference on Numerical Weather Prediction, Amer. Meteor. Soc., 1994, 212-215, Boston, MA.

Ott, Edward, B.R. Hunt, I. Szunyogh, M. Corazza, E. Kalnay, D.J. Patil and J. Yorke, 2002: Exploiting Local Low Dimensionality of the Atmospheric Dynamics for Efficient Kalman Filtering. ArXiv:physics/0203058v1 19 March 2002.

Patil, D.J., B. Hunt, E. Kalnay, E. Ott, J. Yorke, 2001: Local Low Dimensionality of Atmospheric Dynamics. Phys. Rev. Letters, 86, 5878.

Pena, M., E. Kalnay and M. Cai, 2002: The life span of intraseasonal atmospheric anomalies: dependence on the phase relationship with the ocean. WMO, Research activities in atmospheric and oceanic modeling. Report #23, [Available from WMO, C.P. No 2300, CH1211, Geneva, Switzerland].

Pena, M., E. Kalnay and M. Cai, 2002: Statistics of coupled ocean and atmosphere intraseasonal anomalies in Reanalysis and AMIP data. Submitted to the Nonlinear Processes in Geophysics, European Geophysical Society.

Session I

Current Operational Methods and Their Skill

CPC operational methods and skill in the day 15 - day 60 forecast range

Huug van den Dool (CPC)

1. Introduction

The Climate Prediction Center has only one operational forecast in the day 15 - day 60 range, which is, as predicted by Von Neumann(1955), the most difficult of all ranges. We do publish a forecast for monthly mean conditions over the US at a lead of 2 weeks. This forecast has been released once a month since Dec 1994. We will discuss briefly the tools underlying this forecast, in particular OCN (optimal climate normals), CCA (canonical correlation analysis), ENSO composites (when applicable) and, during summer, local and non-local soil moisture tools such as the Constructed Analogue. The weight given to the NCEP two tiered 'coupled' model is rather low so far. Relying on a-priori skill estimates over an historical evaluation period, the tools are combined each month into an official forecast. We present here a discussion of the skill of these official monthly forecasts for 1995-present. A comparison to the skill of the seasonal forecast shows that CPC's monthly forecast is basically a watered down version of the seasonal forecast, but with somewhat lower signal to noise ratio, as expected. Much of the forecast map shows the dreaded CL, a forecast for equal chances.

2. Time scales

The word monthly or seasonal (forecast) sounds like a monthly or seasonal time scale. However, one needs to carefully distinguish three time scales:
-) The lead time, i.e. the time between the issuance of the forecast and the first moment of validity
-) The averaging time (if any), and
-) The time scale of the physical process contributing to the predictability or skill of the forecast

While we can choose the first two time scales, (before 1995 we had a zero lead monthly forecast) we have no control over the third. The great apparent contradiction, as we shall see, is that interdecadal variability contributes to skill of seasonal and, yes, even monthly forecasts.

3. Tools

The tools used at CPC for the ½ month lead monthly forecast include:
1) Optimal Climate Normals (OCN), Huang et al(1996)
2) Canonical Correlation Analysis (CCA), Barnston(1994)
3) NCEP Dynamical Seasonal Forecast Model (CPM)
4) ENSO composites (when judged applicable)
5) Soil Moisture based tools (when judged applicable)
6) MJO extrapolation and more

The grouping reflects the overall importance of these tools. The first three tools are always available. Tools 4 and 5 are important, but are used only occasionally, i.e. ENSO composites are invoked when an ENSO is anticipated, and the soil moisture tools are given some weight during the warm half of the year. With the exception of MJO extrapolation, none of these tools is an atmospheric initial value approach. Rather, the lower boundary, be it SST or soil moisture, is relied upon when formulating the forecast.

In some detail these tools are designed as follows:
1) Optimal Climate Normals (Huang et al 1996a) is essentially a persistence of the climatic anomaly averaged over the last 10 years. This tools picks up on any recent climate trends, whether it be natural or man-made. The fact that a 10 year average is 'optimal' for US temperature is a concise statement about the power spectrum of climate variation in this part of the world.
2) Canonical Correlation Analysis is applied following Barnston(1994). CCA is a multivariate linear regression technique that a-priori compresses the state of the climate is a limited number of modes. Predictors include global SST over the last year, antecedent height fields and local predictors. The predictor can be anything, but for CPC's operations includes all 50 states.
Both OCN and CCA have been trained on data for 1950's present, with much attention for cross validation, i.e. an attempt to estimate a-priori skill honestly.
3) The 2-tiered coupled model (CPM) follows the example of NWP, but now with an ocean model (Pacific only) included. These model components are subject to continual change. A recent description is given in Kanamitsu et al(2002).
4) ENSO warm (cold) composites are essentially an ensemble of realizations during previous warm (cold) events. This tool is invoked when a warm/cold event is anticipated, a decision that includes some subjectivity. The idea goes back at least to Ropelewski and Halpert (1986). The selection of years, and the way one deals with other climate variations issues simultaneously makes composites a somewhat subjective tools.
5) Local effects of soil moisture on temperature have been described in Huang et al (1996b), and a local tool thereof was used. Gradually, a tool including non-local effects (even on precipitation) has subsumed the local tool. The later tool is based on an analogue constructed to 'todays' nation wide soil moisture anomaly (see Van den Dool 1994 for the method). Daily updates can be found at http://www.cpc.ncep.noaa.gov/soilmst/index_jh.html , see CAS forecasts button.
6) When a strong MJO is in progress, some of the forecasters project its evolution into the future month (day 15-day 60). This component is very subjective and could most definitely benefit from an objective underpinning by developing specific MJO tools, a strong theme of this meeting.

4. Skill

With reference to definitions given in Van den Dool et al(1996, 1999), the three class Heidke skill scores for 1995 onward are given in the Table below. The SS1 (0 is useless, 100 perfect) is the Heidke skill score for those areas judged *a-priori* to be high skill areas, where we make a 'non-CL' (i.e. a non-climatological probabilities) forecast, which is about 44% of all places/times (averaged over all leads). The lower SS2 score (=SS1*fractional coverage) is for the whole nation and should be used to intercompare the skill of tools.

{{For those unfamiliar with Heidke: It might help to remember that SS1 is about half the expected correlation, i.e. SS1=25 corresponds to an expected 0.5 correlation, and the permissible probability

anomaly is on average 2/3rds of SS1, i.e. for SS1=25 we are entitled to throw a 34/66 type 'coin', a considerable departure from 50/50 (the no skill lower bound)}}.

	TEMPERATURE			PRECIP'N		
	SS1	SS2	Coverage	SS1	SS2	Coverage
OFF	25	11	44%	10	2	20%
CCA	27	5	20	2	0	6
OCN	26	9	33	10	1	11
CMP	11	3	27	3	0	8

Note that we have little skill in precipitation. For Temperature the official forecast (OFF) appears to combine the strengths of various tools, and has the highest coverage and highest SS2. Of the individual tools OCN has scored the highest over 1995-2001. Each tool is expected to have SS1 in excess of 15, if prepared properly - with the exception of CMP this is the case for Temp, but for Precip we are generally unable to identify the high skill areas a-priori. Appropriately, the coverage is low.

The above Table applies strictly speaking to the seasonal forecast. However, the skill of the monthly forecast (far less studied) follows the above, except that SS2 and coverage are lower. As reported in van den Dool (1998), repeated as a Table below, the comparison of seasonal and monthly forecasts on temperature (2 week lead only) proves that, as expected, the monthly forecast as practiced at CPC just acts as a watered down version of the seasonal forecast, with similar sources of skill, and barely an atmospheric initial value approach. The best single tool is OCN, a crude attempt to harvest 'climate change' as a source of skill for CPC operational forecasts. The coverage of the monthly forecast is low: only 34%, i.e. most of the time we plead a lack of knowledge and or predictability and resort to climatological probabilities.

	TEMPERATURE		
	SS1	SS2	Coverage
OFF	25	13	53 (seasonal from vdDool et al(1998)
OFF	19	6	34 (monthly "

References:

Barnston, Anthony G., 1994: Linear Statistical Short-Term Climate Predictive Skill in the Northern Hemisphere. Journal of Climate: Vol. 7, No. 10, pp. 1513–1564.

Huang, J., H. M. van den Dool and A. G. Barnston, 1996a: Long-Lead Seasonal Temperature Prediction Using Optimal Climate Normals. J. Climate., 9, 809-817.

Huang, J., H. M. van den Dool and K. G. Georgakakos, 1996b: Analysis of model-calculated soil moisture over the US (1931-1993) and applications to long range temperature forecasts. J Climate., 9, 1350-1362.

Kanamitsu, M. Arun Kumar, Hann-Ming Henry Juang, Jae-Kyung Schemm, Wanqui Wang, Fanglin Yang, Song-You Hong, Peitao Peng, Wilber Chen, Shrinivas Moorthi, and Ming Ji,, 2002: NCEP Dynamical Seasonal Forecast System 2000. BAMS, 83, 1019–1037.

Ropelewski, C.F., M.S. Halpert, 1986: North American Precipitation and Temperature Patterns Associated with the El Ni? o/Southern Oscillation (ENSO). Monthly Weather Review: Vol. 114, No. 12, pp. 2352–2362.

Qin, J., and H. M. van den Dool, 1996: Simple extensions of an NWP model.Mon. Wea Rev., 124, 277-287.

Van den Dool, H.M.,1994: Searching for analogues, how long must one wait? Tellus, 46A, 314-324.

Van den Dool, J. Hoopingarner, E.O'Lenic, A.J.Wagner, A.G.Barnston, R.E.Livezey, D.Unger, A.Artusa, M. Masutani, J. Huang and R.Churchill, 1996 : ***1st*** Annual review of skill of CPC real time long lead predictions. Proceedings of the 21rd Annual Climate Diagnostics and Prediction Workshop, Oct. 28-Nov 1, 1996, Huntsville, Alabama. p13-16.

Van den Dool, H. M., J. Hoopingarner, E.O'Lenic, A.J.Wagner, A.G.Barnston, R.E.Livezey, D.Unger, A.Artusa and R.Churchill, 1999: 3rd Annual review of skill of CPC real time long lead predictions: How well did we do during the great ENSO event. Proceedings of the 23rd Annual Climate Diagnostics and Prediction Workshop, Oct. 26-30, 1998, Miami, Florida, pp 9-12.

Von Neumann, J., 1960: Some remarks on the problem of forecasting climatic fluctuations. Proceedings of Dynamics of Climate Conference, 1955 Institute for Advanced Study Princeton, Edited by R. Pfeffer. p9-11.

Monthly Forecasting At ECMWF

Frederic Vitart
European Centre For Medium-Range Weather Forecasts

1. Introduction

Medium-range weather forecasting and seasonal forecasting are currently operational at ECMWF. These two systems have different physical bases. Medium-range forecasting targets the period from day 4 to day 10, and is usually considered as an atmospheric initial condition problem. It is generally believed that the time range is too small for the oceanic variability to play a significant role. Therefore, the medium-range forecasting systems at ECMWF are based on atmosphere-only integrations forced by initially observed SST's. Deterministic medium-range weather forecasts are issued using a single integration of T511 with 60 vertical levels. Probabilistic forecasts called EPS are issued using a 51-member ensemble of T255L40 integrations twice a day.

Seasonal forecasting at ECMWF focuses on the period between 1 and 6 months. It is considered as a boundary condition problem, since most of the predictability at the time scale is justified by the long predictability of the oceanic circulation and its impact on the atmospheric circulation. Because of the strong role of the oceanic variability at such long time-scales, seasonal forecasts at ECMWF are based on coupled ocean-atmosphere integrations. They are probabilistic based on a 40-member ensemble of coupled T95L40 integrations each month.

In order to fill the gap between medium-range weather forecasting and seasonal forecasting, a new project is being developed at ECMWF called monthly forecasting. Its aim is to evaluate the predictability between day 10 and day 30. It is likely to be both an initial condition problem like seasonal forecasting. Therefore, the monthly forecasting system at ECMWF has been designed as a combination of EPS and seasonal forecasting.

2. Description of the monthly forecasting system

The ECMWF monthly forecasting system is based on a 51-member ensemble of coupled ocean-atmosphere integrations. The atmospheric component is IFS (from ECMWF) with a T159L40 resolution. The oceanic component is HOPE (from Max Plank Institute) with a zonal resolution of 1.4 degrees with 29 vertical levels. The oceanic and atmospheric components are coupled every ocean time step (1 hour) using OASIS from CERFACS.

The atmospheric initial conditions are proved by ERA40 or the ECMWF operational analysis. The ocean initial conditions are provided by the last ECMWF ocean analysis. Since the ocean analysis lags 12 days behind real time, ocean-only integrations are performed for 12 days with this ocean analysis as initial condition and forced by atmospheric fluxes from the ECMWF analysis in order to estimate the ocean initial conditions for the coupled run.

The atmospheric perturbations are similar to those used for EPS. They include singular vectors to perturb the atmosphere initial conditions and the use of stochastic phy6sics to perturb the atmospheric model at each time step. The ocean perturbations are identical to those applied for seasonal forecasting. The include SST perturbations in the oceanic initial conditions and wind stress perturbations during the oceanic data assimilation.

The present system displays a systematic error that grows almost linearly with time. This error is quite small during the first 10 days of integrations, but becomes significant after 10 days, and therefore, needs to be corrected. A background set of statistics is created in order to correct the model drift. A 5-member ensemble is integrated at the same calendar date as the real time forecast from 1990 to 2001. This represents a 60-member ensemble, which is run alternately with the real time forecast. This 60-meter ensemble allows us to estimate the drift of the model, and therefore to correct the real-time forecast afterwards.

The background statistics are also very useful to estimate what is the probability distribution function (pdf) of our system. After 10 days, the spread of the real-time forecast ensemble gets very large, and forecasts are issued by comparing the pdf of the real time forecast to the pdf of the model climatology. Statistical tests are used to determine if the 51-member ensemble of the real time forecast is significantly different from the 60-member ensemble of the model climatology.

3. Case Studies

Several monthly forecasts have been performed. Forecasts starting on 1 January 2001 and 10 April 2002 have been displayed. Interestingly, these forecasts suggest that the model still displays some potential predictability by week 4. In the present paper, we say there is potential predictability when the 51-member ensemble distribution of the real time forecast and the 60-member ensemble of the climatological distribution are significantly different, with a significance exceeding 90%. There is of course less potential predictability in week 4 than in week1, but the model is still able to predict something for week 4 that is significantly different from climatology.

The background statistics are also needed to estimate the skill of the coupled system during past years. A time series of the temperature at 850 hPa from 1 January1990 to 1 January 2000, suggests that the model has some skill in predicting its interannual variability up to week 3 over Southern Europe, although the skill for week 3 does not exceed the skill obtained by simply persisting the forecast of week 2. However, over other regions, for instance the eastern U.S., the model displays a skill that beats persistence till week 4. The ensemble size is too small to make definitive conclusions, but this suggests that the monthly forecasting system may produce useful forecasts up to week 4.

Last winter was an interesting test case over Europe, with a blocking even taking place in December followed by a zonal regime in early January. As a consequence, the weather over western Europe was very cold and dry in December and unusually warm and wet in early January. In order to check if the monthly forecasting system was successful in predicting this regime transition, a 51-member ensemble has been created starting on 15 December 2001. The weather patterns have been classified as blocked, zonal and intermediate. Most members of the ensemble predict a blocked regime in the medium range and a zonal regime during the last week of the forecast, but there is considerable variability in the way the transition occurs. As a consequence, the 2-meter temperature forecasts for week 1 and week 4 verify well with observations, whereas the forecasts

for week 2 and week 3 were not as successful. Another ensemble of monthly forecasts was realized starting on 15 November to test the ability of the coupled system in predicting the blocking event. Only 10 members of the ensemble predicted a blocking. About 3 of these members predicted a time evolution till day 25 very consistent with observations.

4. Simulating the MJO

The atmospheric component of the monthly forecasting system displays skill in predicting the evolution of the MJO till day 10. After about 10 days of integrations, the MJO tends to disappear in the model integrations. This is also true with coupled integrations, where the model succeeds in predicting the evolution of the MJO only when it is present in the initial conditions. Changes in the cumulus parameterization have helped improve the simulation of the MJO in the model. However, these changes had undesirable effects in other areas, leading to a degradation of medium-range scores over Europe. Improving the MJO without generating negative impacts elsewhere is still an active area of research at ECMWF. If successful this would likely lead to improved monthly forecasts.

5. Conclusion

A monthly forecasting system has been set up at ECMWF. This model is based on 51-member ensemble integrations. It is an experimental system that is run every 2 weeks and started on 27 March 2002. This system will be routinely integrated for at least a couple of years in order to get enough cases to assess the skill of this coupled model. This system is deficient in simulating a realistic MJO more than 10 days in advance.

The NCEP Global Ensemble: How to Go Beyond 16 Days?

Z. Toth, Y. Zhu, R. Wobus, and T. Marchok
Environmental Modeling Center
NCEP/NWS/NOAA

The NCEP global ensemble system currently generates operational forecasts out to 16 days. In this talk different verification statistics will be presented to explore the skill of these forecasts in predicting daily weather events out to 16 days. Through case studies the possible impact of regime transitions on forecast skill will also be addressed.

Additionally, experimental ensemble forecasts run out to 35 days lead time will be evaluated in terms of their skill. Possible future ensemble configurations that could contribute to a seamless suite of forecasts from day 1 to the climate time scales will also be discussed.

Ensemble Prediction of Blocking

Stephen J. Colucci
Department of Earth and Atmospheric Sciences
1116 Bradfield Hall
Cornell University
Ithaca, New York 14853
sjc25@cornell.edu

Recent unpublished work (Pelly and Hoskins 2002; Watson and Colucci 2002) reveals that ensemble prediction systems (EPSs) from the European Center for Medium-range Weather Forecasts (ECMWF) and the National Centers for Environmental Prediction (NCEP) can skillfully predict the occurrence of blocking over the Northern Hemisphere at extended ranges (ten days in advance and beyond). In the Pelly and Hoskins study, blocking is defined by a persistent, longitudinally coherent reversal of the normal meridional potential temperature gradient on the 2-PVU surface. With this definition, a blocking climatology was constructed from five years of ECMWF data and EPS forecasts were evaluated over one year. In the Watson and Colucci study, blocking is defined by a persistent, longitudinally coherent reversal of the normal meridional 500-mb height gradient over middle latitudes, following Tibaldi *et al.* (1994). With this definition, a blocking climatology was constructed from 40 years of NCEP data; EPS forecasts were evaluated over three winters. In both climatologies, maximum blocking frequency was found over the Atlantic and Pacific Oceans, allowing a separation of the data into Atlantic and Pacific sectors.

Blocking frequency is underpredicted by both the ECMWF and NCEP EPSs. Results are shown for the NCEP forecasts in Figures (1-3). The underprediction bias can be corrected to produce calibrated probabilistic forecasts that extend the range of skillful blocking forecasts in the NCEP EPS, especially over the Atlantic (Figure 4). Block onset is found to be more difficult to forecast than block decay in the ECMWF EPS (not shown).

These results are preliminary, since they are based upon a limited sample (three years of NCEP forecasts, one year of ECMWF forecasts), and therefore need to be checked for authenticity in a larger sample of forecasts.

References

Pelly, J. L., and B. J. Hoskins, 2002: How well does the ECMWF Ensemble Prediction System predict blocking? Submitted to the Quarterly Journal of the Royal Meteorological Society.

Tibaldi, S., E. Tosi, A. Navarra and L. Pedulli, 1994: Northern and Southern Hemisphere seasonal variability of blocking frequency and predictability. Monthly Weather Review, 122, 1971-2003.

Watson, J. S., and S. J. Colucci: Evaluation of ensemble predictions of blocking in the NCEP Global Spectral Model. Conditionally accepted for publication in the Monthly Weather Review.

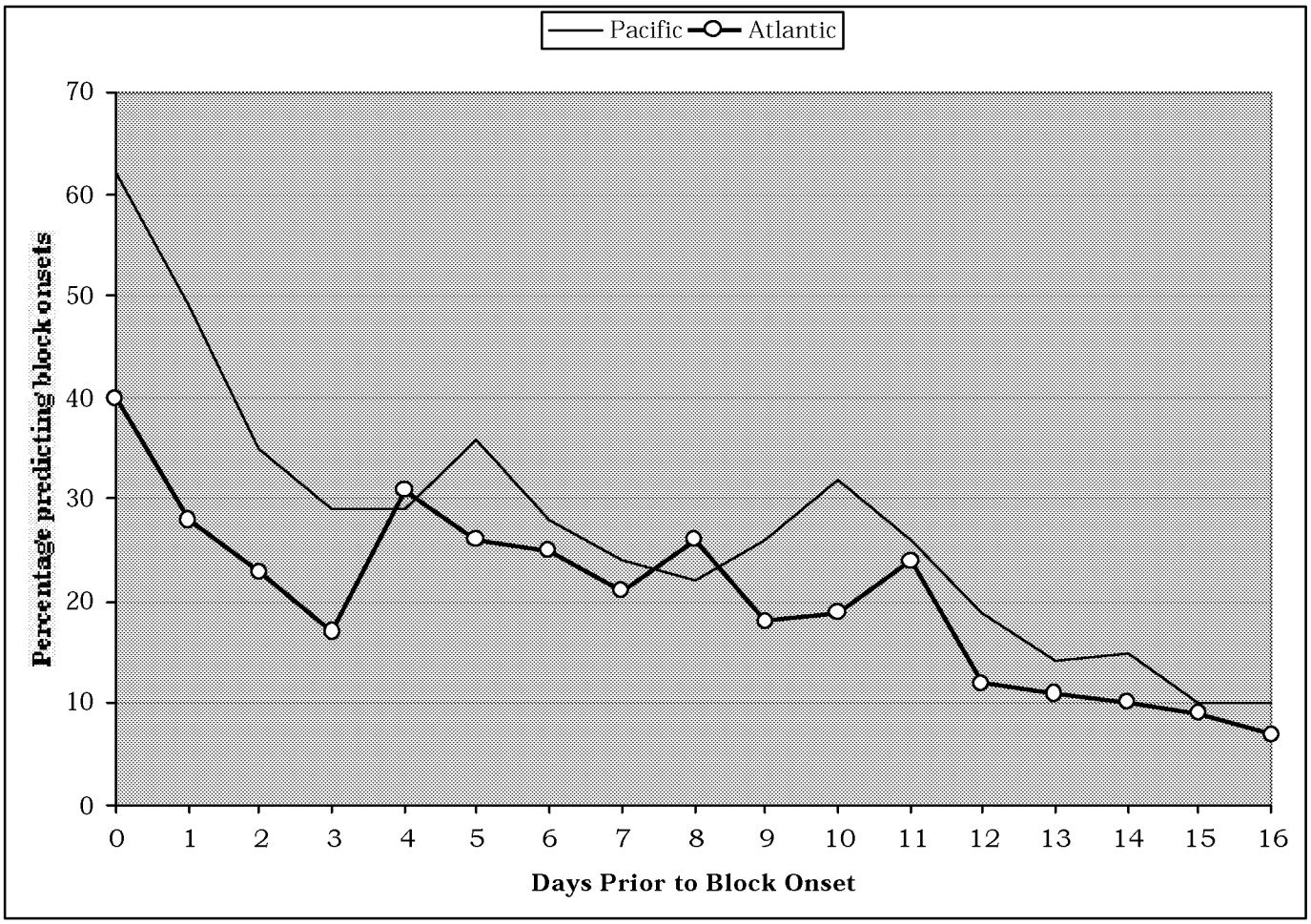

Figure 1. Percentage of available ensemble members (up to 17) predicting blocking on the block onset day, averaged over all three seasons studied (1995-96, 1996-97, 1997-98) as a function of forecast range in the NCEP Global Spectral Model. Forecasts of the probability of block onset from this information would become unskillful relative to climatology (13% probability over the Atlantic, 12% probability over the Pacific) by Day 12 over the Atlantic and Day 15 over the Pacific.

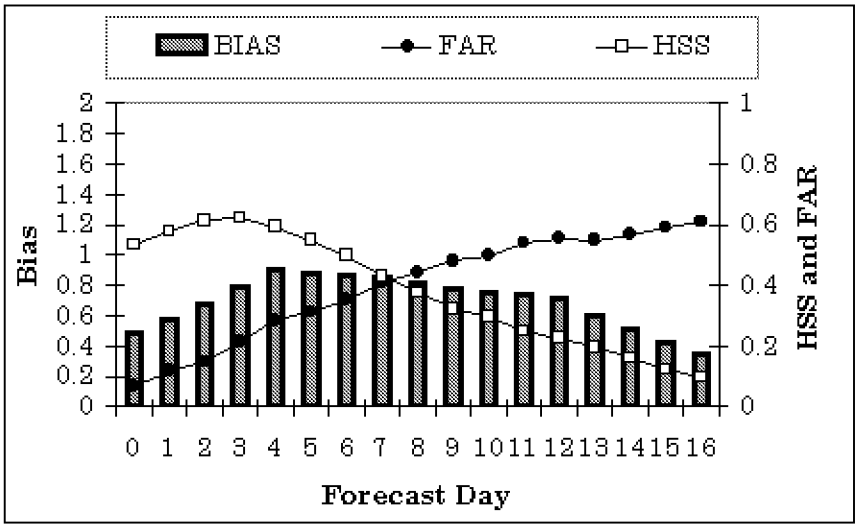

Figure 2. Average skill scores (HSS), biases and False Alarm Ratios (FAR) for NCEP ensemble forecasts of Pacific block onsets. The skill scores were averaged over individual forecast days (0 - 16) over all ensemble members for the three years of verification data.

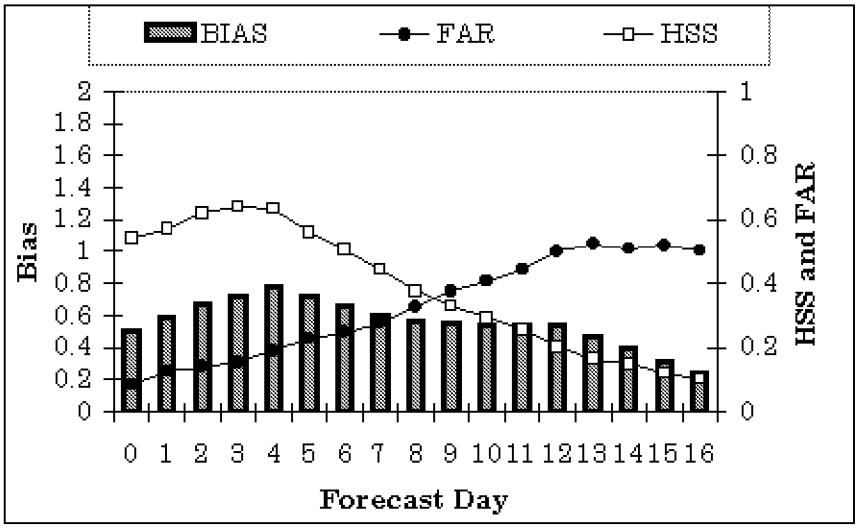

Figure 3. Same as in Fig. 2, but for Atlantic sector forecasts.

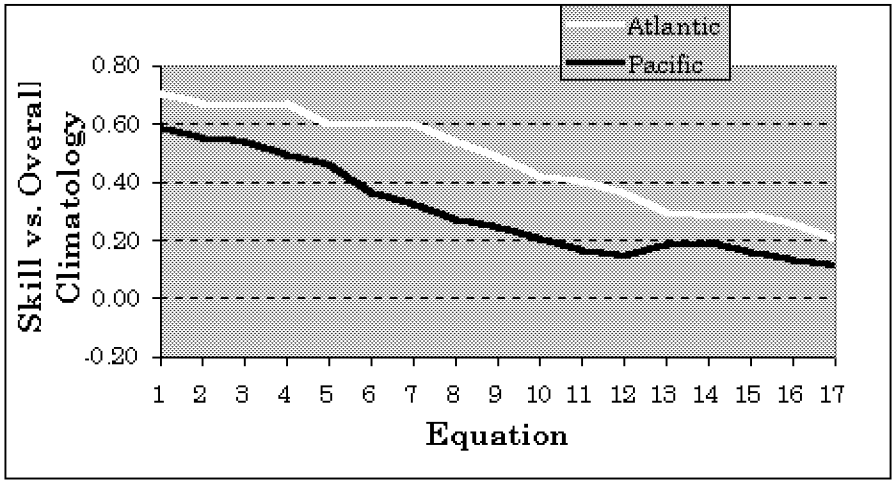

Figure 4. Calibrated NCEP forecast skill relative to climatology for Pacific and Atlantic block onsets, as a function of "equation" (= forecast day plus one). Climatological block relative frequencies for the Pacific (0.115) and Atlantic (0.131) are used as the reference forecasts. Two seasons of forecasts (1996-97, 1997-98) were used to develop the forecast scheme which was tested on the third season (1995-96).

Arun Kumar
CPC/NCEP
5200 Auth Road, Rm 807
Camp Springs, MD 20746

Micheal W. Phelps
COAPS, FSU
Tallahassee, FL

In this analysis AGCM simulations for the monthly mean hindcasts with different lead times are analyzed. For example, for the 1979-99 period, AGCM simulations starting from the atmospheric initial conditions in September, October, November, and December are analyzed for the hindcasts for the month of January. The purpose of this analysis is to evaluate the impact of atmospheric initial conditions on the hindcasts, for it is expected that hindcasts with the shortest lead (for example, the hindcasts from December for the target month of January compared to the hindcasts from September for the month of January) will have a higher level of simulation skill. Different measures to assess the role of initial conditions on the monthly mean variability are used. These include the analysis of internal and external variances with different lead times, the analysis of simulation skill with different lead times, and the analysis of low-frequency modes of the atmospheric variability with different lead times.

The Role of Atmospheric Initial Conditions for Long-Range Predictability

T. J. Reichler and J. O. Roads
Experimental Climate Prediction Center
Scripps Institution of Oceanography,
University of California San Diego, 0224
9500 Gilman Dr.
La Jolla, CA 92093-0224

We examine the relative importance of the atmospheric initial state and boundary forcing for long-range atmospheric predictability using the seasonal forecasting model from the National Centers for Environmental Prediction. A series of ensemble predictability experiments are conducted, using different combinations of initial and boundary conditions. The experiments are verified globally against a reference run with the same model as well as against reanalysis. We analyze the un-averaged forecast skill from day one out to a season and compare it with seasonally averaged data. We find that from initial conditions alone, there is significant instantaneous forecast skill out to 2 months. Different initial conditions show different predictability using the same kind of boundary forcing. Boundary forcing leads to measurable instantaneous forecast skill at any lead time: It starts to impact predictability after 10 days, it is equally important as initial conditions after 4 weeks, and it completely determines the forecast after 6 weeks. During events with strong tropical forcing, these time scales are somewhat shorter. For seasonally averaged skill, using observed atmospheric initial conditions can lead to a significant increase in overall skill, especially during periods with weak tropical forcing. We conclude that the long-term memory of the initial conditions is important for seasonal forecasting, and that good atmospheric initial conditions should be included in current seasonal forecasts.

Session II

Predictability of Extratropical "Modes"

Impacts of the Arctic Oscillation and the PNA Pattern on Weather

Roberta Quadrelli and John M. Wallace
JISAO, Seattle

Over large areas of the Northern Hemisphere, the influence of the AO upon the frequency of occurrence of extreme cold is stronger than one would expect, based on its effect on mean temperature alone. Apparently, the temperature field in these regions exhibits stronger temporal variability when the AO is in its low index polarity, with relatively weak subpolar westerlies, than when it is in its high index polarity. In order to elucidate this behavior, we examine the circulation regimes observed during contrasting polarities of the AO (and the PNA pattern as well). After presenting the phase space defined by the two modes together and its impact on the large scale temperature variability we show a series of "spaghetti diagrams"- selected contours extracted from the 10-day mean maps of the 500-mb height, sea-level pressure, and 1000-500-mb thickness fields for the 30 highest and lowest mean values of each of the indices. The plots reveal that the AO and the PNA pattern do, indeed, exert a strong influence on the frequency of occurrence of the distinctive flow regimes that are often associated with cold air outbreaks in midlatitudes.

RESULTS

In this study the AO and the PNA patterns are defined as the leading modes of wintertime variability of the Northern Hemisphere SLP. Their time series are given by PC1 and PC2 of monthly SLP anomalies, for the months DJFM of the period 1958-99. This follows the standard way of defining the AO (Thompson and Wallace, 1998), while the PNA pattern thus defined differs from the conventional PNA (Wallace and Gutzler, 1981) for the presence of an Atlantic center of action (Wallace and Thompson, 2002). The latter is a real signal though, since it also shows up in the one-point covariance map of the Pacific center of action for 500 hPa data.

Figure 1 presents a simple schematic of how some modes of low frequency variability project onto the phase space defined by the PC1 and PC2 SLP patterns. We notice how the "regional" definitions of NAO (Hurrell, 1995) and PNA (Wallace and Gutzler, 1981) represent an orthogonal basis as well as the "global" definitions offered by the EOF analysis. In figure 2 we show how AO and PNA affect the monthly temperature field on a global scale. At each gridpoint the arrow direction indicates which linear combination of the two modes is that most highly correlated with the local temperature time series.

Warm anomalies over Europe and cold anomalies over North Africa are associated with the positive polarity of AO; the PNA signature is quite strong over the Pacific sector and, somewhat surprisingly, over Eurasia as well.

To investigate the variability of AO (and of PNA) in its contrasting polarities, we show some "spaghetti" diagrams where selected contours of atmospheric variables are plotted for the 30 "highest" and 30 "lowest" index 10-day averages. The Z500 contour presented in figure 3 shows

that the polar vortex is clearly defined during high AO index (H1), while it is broken apart during low index (L1) when the global variability is also much higher.

The SLP contours in figure 4 reveal marked differences: H1 is characterized by a higher frequency of occurrence of anticyclones over the subtropical eastern oceans and an almost complete absence of them over higher latitudes; SLP often drops below 992 hPa in the Davis Straits, over the far North Atlantic and the European sector of the Arctic and much less often in the vicinity of the Aleutian Low; the L1 regime is characterized by a high frequency of occurrence of anticyclones that encompass parts of the Arctic and a relative absence of cyclones at lower latitudes.

The thickness contour shown in figure 5 also exhibits greater variability over the hemispheric domain (with the exception of Eurasia) during L1 than during H1. The favored location of the contour is strikingly different over the European region, hardly touched by it during H1 and always experiencing it during L1; a greater latitudinal spread is observed during L1 all across US, with a much higher possibility of cold outbreaks farther south. An example of dramatic change in variability during the polarities of PNA (H2 and L2) is shown in figure 6 (500 hPa). Focusing on the northwestern American region we notice that during H2 the shape of the contour shows there a sharply defined ridge with an axis along the west coast; during L2 the same region is instead characterized by extremely high variability.

Consistently, figure 7 shows the two types of blocking anomalies that are likely to occur during H2 and L2; the Pacific Nortwest will be warmer and colder than average during the two PNA polarities, respectively.

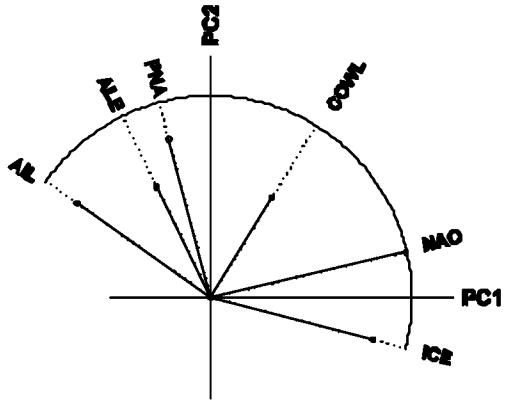

Figure 1: Projections of various indices on the phase space defined by PC 1 and PC2 of monthly DJFM SLP anomalies. ALE and ICE denote time series of monthly SLP anomalies at the center of the Aleutian Low and the Icelandic Low, with signs inverted; COWL denotes the COWL pattern, and NAO denotes seasonal-means of an index of the North Atlantic Oscillation. Length of solid line proportional
to the explained correlation (from 0 to 1).

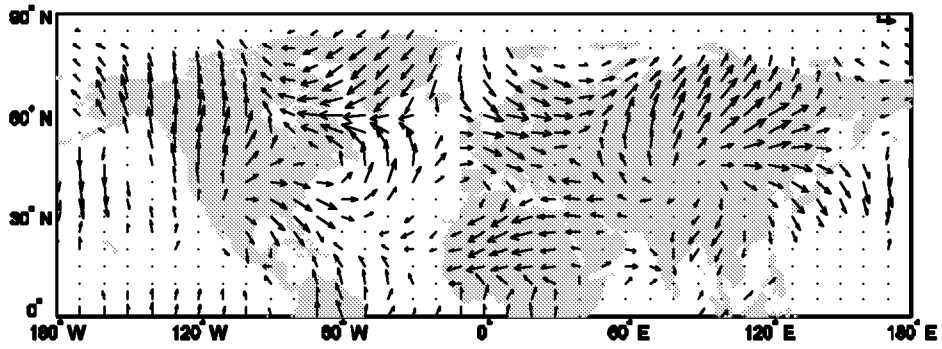

Figure 2: Vectorial map showing correlation coefficients between monthly mean 850-hPa temperature and PCs 1 (x-component) and 2 (y-component) of monthly DJFM SLP anomalies. Only correlation coefficients significant at 95{\%} level for both PC's 1 and 2 are shown. Upper right arrow corresponds to a correlation coefficient of 0.5.

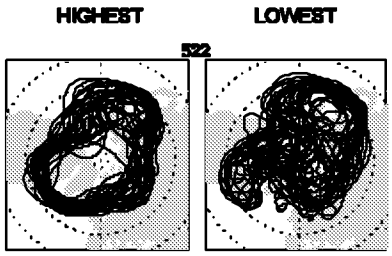

Figure 3: Plots of the 5220 m contour of Z500 for the 30 10-day mean maps with the most positive and the 30 10-day mean maps with the most negative projections upon EOF 1 of monthly-mean SLP.

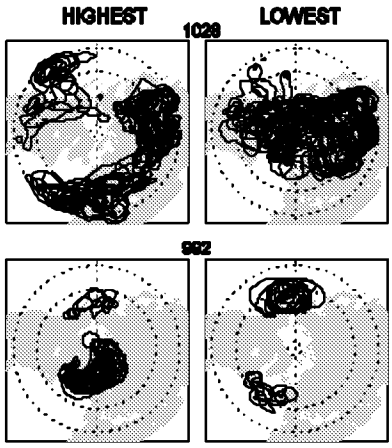

Figure 4: Plots of specified SLP contours for the 30 10-day mean maps with the most positive and the 30 10-day mean maps with the most negative projections upon EOF 1 of monthly-mean SLP.

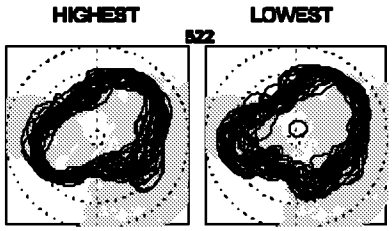

Figure 5: Plots of the 5220 m contour of the 500 hPa-1000 hPa thickness for the 30 10-day mean maps with the most positive and the 30 10-day mean maps with the most negative projections upon EOF 1 of monthly-mean SLP.

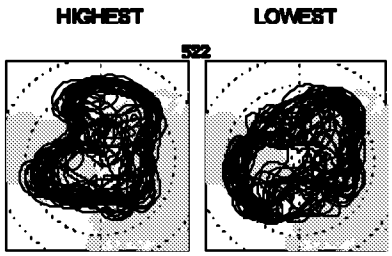

Figure 6: Plots of the 5220 m contour of Z500 for the 30 10-day mean maps with the most positive and the 30 10-day mean maps with the most negative projections upon EOF 2 of monthly-mean SLP.

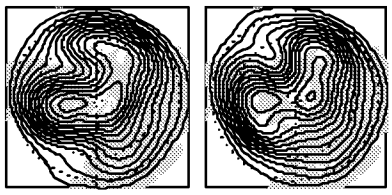

Figure 7: Composite mean of 500 hPa height for the 20 10-day mean maps with the highest anomalies at the grid point (150 W, 65 N) based on the subset of the data consisting of the 80 10-day mean maps with the strongest positive (left) and negative (right) projections upon EOF 1. Contour interval: 60 m; the 5100, 5400 and 5700 m contours are bold.

REFERENCES

Hurrell, J.W., 1995: Decadal trends in the North Atlantic Oscillation: Regional temperatures and precipitation, Science, 269, 676-679.

Thompson, D.W.J., and J.M. Wallace, 1998: The Arctic Oscillation signature in the wintertime geopotential height and temperature fields, Geophys. Res. Letters, 25, 1297-1300.

Wallace, J.M., and D.S. Gutzler, 1981: Teleconnections in the geopotential height field during the northern hemisphere winter, Mon. Wea. Rev, 109, 784-812.

Wallace, J.M., and D.W.J. Thompson, 2002: The Pacific center of action of the Northern hemisphere annular mode: real or artifact?, J. Climate, 2002, 15, 1987-1991.

Statistical Prediction of the Arctic Oscillation

Mark P. Baldwin and Timothy J. Dunkerton
Northwest Research Associates, Bellevue, WA USA
mark@nwra.com, tim@nwra.com

The Arctic Oscillation (AO) is the surface expression of the Northern Annular Mode (NAM), which can be defined at any pressure level from 1000 hPa to the mesosphere. Here we explore the possibility of predicting the average value of the AO 10–40 days in the future, based on today's value of the AO and values of the NAM at stratospheric levels.

We first note that there is a strong seasonality in the autocorrelation of the AO; it is substantially more persistent during the winter season (the season when planetary wave coupling to the stratosphere is strongest). Outside the winter season, the e-folding time scale of the AO is ~15–20 days during DJF, and ~5–6 days from April–October (Figure 1). The NAM is more persistent at stratospheric levels, peaking at 150 hPa in the lowermost stratosphere, where the DJF e-folding time scale exceeds 30 days.

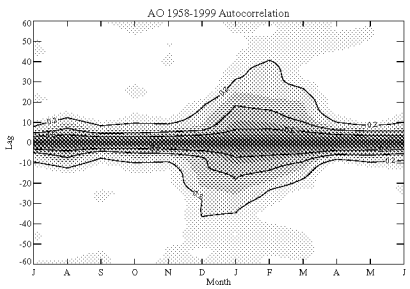

Figure 1

As predictors of the average value of the AO 10–40 days in the future, we use either today's AO value or the NAM at 150 hPa. Outside of the winter season, persistence of the AO provides almost no skill; during DJF the AO value accounts for ~13% of the AO 10–40 days in the future (gray curve in Figure 2).

Our previous work suggested that the effect of stratospheric NAM anomalies on the AO is confined to extreme events (of either sign) which appear to propagate from the upper stratosphere down to Earth's surface. We find here that the effect is simpler, with a linear relationship between the lower stratospheric NAM (150 hPa) and the average AO 10–40 days later (Figure 3). The cloud of points shows all of the DJF daily NAM-150 values plotted against the AO 10–40 days later. The straight line is a linear fit to the data, and the solid line shows the average AO values for the range of NAM-150 values. Similar linear results are obtained for other NAM levels from 1000 to 10 hPa.

We find that 150 hPa is the optimum single NAM level for forecasting future values of the AO, far better than using the AO itself to predict the AO. The 150-hPA NAM provides not only greater predictability during DJF, but extends the season of predictability to include November and March (black curve in Figure 2). It is also possible to combine levels in a multiple regression (dotted curve, which uses 1000, 150, and 10 hPa) to account for somewhat more variance, especially in early winter.

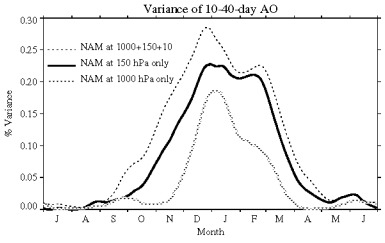

Figure 2

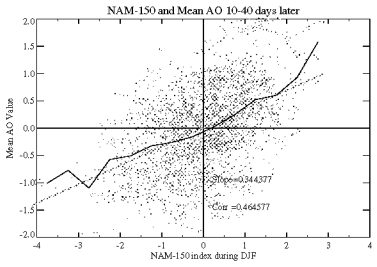

Figure 3

Our results are not sensitive to the time interval predicted or the exact level of the NAM used. The results are nearly identical if we predict the NAO instead of the AO (the daily AO and NAO have a year-round correlation of 0.93). We have assumed that only today's NAM values are available from data analysis. If the NAM can be predicted numerically (especially at 150 hPa) several days in the future, then the 10–40 day range would effectively be extended.

We have performed a similar study in the Southern Hemisphere. We find that the AAO shows enhanced persistence not during Austral winter, but rather during March–May and November–December—the seasons when planetary wave coupling to the stratosphere is strongest in the Southern Hemisphere.

Dynamical Mechanisms Associated With the Growth and Decay of the North Atlantic Oscillation (NAO) Teleconnection Pattern

Steven Feldstein
EMS Environment Institute
The Pennsylvania State University

This investigation performs both diagnostic analyses with NCEP/NCAR Reanalysis data and forced, barotropic model calculations to examine the dynamical mechanisms associated with the growth and decay of the North Atlantic Oscillation (NAO) teleconnection pattern. The diagnostic calculations include projection and composite analyses of each term in the streamfunction tendency equation.

The results of the analyses reveal a complete lifecycle of growth and decay within approximately two weeks. The positive NAO phase is found to develop after anomalous wavetrain propagation across the North Pacific to the east coast of North America. This contrasts with the negative NAO phase which appears to develop in-situ.

Both high-frequency (period 10 days) and low-frequency (period 10 days) transient eddy fluxes drive the NAO growth. After the NAO anomaly attains its maximum amplitude, the high-frequency transient eddy fluxes continue to drive the NAO anomaly in a manner that is consistent with a positive feedback process. The decay of the NAO occurs through both the divergence term and the low-frequency transient eddy fluxes. The temporal and spatial properties of the divergence term are found to be consistent with Ekman pumping. These results illustrate many important differences between the NAO and Pacific/North American (PNA) teleconnection patterns, perhaps most striking being that the NAO lifecycle is dominated by nonlinear processes, whereas the PNA evolution is primarily linear. In addition, the relation between the NAO and the zonal index is discussed.

To appear in proceedings of workshop on *Prospects for Improved Forecasts of Weather and Short-term Climate Variability on Subseasonal (2 week to 2 month) Time Scales*, NASA/GSFC, April 16-18, 2002

Distant Teleconnections via the Tropospheric Jetstream Waveguide

Grant Branstator

National Center for Atmospheric Research,
Boulder, CO 80307

Planetary wave theory suggests that low-frequency covariability between widely spaced points on the globe can be achieved without resorting to annular disturbances. This is able to happen because the time averaged tropospheric jets can act as waveguides which meridionally trap and zonally elongate wavetrains in their vicinity, as seen in solutions of the barotropic vorticity equation linearized about boreal winter upper tropospheric conditions. We examine the behavior of seasonal and subseasonal mean circulation anomalies in nature and in NSIPP and NCAR general circulation models to determine whether this behavior is observed.

We find that indeed there are locations on opposite sides of the North Hemisphere that covary during winter. An example of such behavior is shown in Fig. 1a, which portrays a one point correlation map for a base point in the waveguide when seasonal mean internal DJF 300mb streamfunction variability from an ensemble of AMIP-like integrations is analyzed. The meridional confinement and zonal elongation of the pattern in this example is quite distinct and contrasts with the more familiar arching structure of the pattern in Fig. 1b, which represents the situation for a base point not in the waveguide. This comparison indicates how the waveguide can lead to covariability between much more widely separated points than usually considered. A systematic investigation of one-point correlation plots indicates that this property is generic; pairs of midlatitude points that are both widely separated and strongly temporally correlation are invariably near the core of the time-averaged jet.

The example in Fig. 1 has a prominent zonal mean component, but further calculations show that this is not essential for distant teleconnections to exist. If similar calculations are done with the v-component of the nondivergent wind (which has no zonal mean), one still finds that locations on the opposite side of the globe can be highly correlated. Rather than possession of a zonal mean component, what is important for a field to capture the effect of the waveguide is that it have significant amplitude in the subtropics, where the mean jets tend to be located in boreal winter. This means that streamfunction and the v-component of the wind are

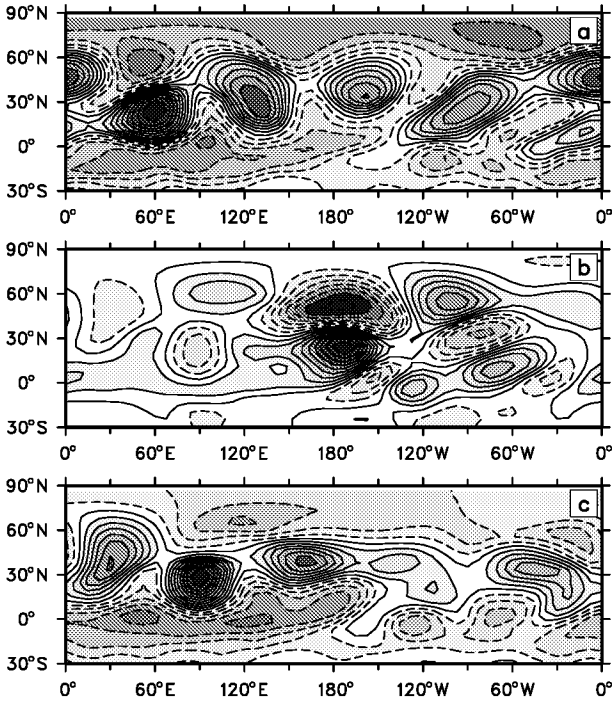

Figure 1. One point correlation plots of DJF 300mb streamfunction internal variability from a CCM3 22 member ensemble of 45 year integrations with observed SSTs. The base point is at a) (60E, 24N), b) (172W, 24N), c) (90E, 29N). Contour interval is 0.1.

effective choices for investigating the waveguide while the more commonly used geopotential height is not.

A distinguishing characteristic of waveguide patterns of variability is that within the jet they do not appear to have a preferred longitudinal phase. If, as in Fig. 1c, one chooses a basepoint to the east of that used in Fig. 1a, the portion of the pattern in the Asian jet retains its zonal wave five structure and shifts eastward. On the other hand, from a *global* perspective the waveguide pattern is sensitive to phase; for the phase in Fig. 1c, the pattern of variability is not as global in extent with a gap appearing over the eastern North Pacific and North America. So the pattern of Fig. 1a is special and

might be thought of as being *the* circumglobal waveguide teleconnection pattern.

Additional analysis indicates that for a number of reasons waveguide disturbances should be important for the subseasonal forecasting problem. First, they can act to connect widely separated locations in surprisingly short times. Calculations using a linear inverse model as a diagnostic tool indicate that waveguide-trapped disturbances in one part of the globe can affect locations on the opposite side of the hemisphere within about a week. Second, these disturbances influence not only the time mean circulation but also weather parameters including bandpass eddy statistics and rainfall rates. Third, calculations show that waveguide influenced variability is embedded in and thus affects the structure of some of the best known atmospheric teleconnection patterns, including the NAO and the response of the extratropics to El Nino. That the pattern of variability associated with the NAO appears to be affected by the waveguide can be seen in Fig. 2a, which shows contours of the correlation between upper tropospheric streamfunction, again for internal variability in an AMIP-like ensemble, and a near surface North Atlantic sector index of the NAO. In addition to the familiar North Atlantic and zonally symmetric features of variability associated with the NAO, the five centers of variability seen in Fig. 1a are seen in this diagram. Whether this indicates a physical link between these two phenomena or simply reflects the similarity in their structure over the North Atlantic is not clear.

As explained in Branstator (2002), most of our analysis is carried out with GCM data because of the high statistical significance of results produced when GCM data are used. A similar analysis with data from nature shows similar characteristics, to the extent that the short record allows conclusions to be drawn. As an example of the situation in nature, Fig. 2b shows correlations between intraseasonal 300mb streamfunction and a near surface North Atlantic index of the NAO, calculated in an analogous way to that for Fig. 2a. Again, the influence of the waveguide pattern on the centers of covariability that are remote from the North Atlantic are apparent, an indication that the effects of the waveguide need to be taken into account when considering subseasonal and longer variability in nature as well as in GCMs.

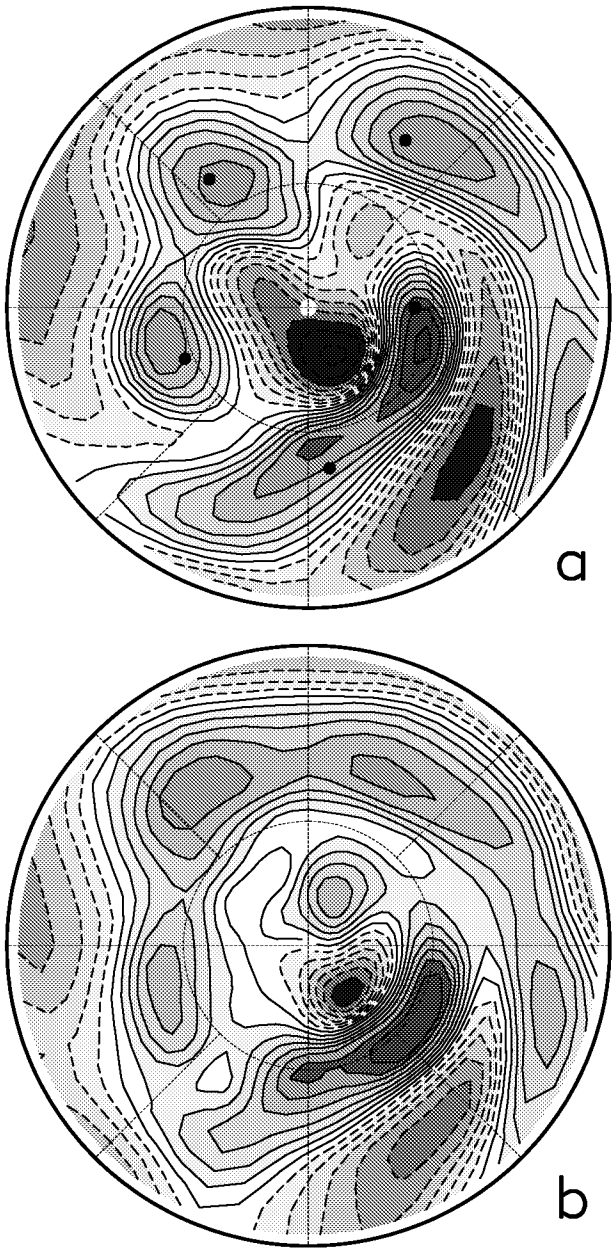

Figure 2. a) Correlation between DJF 300mb streamfunction CCM3 internal variability and projections onto the leading EOF of North Atlantic sector 850mb streamfunction. b) Same as a) for intraseasonal reanalysis perturbations. Contour interval is 0.1.

Reference

Branstator, G., 2002: Circumglobal teleconnections, the jet stream waveguide, and the North Atlantic oscillation. *J. Climate,* in press.

On the Origin and Mature-Phase Dynamics of PNA Variability

Sumant Nigam
University of Maryland

A prominent mode of winter climate variability is the geographically well-defined Pacific North American (PNA) pattern, which represents circulation and precipitation variability on both intraseasonal and seasonal time-scales. The mode is linked with midlatitude Pacific SST variability, but has sometimes been erroneously associated with ENSO variability as it can be excited during ENSO winters as well. The talk will focus on the extraction of PNA structure (rotational and divergent circulations) and forcing (diabatic heating, vorticity and thermal transients) from reanalysis data sets. The pattern is then simulated from the diagnosed forcing using a steady linear primitive equation model. A good simulation allowed pursuit of the dynamical diagnosis strategy, the objective of which is to reveal the mature-phase maintenance mechanisms. Modeling analysis indicates the considerable role of zonal/eddy coupling and sub-monthly vorticity transients in the pattern's generation.

Ongoing analysis of PNA evolution at weekly resolution indicates that a typical 2-week long episode begins with an eastward extension of the east Asian jet, with zonal wind anomalies at 200mb extending 20-30° beyond the dateline. From this point onwards, a sequence of events, including displacement of Pacific storm tracks, occur, spurred, in part, by the balance-restoring secondary circulations. The origin of the precursor phase jet extensions is unclear at present, although linkage with Kuroshio variability is being investigated. A better understanding of PNA excitation and dynamics can clearly influence predictions of short-term climate variability.

Limits of Predictability Determined by Optimal Persistence Patterns

Tim Delsole
Center for Ocean-Land-Atmosphere Studies

In this talk I introduce the concept of an optimal persistence pattern and discuss how it can be used to define limits of predictability strictly from observations. An optimal persistence pattern (OPP) is a component of a time-varying field that remains auto-correlated for the longest time-lags. Techniques for extracting OPPs provide an efficient method not only for isolating persistent patterns in stationary time series, but also for detecting trends, discontinuities, and other low-frequency signals in nonstationary time series. In this talk, we discuss how OPPs can be used to filter out low-frequency signals to render a time series stationary, then used to determine the patterns with the maximum decorrelation time. This approach clarifies the fundamental time scales of phenomena such as the PNA, NAO, etc. The resulting patterns can be shown to provide a rigorous upper limit of predictability for all linear prediction models. The skill of statistical predictions of the leading OPPs will be discussed.

Variability Within the PNA, NAO, and AO Regimes On Sub-Seasonal Time Scales

Wilbur Y. Chen
Climate Prediction Center
NCEP/NWS/NOAA

Variability over the oceans is much more prominent than over the lands, as shown in Fig. 1. Its impacts on remote regions through teleconnections are well recognized. For instance, PNA and TNH patterns show impact of the Pacific sector on North America sector. Both PNA and TNH teleconnections can develop due to tropical forcing and/or intrinsic internal dynamics. This study focuses on the latter. That is, through the intrinsic internal dynamical processes, how does a large oceanic variability impact North America? Particular attention is focused on the variability of a telconnection pattern within the PNA, NAO, and AO regimes.

Variability and teleconnectivity are examined for various sub-seasonal time-scales (figs. 1 and 2). Variability decreases rapidly as time-scale increases, as shown in Fig. 1. Also, as timescale increases, the teleconnection not only become stronger and better established but also much more organized and located in certain restricted regions, as illustrated in Fig. 2. The main points relevant to medium-range predictions over the North America are:

1. Significant variability within the PNA, NAO, and AO regimes, as shown in Figures 3 to 5.

2. A gradual transformation from PNA to TNH pattern (top panels of Fig. 3). Large anomalies over most of the North Pacific basin induce a development of a same-signed anomaly over the Southeast of the U.S. However, a reverse-signed anomaly will develop ranging from Alaska to eastern Canada depending on the location of the Pacific anomaly, as shown in Fig. 3. Also shown is the gradual transformation between PNA and TNH patterns (top 3 panels).

3. In Fig. 4: The large-scale anomalies over the North Atlantic along 40 N (which may be considered to be the southern components of the NAO) make same-signed impacts on various interior parts of the U.S. If the Atlantic anomaly is over the Europe, the impact is then over the eastern U.S. If the Atlantic anomaly is located over the mid-western ocean, the impacted area then extends westward across the U.S. interior, reaching as far as southern New Mexico. It is interesting to note that the impacts take on an arch shape, from Florida coastal areas up to the Great Lakes and northern Plains and then down to New Mexico.

4. In Fig. 5: Here we focus on large anomaly located over north of 65N (the green circle). If a large anomaly is located at 11 O'clock position, the impact is over the northern China. When the Arctic anomaly shifts eastward, another impacted region start to develop over the Europe, as shown in the top-right panel. Further movement of the Arctic anomaly to the 5 O'clock position, a third impacted region develops over the mid-Atlantic region of the U.S.

5. An Arctic anomaly that is heavily weighted in the Pacific side (say, at 7-9 O'clock position) is found not to affect the North Pacific and the U.S. mainland. This result is somewhat surprising, when comparing to the conventional AO loading pattern. Could it be an artifact of an EOF analysis?

6. Within a conventional AO index, there can be large variations of anomaly distribution. The variations of action center within Arctic region can make the impacted remote region to be half the world apart. The longitudinal position of a large anomaly appears to be an important consideration in sub-seasonal prediction applications.

Fig. 1 Wintertime Z500 Variability on various time-scales
evaluated for Dec-Mar during the period of 1971-2001

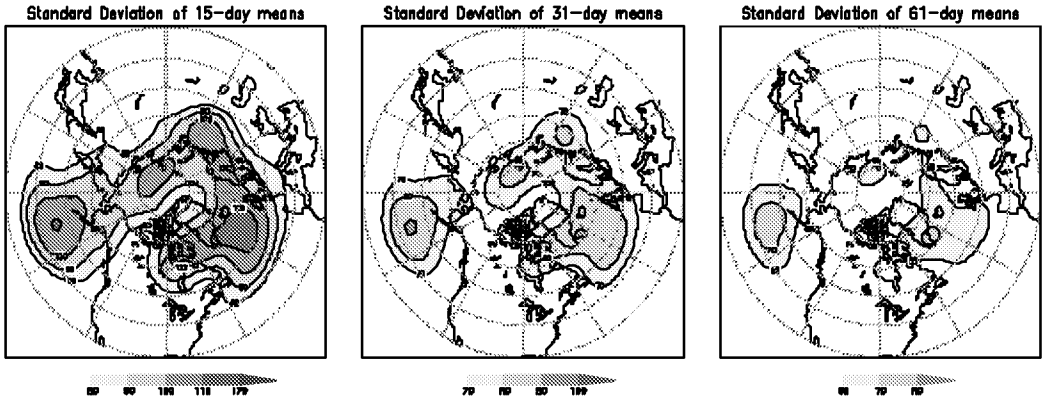

Fig. 2 Correlation Coef with N PAC Maximum Variability Center
(160W & 45N) on various timescales evaluated for Dec-Mar 1971-2001

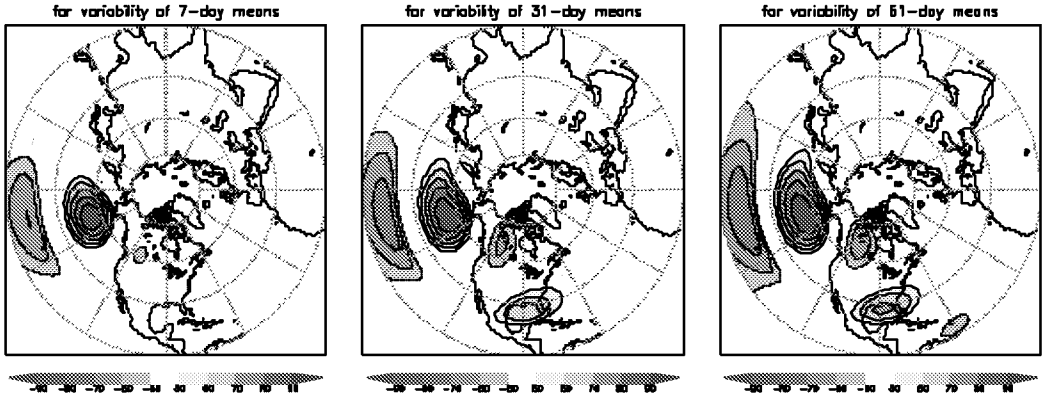

Fig. 3 Teleconnection Pattern with N Pac Variability Center at various locations, evaluated for Jan–March (1971–2001)

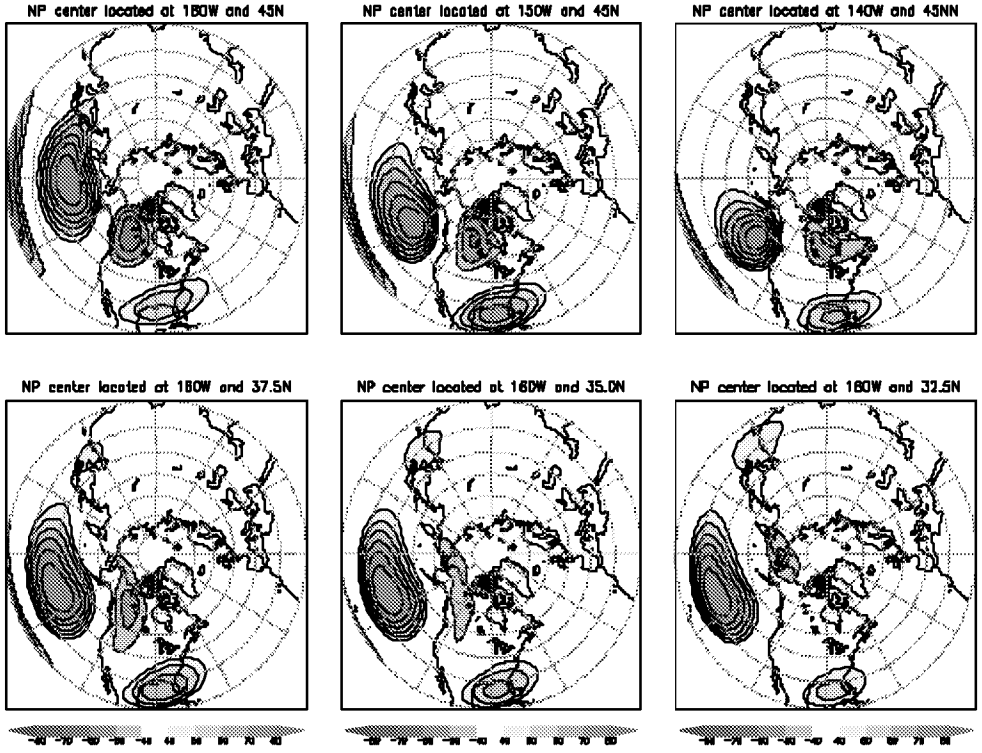

Fig. 4 Teleconnection Pattern with N Atl Variability Center at various locations, evaluated for Jan–March (1971–2001)

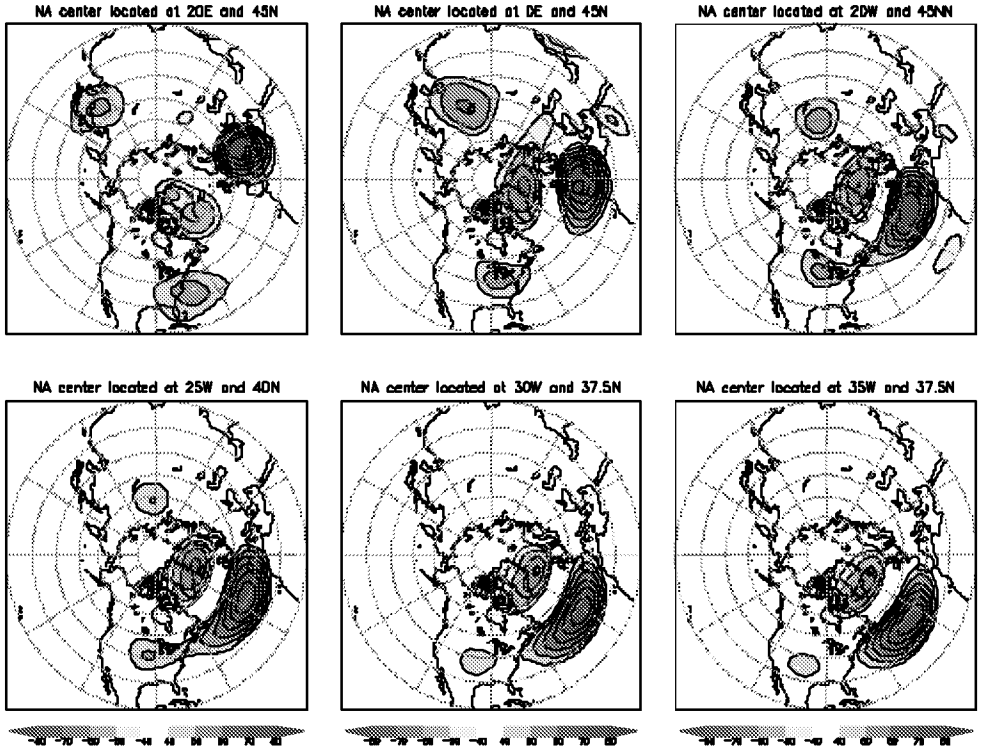

Fig. 5 Teleconnection Pattern with Arctic Center at various longitudes, evaluated for wintertime Jan–March (1971–2001)

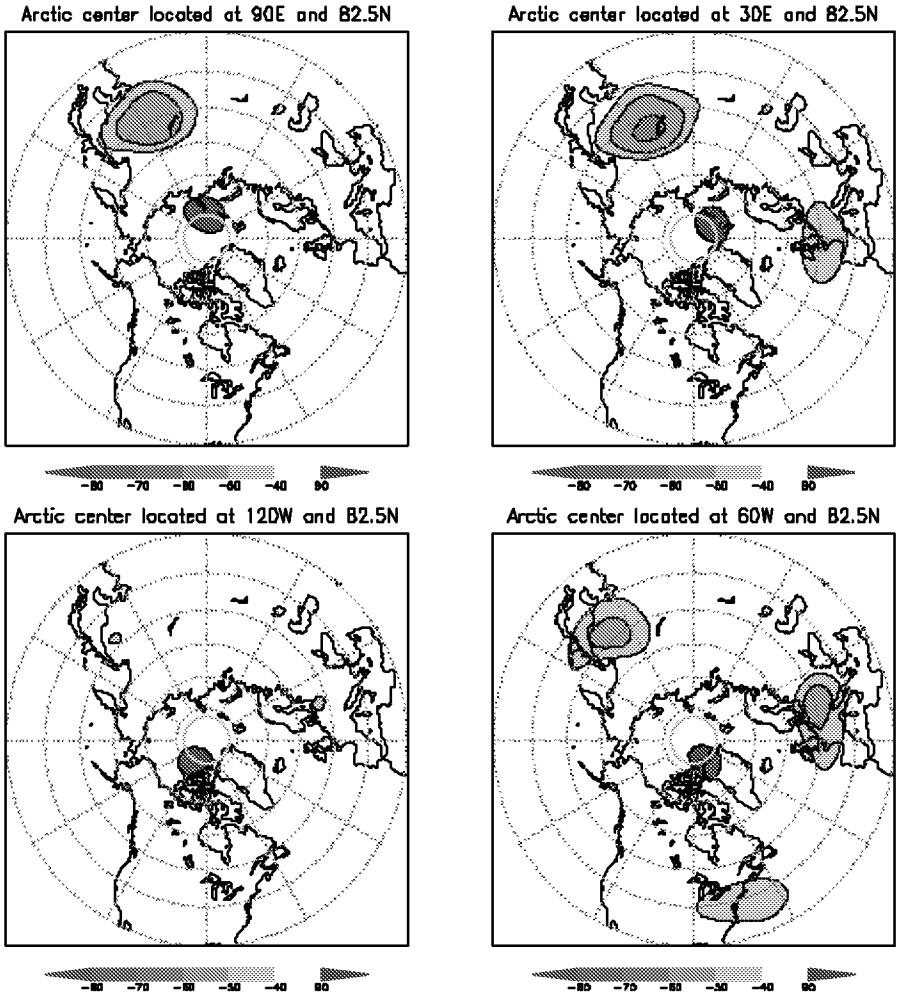

Monitoring the AO/PNA Indices Using NCEP/NCAR CDAS/Reanalysis

Hyun-kyung Kim and Wayne Higgins
CPC/NCEP

The Arctic Oscillation (AO) and the Pacific / North American pattern (PNA) are two of the dominant modes of atmospheric variability in the Northern Hemisphere (NH), in particular during cold season. These indices are strongly associated with weather and climate variability over a large portion of the NH.

For the purpose of improving weather and climate prediction at NCEP, these indices were developed for the period from January 1950 to the present using the NCEP/NCAR CDAS/Reanalysis. Since there is no explicit way to predict these indices yet, the "predicted" indices are generated by projecting the loading pattern of each mode onto the MRF and Ensemble forecast data in order to help the weather and climate prediction.

The indices and forecasts for the most recent 120 days are posted on the monitoring weather and climate web site of NCEP/CPC and updated daily. (http://www.cpc.ncep.noaa.gov/products/precip/CWlink)

For the comparison with AO, the North Atlantic Oscillation (NAO) has also been monitored. The Antarctic Oscillation (AAO) has also been monitored as the counterpart of the AO in the Southern Hemisphere. All monitoring products are updated on a daily basis. Several of these will be demonstrated in our talk.

Session III

Predictability of the ISO/MJO

Predictability and Forecast Issues Associated with the MJO/ISO

Duane E. Waliser
Institute for Terrestrial and Planetary Atmospheres
State University of New York, Stony Brook, NY 11794-5000
duane.waliser@sunysb.edu; (631) 632-8647 (voice) –6252(fax)

Since its discovery by Madden and Julian (1971) over two decades ago, the Madden and Julian Oscillation [MJO/ISO; a.k.a. Intraseasonal Oscillation (ISO)] has continued to be a topic of significant interest due to its complex nature (Madden and Julian, 1994) and the wide range of phenomena it interacts with. The onset and break activity of the Asian-Australian monsoon system are strongly influenced by the propagation and evolution of MJO/ISO events (e.g., Yasunari, 1980; Hendon and Liebmann, 1990). Apart from this significant local influence, there are also important downstream influences that arise from the MJO/ISO. For example, the development of persistent North Pacific (PNP) circulation anomalies during Northern Hemisphere winter has been linked to the evolution and eastward progression of convective anomalies associated with MJO/ISO events (e.g., Liebmann and Hartman 1984; Weickmann et al. 1985; Higgins and Mo 1997). In fact, a strong link has been shown to exist between rainfall variability along the western United States, including extreme events, and the longitudinal position of MJO/ISO convective anomalies (Mo and Higgins 1998a; Jones 2000; Higgins et al. 2000). In addition, MJO/ISO convective activity has been linked to Northern Hemisphere summer time precipitation variability over Mexico and South America as well as to wintertime circulation anomalies over the Pacific – South American Sector (Mo and Higgins 1998b; Jones and Schemm 2000; Paegle et al. 2000; Mo 2000). Recently, studies have also shown that particular phases of the MJO/ISO are more favorable than others in regards to the development of tropical storms/hurricanes in both the Atlantic and Pacific sectors (Maloney and Hartmann, 2000; Mo, 2000; Higgins and Shi, 2001). Finally, the passage of MJO/ISO events over the western Pacific Ocean has been found to significantly modify the thermocline structure in the equatorial eastern Pacific Ocean via their connection to westerly wind bursts (e.g., McPhaden and Taft, 1988). This latter interaction has even been suggested to play an important role in triggering variations in El Nino - Southern Oscillation (ENSO) (e.g., Lau and Chan 1988; Weickmann 1991; Kessler and Kleeman 2000).

As influential as the MJO/ISO is on our weather and climate, a fundamental question yet to be adequately addressed concerns its theoretical limit of predictability. For example, it is well known that useful skill associated with deterministic prediction of most "weather" phenomena is limited to about 6-10 days (e.g., Lorenz 1965; Palmer 1993; van den Dool 1994). Similarly, it has been found that the likely limit of predictability for ENSO is on the order of 12-18 months (e.g., Cane et al. 1986). However, it is still yet to be determined what the corresponding metric is for the MJO/ISO phenomenon. The somewhat well behaved nature of the MJO/ISO (e.g., equatorially-trapped; preference for warm SSTs, seasonality) along with its intraseasonal time scale suggests that useful predictive skill might exist out to at least 15-25 days and maybe longer. Support for this suggestion comes from statistical predictive models of the MJO/ISO, which indicate useful skill out to at least 15-20 days lead time (e.g, Waliser et al. 1999a; Lo and Hendon 2000; Wheeler and Weickmann 2001; Mo 2001). However, as with any statistical model, these models are sorely limited in the

totality of the weather/climate system they can predict, their ability to adapt to arbitrary conditions, and their ability to take advantage of known physical constraints.

While there have been a number of dynamical predictive skill studies of the MJO/ISO (i.e., comparing forecasts to observations), these studies typically were performed with forecast models that exhibited rather poor simulations of the MJO/ISO. For example, the studies by Chen and Alpert (1990), Lau and Chang (1992), Jones et al. (2000), Hendon et al. (2000) were all performed on the most recent or previous versions of the NCEP (or NMC) medium range forecast (MRF) model's Dynamic Extended Range Forecasts (DERFs). In general these studies showed useful skill out to about 7-10 days. However, these skill limits are likely to be significant underestimates of the potential predictability due to the very weak MJO/ISO signature in the model. Moreover, since these studies were really measuring forecast skill of the model, their skill versus lead-time estimates are additionally hampered by the difference in phase speeds between the model and observations and the influence from poorly known/specified initial conditions. Thus, ascertaining even a gross estimate of the limit of predictability for the MJO/ISO from these studies is neither appropriate nor feasible.

In addition to the above dynamical studies, there have also been a number of predictive skill studies of the MJO/ISO (i.e., comparing forecasts to observations) using statistical forecast models (e.g, Waliser et al. 1999a; Lo and Hendon 2000; Mo 2001; Wheeler and Weickman, 2001). While these sorts of models are typically more adept at forecasting MJO/ISO variability than present-day dynamical forecast models, they still may not provide a useful or adequate measure of MJO/ISO predictability due to their relatively simplistic, and thus far linear, nature.

The remaining portion of this abstract will describe the results of two recent studies (Waliser et al., 2001, 2002) designed to more directly estimate the theoretical limit of dynamic predictability of the MJO/ISO using sets of twin numerical predictability experiments (e.g., Lorenz 1965; Shukla 1985). These studies utilized the NASA GLA general circulation model due to its relatively realistic MJO/ISO representation (e.g., Slingo et al. 1996; Sperber et al.1996). A 10-year control simulation using specified annual cycle SSTs was performed in order to provide initial conditions from which to perform an ensemble of twin predictability experiments. Note that the predictability analysis described below was performed separately on N.H. winter MJO/ISO activity (i.e. that which typically travels eastward along the equator and SPCZ) and N.H. summer MJO/ISO activity (i.e. that which typically travels northeastward into Indian/S.E. Asia). The analysis framework below describes the N.H. winter study and any item in [parenthesis] describes the differences associated with the N.H. summer analog.

Initial conditions were taken from periods of strong MJO/ISO activity identified via extended empirical orthogonal function (EOF) analysis of 30-90 day bandpassed tropical rainfall during the Oct-Apr [May-Sep] season. From the above analysis, 15 cases were chosen when the MJO/ISO convection was located over the Indian Ocean, Maritime continent, western Pacific Ocean, and central Pacific Ocean [central Indian Ocean, N.E. Indian Ocean, S.E. Asia, and northwestern Tropical Pacific Ocean], respectively, making 60 cases in total. In addition, 15 cases were selected which exhibited very little to no MJO/ISO activity. Two different sets of small random perturbations were added to these 75 initial states. Simulations were then performed for 90 days from each of these 150 perturbed initial conditions. A measure of potential predictability was constructed based on a ratio of the signal associated with the MJO/ISO, in terms of bandpassed rainfall or 200 hPa velocity potential (VP200), and the mean square error between sets of twin

(bandpassed) forecasts. Predictability was considered useful if this ratio was greater than one, and thus if the mean square error was less than the signal associated with the MJO/ISO. The results (see Figure 1) indicate that useful predictability for this model's MJO/ISO extends out to about 20 to 30 days for VP200 and to about 10 to 15 days for rainfall. This is in contrast to the time scales of useful predictability for persistence, which for this model is about 12 days for VP200 and 7 days for rainfall. Note that the persistence forecasts gain additional skill from the bandpassing operation performed on the forecasts.

The predictability measure exhibited (not shown) modest dependence on the phase of the MJO/ISO, with greater predictability for the convective phase at short (< ~5 days) lead times and for the suppressed phase at longer (> ~15 days) lead times. In addition to the dependence on the convective phase of the MJO/ISO, the model's predictability also exhibits dependence on the strength of the MJO, particularly for the N. H. winter mode. During periods of weak MJO activity, the predictability associated with the region of strong MJO variability (i.e. Eastern Hemisphere) is diminished compared to periods of strong MJO activity. Effectively, the same predictability ratios are found at significantly shorter lead times (~ 5-10 day difference) for the null cases versus the active MJO events. This diminished predictability is a result of an error growth rate comparable to the strong MJO activity cases in combination with weaker intraseasonal signals. Mean square forecast errors were also computed for EOF amplitude time series of the bandpassed model output to highlight the fact that the enhanced predictability at extended range is derived mostly from the first 2 modes, i.e., those that capture the model's representation of the MJO/ISO.

The above results have important implications for both the local regions that the MJO/ISO rainfall variations impact directly as well as regions that are influenced by the MJO/ISO via teleconnections. Present day atmospheric forecasts are largely directed toward predicting short-term weather variations from analyzed initial conditions as well as seasonal climate variations associated with seasonal/interannual changes in surface boundary conditions, namely from tropical SSTs. As yet, operational weather forecasts have largely been unable to exploit the relatively strong signal and slow evolution associated with the MJO/ISO (e.g., Waliser et al. 1999a; Jones et al. 2000; Hendon et al. 2000). This is due to the generally poor representation of the MJO/ISO in most AGCMs, except for a few research-oriented models (e.g., Slingo et al. 1996). However, if the MJO/ISO could be better represented in operational weather forecast models, the above results imply that extended-range tropical forecasts in the regions directly impacted by the MJO/ISO could be greatly enhanced and/or extended. This includes a means to better predict the onset and break periods of the Asian-Australian summer monsoons that are so strongly determined by intraseasonal variations such as the MJO/ISO. In this regard, the improvement in forecast skill that might be possible with a model capable of simulating the MJO/ISO over one that poorly represents the MJO/ISO can be inferred from the enhanced predictability associated with the active versus null MJO cases discussed above (i.e. about 10 day improvement in lead time).

In addition to the local impacts that improved MJO/ISO prediction might offer, there are a number of remote processes whose prediction may improve as well. These were discussed in the introduction and include winter time mid-latitude circulation anomalies (e.g., Ferranti et al., 1992), summer time precipitation variability over Mexico and South America, extreme events in rainfall variability along the western United States, and the development of tropical storms/hurricanes in both the Atlantic and Pacific sectors.

There are a number of caveats that should be noted regarding the above results. For example, there are model shortcomings that suggest the above results might be an underestimate of predictability of

the MJO/ISO. First, the model tends to have too much high frequency, low wave-number activity (Slingo et al. 1996). Relative to the MJO/ISO, this variability would be considered to be un-organized, errant convective activity that may erode the relatively smooth evolution of the MJO/ISO and thus diminish its predictability. Second, these simulations were carried out with fixed climatological SST values. A previous study with this model showed that coupled SSTs tend to have an enhancing and organizing influence on the MJO/ISO, making it stronger and more coherent (Waliser et al. 1999b). Thus the exclusion of SST coupling may lead to an underestimate of the predictability as well. The third aspect that may lead to an underestimate the predictability is the fact that the model contains too little variability over the western Indian Ocean and southern Maritime continent region. The weakened MJO/ISO rainfall variations over this region may lead to a reduced predictability due to the model's relatively weak convection passing through this region, a region that exhibits a relatively robust convective signal in the observations.

A number of aspects associated with the model and/or analysis suggest that the above results might over estimate the predictability of the MJO/ISO. The first is that the model's coarse resolution and inherent reduced degrees of freedom relative to the true atmosphere may limit the amount of small-scale variability that would typically erode large time and space scale variability. However, it is important to note in this regard that the low order EOFs of intraseasonally filtered model output typically do not capture as much variability as analogous EOFs of observed quantities. Thus the model's MJO/ISO itself still has room to be more robust and coherent which would tend to enhance predictability. In addition to model shortcomings, the simple manner that perturbations were added to the initial conditions may also lead to an overestimate of the predictability. The perturbation structure and the size of the perturbations may be too conservative and not adequately represent the type of initial condition error that would be found in an operational context. However, even if that is the case, it would seem that adequate size "initial" errors would occur in the forecast in a matter of a day or two and thus one would expect this aspect to overestimate the predictability by only a couple days, if at all. Future studies will examine the sensitivity of these results to the AGCM used, to SST coupling, mid-latitude variability, and El Nino state, as well as examine how sensitive these results are to the initial condition perturbations and definition of predictability.

References

Cane, M., and S. E. Zebiak, and S. C. Dolan, 1986: Experimental forecasts of El Niño. Nature, 321, 827–832.

Chen, T.-C., and J. C. Alpert, 1990: Systematic errors in the annual and intraseasonal variations of the planetary-scale divergent circulation in NMC medium-range forecasts. J. Atmos. Sci., 118, 2607-2623.

Ferranti, L., T.N. Palmer, F. Molteni, and K. Klinker, 1990: Tropical -extratropical interaction associated with the 30-6- day oscillation and its impact on medium and extended range prediction. J. Atmos. Sci., 47, 2177-2199.

Hendon, H. H., and B. Liebmann, 1990: The intraseasonal (30-50 day) oscillation of the Australian summer monsoon. J. Atmos. Sci., 47, 2909-2923.

Hendon, H.H., B. Liebmann, M. Newman, J.D. Glick, and J. Schemm, 2000: Medium range forecast errors associated with active episodes of the Madden-Julian oscillation. Mon. Wea. Rev., 128, 69–86.

Higgins, R. W., and K. C. Mo, 1997: Persistent North Pacific circulation anomalies and the tropical intraseasonal oscillation. J. Clim., 10, 224-244.

Higgins, R. W., J. K. Schemm, W. Shi and A. Leetmaa, 2000: Extreme precipitation events in the western United States related to tropical forcing. J. Climate, 13. 793-820.

Higgins, R.W., and W. Shi, 2001: Intercomparison of the principal modes of intraseasonal and interannual variability of the N. American monsoon system. J. Climate. In Press.
Jones, C., 2000: Occurrence of extreme precipitation events in California and relationships with the Madden-Julian Oscillation. J. Climate, 13, 3576-3587.
Jones, C., D. E. Waliser, J. K. Schemm, and W. K. Lau, 2000: Prediction skill of the Madden-Julian Oscillation in Dynamical Extended Range Forecasts. Clim. Dyn., 16, 273-289.
Jones, C., and J-K. E. Schemm, 2000: The influence of intraseasonal variations on medium-range weather forecasts over South America. Mon. Wea. Rev. 128, 486-494.
Kessler, W. S. and R. Kleeman, 2000: Rectification of the Madden-Julian Oscillation into the ENSO cycle. J.Climate, 13, 3560-3575.
Lau, K.M. and P. H. Chan, 1988: Interannual and intraseasonal variations of tropical convection: A possible link between the 40-50 day oscillation and ENSO? J.Atmos. Sci., 44, 506-521.
Lau, K. M. and F. C. Chang, 1992: Tropical intraseasonal oscillation and its prediction by the NMC operational model. J. Climate, 5, 1365-1378.
Lo, F., and H. H. Hendon, 2000: Empirical Prediction of the Madden-Julian Oscillation. Mon. Wea. Rev., 128, 2528-2543..
Lorenz, E. N., 1965: A study of the predictability of a 28-variable atmospheric model. Tellus, 17, 321–333.
Madden, R.A and P.R. Julian, 1971: Dection of a 40-50 day oscillation in the zonal wind in the tropical pacific. J.Atmos.Sci., 28, 702-708.
Madden, R.A and P.R. Julian, 1994: Observation of the 40-50 day tropical oscillation--A review. Mon.Wea.Rev., 12, 814-837.
Maloney E.D., Hartmann D.L., 2000: Modulation of eastern North Pacific hurricanes by the Madden-Julian oscillation. J. Climate, 13: (9) 1451-1460.
McPhaden , M. J., and B. A. Taft, 1988: Dynamics of seasonal and intraseasonal variability in the eastern equatorial Pacific. J. Phys. Oceanogr., 18, 1713-1732.
Mo, K, C., R. W. Higgins, 1998a: Tropical Convection and Precipitation Regimes in the Western United States. Journal of Climate: Vol. 11, No. 9, pp. 2404–2423.
Mo, K. C., and R. W. Higgins, 1998b: The Pacific–South American Modes and Tropical Convection during the Southern Hemisphere Winter. Mon. Wea. Rev. 126, 1581–1596.
Mo, K. C.,2000: Intraseasonal Modulation of Summer Precipitation over North America. Monthly Weather Review: Vol. 128, pp. 1490–1505.
Mo, K. C., 2001: Adaptive Filtering and Prediction of Intraseasonal Oscillations. Monthly Wea. Rev. In Press.
Paegle, J. N., L. A. Byerle, K. C. Mo, 2000: Intraseasonal Modulation of South American Summer Precipitation. Monthly Weather Review: Vol. 128, No. 3, pp. 837–850.
Palmer, T.N., 1993: Extended-Range Atmospheric Prediction and the Lorenz Model. Bull. Am. Meteor. Soc., 74, 49–66.
Shukla, J. 1985: Predictability, Adv. Geophys., 28B, 87-122.
Slingo, J. M., K. R. Sperber, J. S. Boyle, et al., 1996: Intraseasonal oscillations in 15 atmospheric general circulation models: results from an AMIP diagnostic subproject. Climate Dynamics, 12, 325-357.
Sperber K.R, J.M. Slingo, P. M. Inness, and K-M Lau, 1996: On the maintenance and initiation of the intraseasonal oscillation in the NCEP/NCAR reanalysis and the GLA and UKMO AMIP simulations. Clim. Dyn., 13, 769-795.
van den Dool, H. M., 1994: Long-range weather forecasts through numerical and empirical methods. Dyn. Atmos. Oceans, 20, 247-270.

Waliser, D. E., C. Jones, J. K. Schemm and N. E. Graham, 1999a: A Statistical Extended-Range Tropical Forecast Model Based on the Slow Evolution of the Madden-Julian Oscillation. J. Climate, 12, 1918-1939.

Waliser, D.E, K.M. Lau and J-H Kim, 1999b: The influence of coupled sea surface temperatures on the Madden-Julian Oscillation: A model perturbation experiment. J. Atmos. Sci. 56, 333-358.

Waliser, D. E., K. M. Lau, W. Stern, C. Jones, 2001: Potential Predictability of the Madden-Julian Oscillation, Bull. Amer. Meteor. Soc., Submitted.

Waliser, D. E., W. Stern, S. Schubert, K. M. Lau, 2002: Dynamic Predictability of Intraseasonal Variability Associated with the Asian Summer Monsoon, Quart. J. Royal Meteor. Soc., Submitted.

Weickmann, K. M., G. R. Lussky, and J. E. Kutzbach, 1985: Intraseasonal (30-60 day) fluctuations of outgoing longwave radiation and 250 mb stream function during northern winter. Mon. Wea. Rev., 113, 941-961.

Weickmann, K., M., 1991: El Nino/Southern oscillation and Maddern-julian (30-60 day) oscillations during 1981-1982. J. Geophys. Res., 96, 3187-3195.

Wheeler, M. and K. Weickmann, 2001: Real-time monitoring and prediction of modes of coherent synoptic to intraseasonal tropical variability. Mon. Wea. Rev., 129, 2677-2694.

Yasunari, T., 1980: A quasi-stationary appearance of the 30-40 day period in the cloudiness fluctuations during the summer monsoon over India. J. Met. Soc. Japan., 59, 336-354.

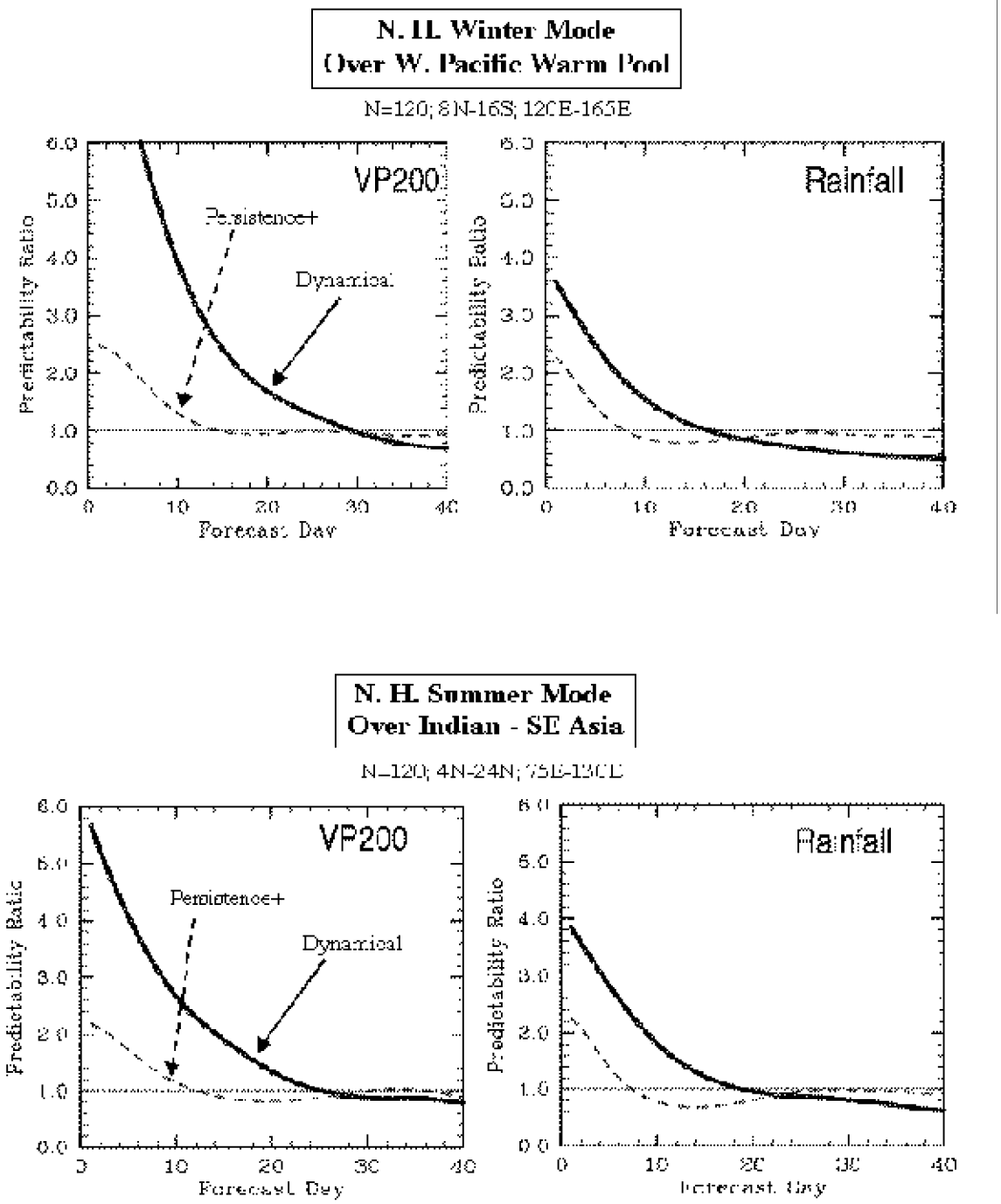

Figure 1. (top) Predictability ratio for N.H. winter mode VP200 (left) and rainfall (right) from the dynamical (solid) and persistence+ (dotted; see text for details) forecasts for the region 8N-16S and 120-165E. (bottom) The same but for the N.H. summer mode and for the region 4-24N and 75-130E.

The MJO-ENSO Relationship: A re-assessment

William K. M. Lau and K. M. Kim
Climate and Radiation Branch, Laboratory for Atmospheres
NASA/Goddard Space Flight Center
Greenbelt, MD 20771

1. Introduction

Noting the similarities among the spatial patterns of outgoing longwave radiation among MJO and ENSO, Lau and Chan (1987, 1988) speculated a possible relationship between the two phenomena. This speculation received a substantial boost in credibility after the 1997-98 El Nino, when MJO activities were found to be substantially enhanced prior to the onset of the warm phase, and clear signals of oceanic Kelvin waves forced by MJO induced anomalous surface wind were detected as possible triggers of ENSO (McPhaden 1999, McPhaden and Yu 1999). Yet statistical and modeling studies have so far yielded either nil or at best, very weak relationship between MJO activities and SST (Hendon et al. 1999, Fink and Speth 1997, and Slingo et al. 1999). Recently Kessler (2001) suggested using an MJO index which includes convective variability in the equatorial central Pacific lead to a more robust MJO-ENSO relationship. Clearly, while MJO might have been instrumental in triggering some El Nino, there are other events that can occur without any MJO trigger.

A possible reason for the above conundrum is that MJO-ENSO relationship, if exists, is likely to be strongly nonlinear, and therefore will not have a one-to-one correspondence in individual cases. Even within the 20-70 or 20-90 day windows commonly used by most investigators to capture the MJO, there are possibly different modes of variability that may act as trigger, or merely response to, or simply independent of ENSO SST variability. Many previous studies of MJO-ENSO relationship focused on MJO in one particular season, particular boreal winter or summer. Yet, MJO wind forcings on the ocean are likely to be continuously modulated throughout the year. Indeed, oceanic Kelvin waves forced by MJO are likely to be found along the equatorial waveguides, when the forcing is symmetric with respect to the equator, i.e. during the spring and fall, and not during boreal winter or summer when the center of MJO activities are away from the equator. Furthermore, although MJO has dominant signals in the tropics, it also has strong extratropical expressions, suggesting interaction between tropics and the extratropics. Hence identifying the full spectrum of variability associated with MJO, including seasonality, tropical and extratropical variabilities , and separating modes of intraseasonal variability with respect to SST forcings are essential in understanding MJO-ENSO relationship.

In this paper, we re-assess the MJO-ENSO relationship, by identifying dominant space-time modes of intreaseasonal variability and their possible separate roles in triggering or respond to ENSO. Using 50 years of NCEP wind reanalysis, we have computed the space-time extended empirical orthogonal functions (EEOF) of 20-70 filtered 850 mb streamfunctions to identify dominant modes of intraseasonal variability all year round. The first EEOF mode describes an eastward, circum-propagating planetary pattern identified as the "classical" MJO. The second

mode depicts the quasi-stationary component of the MJO, associated with wave signals emanating from the Indo- Pacific region along the subtropical jetstreams. Two indices of MJO activities have been constructed based on the 90-day windowed variances of the principal components of these two modes. The MJO activities show strong seasonality, with the eastward propagating mode (EPM) and the standing mode (SM) having its peak activity in the boreal spring, and winter respectively (not shown).

2. Results

Figure 1 shows a composite of the EPM with respect to Nino –3 SST variation. Enhanced EPM (PC 1+2) activity is found during the cold-to-warm transition of El Nino. Immediately after entering into the warm phase of El Nino, EPM activity is drastically reduced.,and remains suppressed throughout the entire warm phase. This suggests that the EPM may be instrumental in triggering or promoting the onset of El Nino. Yet, as a response to the spreading out of the warm water, the global eastward propagation of the MJO is stalled in favor of the development of the stationary component. As seen in the lower panel, SM activity appears to evolve coherently with the Nino-3, with a delayed response of about 3 to 6 months.

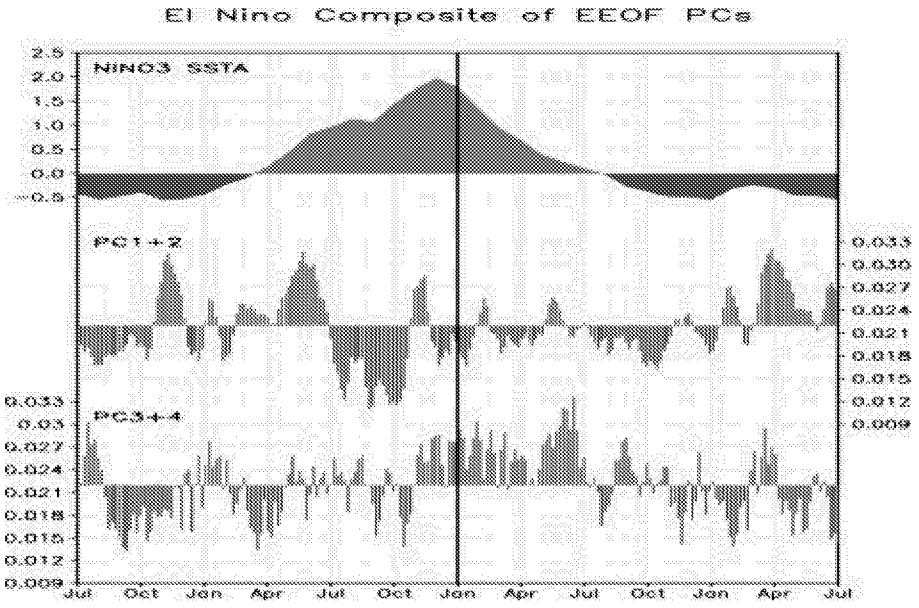

Figure 1 Composite as a function of calendar months for a) Nino-3 SST (°C) , b) PC1 +2 and c) PC3+4. The PCs are in relative units

The possible triggering of EL Nino by the EPM can be seen in the lagged time-longitude cross sections of EPM index with respect to monthly 850mb zonal wind and SST along the equator, shown in Figs. 2 a and b. Before enhanced EPM activity, the evolution patterns are quite disorganized. However, simultaneous with and immediately following EPM activity, there are clearly eastward propagating wind signals from the Indian Ocean to the eastern Pacific (Fig.2a), accompanied by coherent SST signals over the eastern Pacific (Fig.2b). Note that the

dominant time scale is quasi-biennial and not ENSO. In contrast, similar time lagged cross-sections of SM (Figs.3 a and b) depict a space-time pattern characteristics of El Nino and with a dominant time scale of 3.5 to 4 years. Also clear is that the enhanced SM activity lagged the warm SST by about 3 months- further evidence that it may be a response to El Nino.

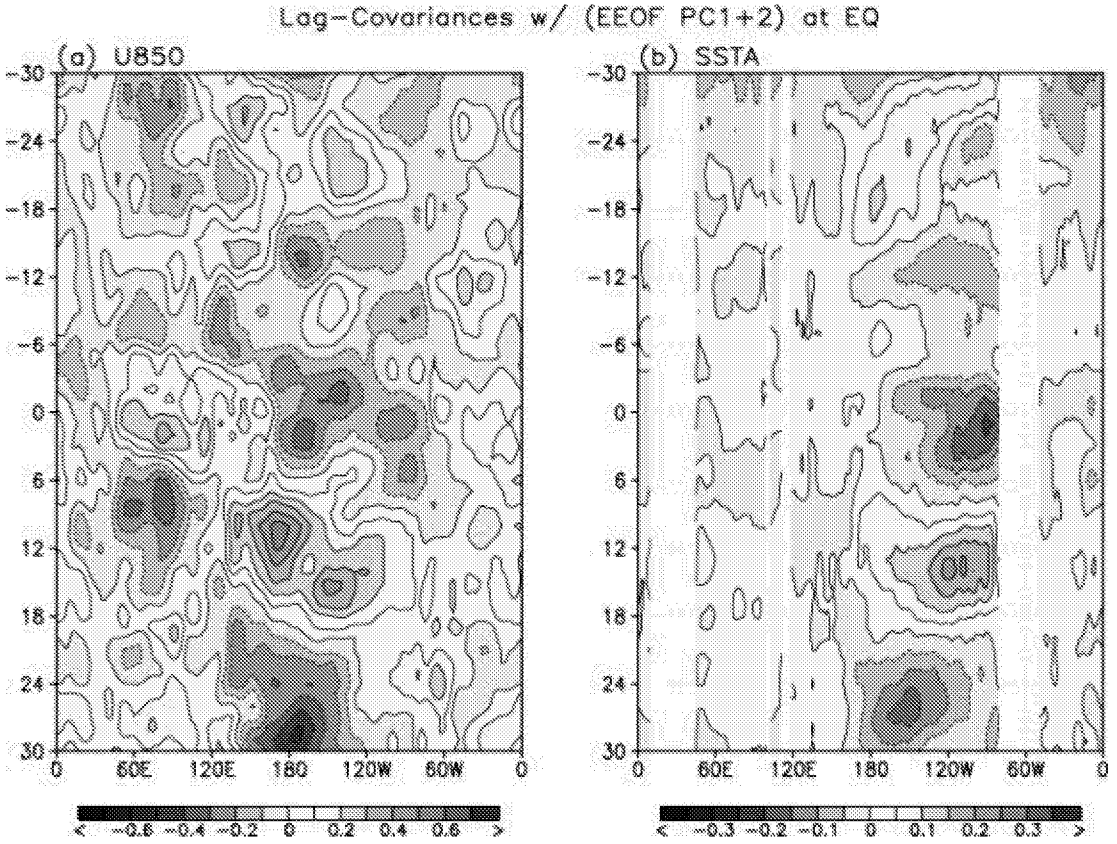

Figure 2 Lagged-time-longitude corrvariance of EPM with respect to a) 850 mb zonal wind, and b) SST , along the equator. Units are in m/s and °C per 1-? changes in the PC.

3. Conclusion

Our results show that the EPM component of the MJO, by virtue of its enhanced activity during boreal spring may be instrumental in exciting a warm event. When the naturally occurring El Nino is properly phased with enhanced EPM activity in boreal and summer, a rapidly warming phase, following by a rapidly cooling phase may occur. Recently Kim and Lau (2001) has suggested a combination of winter and summer monsoon anomalous surface wind forcings in the equatorial western Pacific may induce a biennial tendency in the ENSO cycle. The present results suggest such biennial tendency in ENSO may be effected through the seasonal modulation of the MJO.

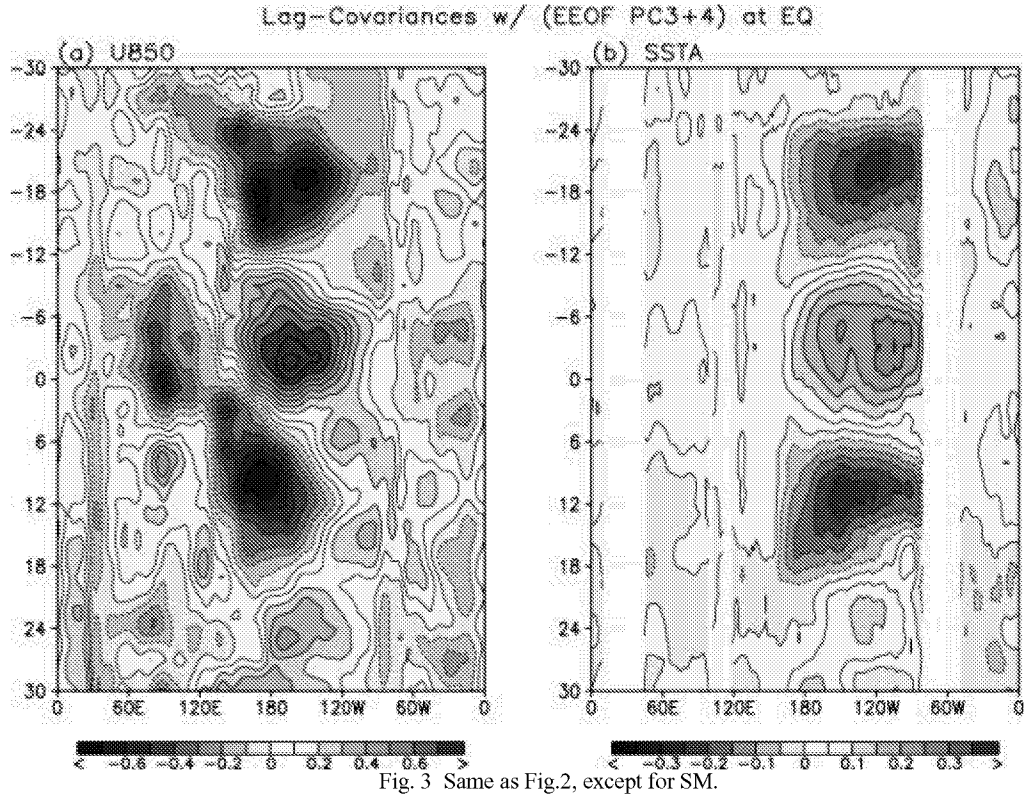

Fig. 3 Same as Fig.2, except for SM.

Reference

Kim, K. M., and K. M. Lau, 2000: Dynamics of monsoon-induced biennial variability in ENSO. *Geophys. Res. Letters* , 28, 315-318.

Lau, K. M. and P. H. Chan, 1986: The 40-50 day oscillation and the El Nino/Southern Oscillation: a new perspective. Bull. Amer. Meteor. Soc., 67, 533-534.

Lau, K. M. and P. H. Chan, 1988: Intraseasonal and interannual variability of tropical convection: a possible link between the 40-50 day oscillation and ENSO. *J. Atmos. Sci.*, **45**, 506-521

Weickmann, K. M., 1991: El Nino/Southern Oscillation and the Madden and Julian (30-60 day) oscillations during 1981-82. *J. Geophys. Res.*, **96**, 3187-3195.

McPhaden, M. J., 1999: Climate oscillations – Genesis and evolution of the 1997-98 El Nino. *Science* **283**, 950-940.

McPhaden, M. J., and X. Yu, 1999: Equatorial waves and the 1997-98 El Nino. *Geophys. Res. Lett.*, **26**, 2961-2964.

Kessler, W. S., 2001: EOF representations of the Madden-Julian Oscillation and its connection with ENSO. *J. Climate*, **14**, 3055-3061

Slingo J.M., Rowell D. P., Sperber K. R., 1999: On the predictability of the interannual behaviour of the Madden-Julian Oscillation and its relationship with El Nino, Q J Roy Meteor Soc 125: (554) 583-609.

Hendon, H. H., C. Zhang, J. D. Glick, 1999: Interannual Variation of the Madden–Julian Oscillation during Austral Summer. Journal of Climate: Vol. 12, No. 8, pp. 2538–2550.

Recent Failures of Monsoon-ENSO Relationships Viewed From Coupled Model Results

Arun Chakraborty and T. N. Krishnamurti
Department of Meteorology
Florida State University
Tallahassee, Florida 32306-4520

We are in the course of preparing data sets for a multimodel ensemble of seasonal forecasts. These are based on eight versions of the FSU global coupled model following LaRow and Krishnamurti (1998, Tellus). In addition to those we have prepared parallel data sets for as many as four external non-FSU global coupled model runs. Although the entire array covering several decades of seasonal forecasts experiments are not yet completed, some preliminary results from several single model runs were possible at this stage. One of the questions we address here is on the recently reported failures of the ENSO – Monsoon relationship. Prior to 1995 there was the general feeling that El-Niño years were to be treated as deficient in Indian monsoon rainfall with the converse being the case for the La-Niña years. Recent papers by several authors observed the failure of this relationship since roughly 1995. Our study examines the coupled model results on the relationship of ENSO index and the all India summer monsoon rainfall (AISMR). We find that the model output does confirm a breakdown of this relationship. In the course of further diagnosis of this relationship, we noted a prominent feature that prevailed prior to 1995 that was absent in the subsequent years. The model output showed that the amplification of the MJO signals in the zonal winds at 850hPa levels and of the ENSO signals were both large during years of above normal AISMR. During years of deficient AISMR the MJO signal amplitudes were small. The differences in the amplitudes of ENSO and MJO signals were inversely related to the AISMR. Even that relationship broke down after 1995. Since the complete global coupled model output is available at intervals of every week we feel that this data sets provides an opportunity for the examination of other non-conventional parameters that might provide a clue to the behavior of the breakdown of these relationships and to search for other possible candidates. These results will be presented at the workshop on subseasonal climate prediction.

Variability of Tropical Intraseasonal Convective Anomalies and Their Statistical Forecast Skill

Charles Jones, Leila M. V. Carvalho, Wayne Higgins, Duane Waliser and Jae-K. E. Schemm
Institute for Computational Earth System Science (ICESS)
University of California
Santa Barbara, CA 93106-3060

The tropical atmosphere exhibits significant amounts of variance on time scales of 20-90 days. In particular, the Madden-Julian Oscillation (MJO) is the main mode of tropical intraseasonal variation with significant influences on the Asian-Australian Monsoons, Indo-Pacific thermocline variability and mid-latitude teleconnections. Previous works have shown that tropical intraseasonal convective anomalies (TICA) display different modes of eastward propagation, seasonal and interannual occurrences.

This study examines the characteristics of eastward propagating TICA events. An objective-tracking algorithm is applied to 22 years of Outgoing Longwave Radiation (OLR) data to characterize their propagation, life cycle, zonal displacement and structural properties (minimum OLR anomaly, variance of OLR anomaly, area, number of cold clusters, rate of growth and decay). The zonal wind (U) components at 850 hPa and 200 hPa from 22 years of NCEP/NCAR reanalysis are used to describe the large-scale circulation associated with TICA events. Four main TICA types are recognized depending on their eastward propagation and region of most significant influence (Indian Ocean, India/China Sea, SPCZ and Pacific Ocean). A statistical analysis is carried out to determine if differences in structural properties of convective anomalies are also associated with different TICA types. Probability curves are then constructed to determine the likelihood of TICA occurrences according to their zonal displacement and frequency per season. In the last part of this work, a combined (CEOF) analysis of OLR, U850, and U200 is performed to build a statistical forecast model based on multiple linear regressions using the first two leading EOF modes. The statistical forecast skills of different TICA types are analyzed and their implications for midlatitude teleconnections are discussed.

An All-Season Real-time Multivariate MJO Index: Development of the index for monitoring and prediction in Australia

Matthew C. Wheeler and Harry H. Hendon
Climate Forecasting Group
Bureau of Meteorology Research Centre
P.O. Box 1289K
Melbourne, Victoria 3001
m.wheeler@bom.gov.au & h.hendon@bom.gov.au

1. Introduction

As part of an ongoing research project at the Australian Bureau of Meteorology on the use of the Madden-Julian Oscillation (MJO) for forecasting on the intraseasonal time scale, we have developed an index for the MJO based on the first two Empirical Orthogonal Functions (EOFs) of the combined fields of near-equatorial 850 hPa zonal wind, 200 hPa zonal wind, and satellite-observed outgoing longwave radiation (OLR). Projection of the daily observed data onto such multivariate EOFs, with the annual cycle and El Nino variability removed, yields principal component (PC) time series that vary mostly on the intraseasonal time scale of the MJO only. That is, the projection of daily data onto the two EOFs is a very effective filter for the MJO, without the need for time filtering, and thus an effective index for real-time use. In this way, it is thought to be an improvement over the method that is currently performed daily at the Bureau, of Wheeler and Weickmann (2001). This paper explores the properties of the index along with its relationship to other important weather and climate parameters. Prediction of the index will follow in later work and publications.

2. Data and Analysis

Perform EOF analysis on the daily fields of equatorially-averaged (10°S to 10°N) OLR, 850 hPa zonal wind, and 200 hPa zonal wind for the period of 1979 to 2001 (23 years). EOF analysis is of the covariance matrix. For the combined (multivariate, i.e. OLR and winds) analysis, each field is normalized by its global variance first. Before the EOF analysis, however, we do the following: Remove the mean and annual cycle (3 harmonics) from each field at each grid-point. Remove the variability associated with El Nino (that which is linearly related an ENSO SST index). Remove a 120-day mean of the most recent 120 days at each point. All of these steps can be performed in real-time. Figure 1 presents the first two EOFs, which we feel capture the variability of the MJO well.

3. Initial Results

We call the two PC time series that form the index the Real-time Multivariate MJO series 1 (RMM1), and RMM2. For the 1979 to 2001 period, for all seasons, RMM1 and RMM2 respectively have 58 and 61% of their total variance occurring for the 30- to 80-day time scale (Fig. 1), and their cross-spectrum reveals a coherence-squared value of ~0.8 on this time scale with RMM1 leading RMM2 by a quarter cycle. In the two-dimensional phase-space defined by the vector M = (RMM1,RMM2) (Fig. 2), the MJO thus manifests itself as an anti-clockwise rotation with time, while times of little or no MJO activity are represented by seemingly random movement of the vector M near the origin.

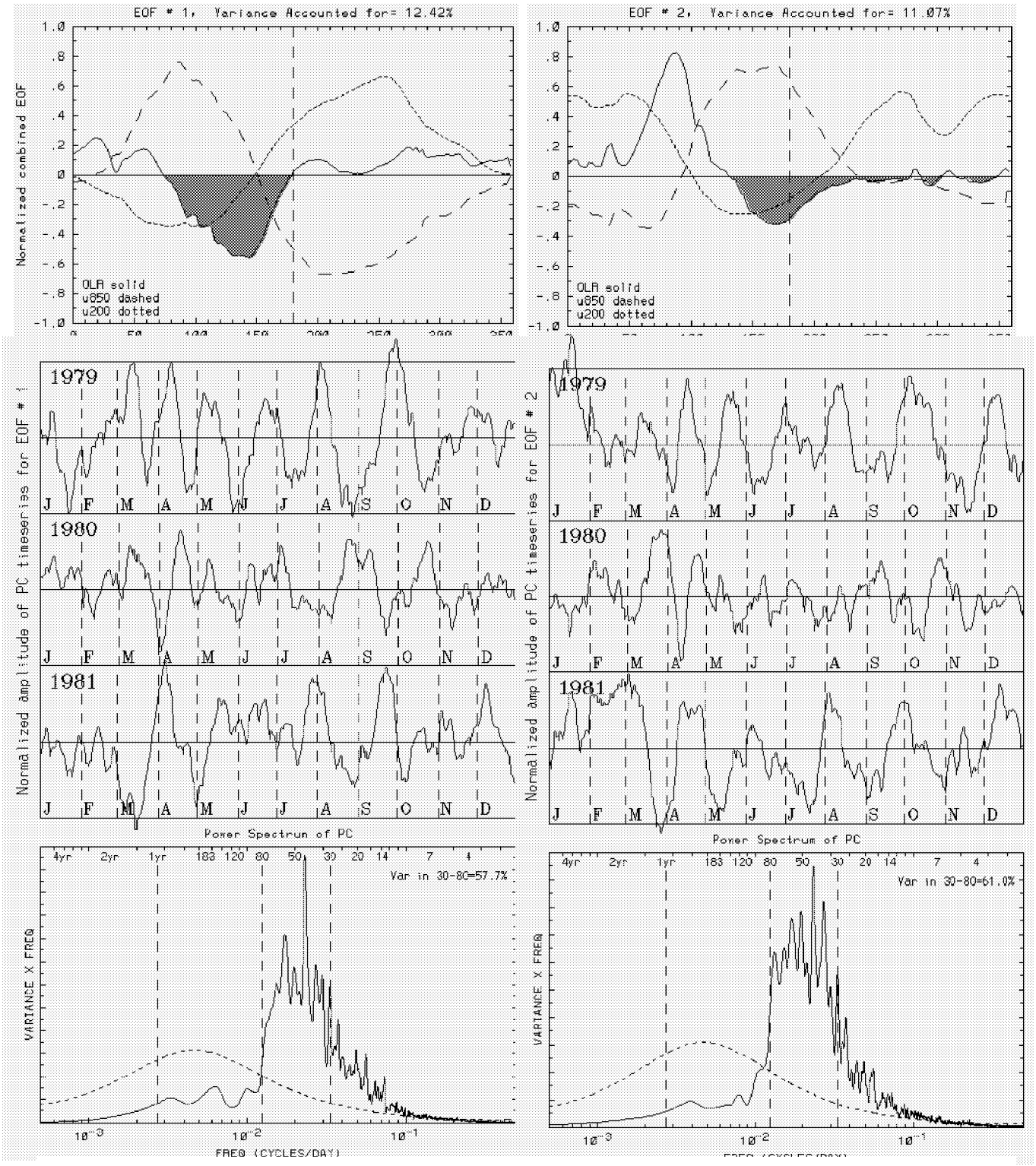

Figure 1: Spatial structure, example time series, and spectra of those time series, for the first two empirical orthogonal functions of the combined fields of OLR, 850 hPa zonal wind, and 200 hPa zonal wind. We call the principal component timeseries resulting from the projection of the daily data onto these EOFs RMM1 and RMM2.

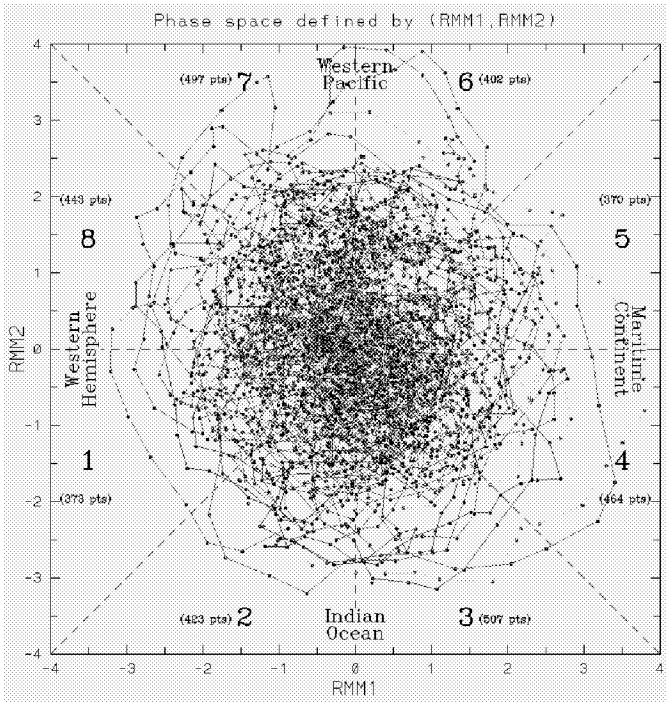

Figure 2: The phase space representation of the RMM1 and RMM2 indices for the southern summer months of December, January, February, March, and April for the full 23 years of data. When the MJO is active the (RMM1,RMM2) vector describes large anti-clockwise circles.

This phase-space representation of the two RMM series is one of a number of ways to use the index for the purpose of producing composites and forming relationships with other climate or weather indicators.

a. Composites

Given that the RMM series are computed using the near-equatorial (10°S to 10°N average) OLR and winds for any season, one aspect that is important to demonstrate is whether they can capture the known varied structure and influence of the MJO from season to season. Composites of total OLR and wind fields for eight defined phases of the MJO for the different seasons show that indeed they do capture such seasonal changes. The strongest direct influence of the MJO on the OLR field (and presumably rainfall) is strongest over Australia in southern summer, but it is mostly confined north of about 20°S. There is no discernible influence over the Australian continent in northern summer, but in autumn, there is some indication of an influence through northwest cloudbands stretching to western Australia from the Indian Ocean.

b. Relationship with the onset of the Australian monsoon at Darwin

Relationships with a completely independent indicator of the onset and retreat of the Australian monsoon can also be demonstrated. Figure 3 shows the location of the (RMM1,RMM2) vector in its phase space when the monsoon was defined to onset at Darwin by a measure defined by Drosdowsky (1996). This measure is determined by the radio-sonde westerly winds at Darwin only, and is thus a very strict point measurement of the monsoon, that is, not a large-scale indicator like the MJO. Yet we see in Fig. 3 that the monsoon for the last 23 years has only onset at times when the MJO is in only about half of its 8 defined phases. The monsoon at Darwin rarely "onsets" when the convection of the MJO is over the

Indian Ocean or the Western hemisphere. Such a relationship is instructive for the potential use of the MJO and the RMM series for prediction.

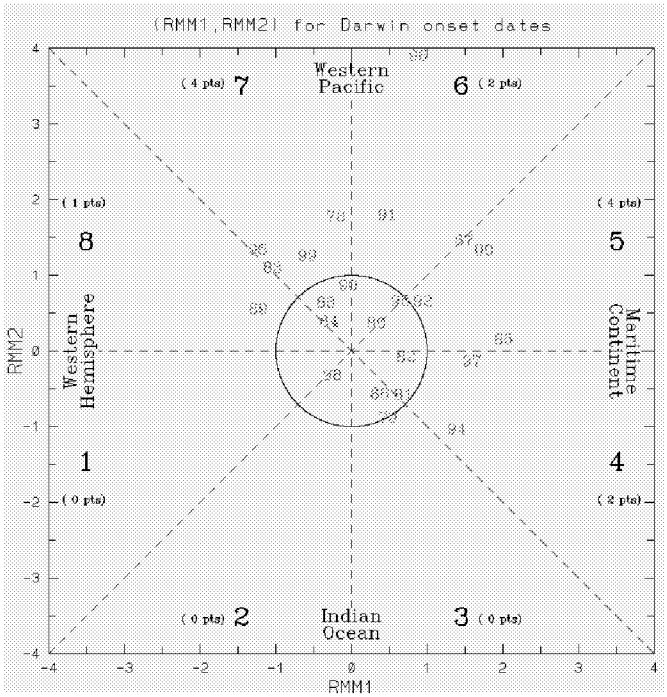

Figure 3: The location of the (RMM1,RMM2) vector each year when the monsoon is determined to onset at Darwin. Each point is labeled according to the year of the December of the monsoon season. For example, the point indicating the position for the 1978/1979 monsoon onset is labeled as "78".

c. Prediction of the RMM1 and RMM2 series

Prediction of the RMM series, and thus prediction of the MJO, is work to be described in future publications. One method of prediction is along the lines of the work of Lo and Hendon (2000), an empirical technique utilizing multiple step-wise lag regression. Predictions from numerical models could also be projected onto the same EOFs to obtain the RMM series.

References

Drosdowsky, W., 1996: Variability of the Australian Summer Monsoon at Darwin: 1957-1992. *J. Climate*, **9**, 85-96.

Lo, F. and H. H. Hendon, 2000: Empirical extended-range prediction of the Madden-Julian Oscillation. *Mon. Wea. Rev.*, **128**, 2528-2543.

Wheeler, M. and K. M. Weickmann, 2001: Real-time monitoring and prediction of modes of coherent synoptic to intraseasonal tropical variability. *Mon. Wea. Rev.*, **129**, 2677-2694.

Evidence of an Intrinsic Intraseasonal Oscillation over Tropical South America during Austral Summer

Jiayu Zhou[1?] and William K.-M. Lau[2]

[1]Goddard Earth Sciences and Technology Center, UMBC, Baltimore, MD 21250

[2]Climate and Radiation Branch, Laboratory for Atmospheres, *NASA/GSFC,* Greenbelt, MD 20771

1. Introduction

The intraseasonal variation (ISV) in the 30-60 day band, also known as Madden-Julian oscillation (MJO), has been studied for decades. Madden and Julian (1971, 1972, 1994) showed that the oscillation originated from the western Indian Ocean, propagated eastward, got enhanced over the maritime continent and weakened after passing over the dateline. Composite studies showed evidences of a signal in upper and lower level zonal wind propagating around the globe during an oscillation (Knutson and Weickmann 1987). Theoretical studies pointed out that the interaction with the warm ocean surface and the coupling with the convective and radiative processes in the atmosphere could manifest the oscillation, which propagates eastward via mutual feedbacks between the wave motions and the cumulus heating (Chang 1977; Yamagata and Hayashi 1984; Lau and Peng 1987; Salby and Garcia 1987; Wang 1988; Hu and Randall 1994).

Over tropical South America, no independent 30-60 day oscillation has been reported so far, despite that Amazon is the most distinct tropical convection center over the western hemisphere and the fluxes from its surface of tropical rainforests are close to that from the warm tropical ocean. Liebmann *et al.* (1999) showed a distinct spectral peak of 40-50 day oscillation in outgoing longwave radiation (OLR) over tropical South America and considered that was manifested by the MJO propagation. Nogues-Paegle *et al.* (2000) focused on a dipole pattern of the OLR anomaly with centers of action over the South Atlantic Convergence Zone (SACZ) and the subtropical plain. They used the regional 10-90 day filtered data and demonstrated this pattern could be represented by the fifth mode of the rotated empirical orthogonal function. Its principal component was further analyzed using the singular spectrum analysis. Their result showed two oscillatory modes with periods of 36-40 days and 22-28 days, of which the former was related to the MJO influence and the latter linked to the remote forcing over southwest of Australia, which produced a wave train propagating southeastward, rounding the southern tip of South America and returning back toward the northeast. The 22-28 day mode has distinct impact on SACZ, responsible for the regional seesaw pattern of alternating dry and wet conditions.

In this study we will focus on the 30-60-day spectral band and investigate whether the independent oscillation source over tropical South America is existed. First, we will show the seasonal dependence of the tropical South American ISV in Section 3. Then, the leading principal modes of 30-60 day bandpass filtered 850-hPa velocity potential (VP850) will be computed to distinguish the stationary ISV over tropical South America (SISA) from the propagating MJO in the austral summertime in Section 4. The importance of SISA in representing the regional ISV over South America will be discussed. In Section 5, we will demonstrate the mass oscillation regime of SISA, which is well separated from that of MJO by the Andes, and the convective coupling with rainfall. The dynamical response of SISA and the impact on

[?] **Corresponding author address:** Dr. Jiayu Zhou, GEST, Code 913, NASA/GSFC, Greenbelt, MD20771.
E-mail: zhou@climate.gsfc.nasa.gov

the South American summer monsoon (SASM) will be presented in Section 6. Finally, we will give the concluding remarks.

2. Data

The data used in this study are the Goddard Earth Observing System of version one (GEOS-1) reanalysis (Schubert *et al.* 1993), the European Center for Medium Range Weather Forecast (ECMWF) reanalysis (Gibson *et al.* 1997), the National Oceanic and Atmospheric Administration / National Centers for Environmental Prediction (NOAA/NCEP) OLR (Janowiak *et al.* 1985), and CPC (Climate Prediction Center) Merged Analysis of Precipitation (CMAP) (Xie and Arkin 1997). To focus on the 30-60 day band, the Lanczos filter (Duchon 1979) was used, prior to which the pentad mean was constructed. A 9-grid spatial smoother was also applied to the CMAP rainfall data to remove small-scale features. The austral summer half-year is defined as from mid-October to the following mid-April.

3. Seasonal dependence of ISV over South America

The seasonal variations of precipitation, wind and temperature over South America have been addressed by many previous studies (Aceituno 1988, Horel *et al.* 1989, Kousky and Ropelewski 1997, among others). It is now recognized that these variations are organized by the South American monsoon system (Nogues-Paegles *et al.* 2002), which is forced by the summertime regional thermal infrastructure, responding to the annual cycle of solar heating in an interactive ocean-atmosphere-land entity and being characterized by the systematic rainfall migration and the reversal of seasonal perturbation wind in the tropical and subtropical regions. Zhou and Lau (1998) showed coherent convective 40-45 day oscillations over tropical-subtropical South America during 1989/90 summer monsoon season. These oscillations were related to pre-monsoon, monsoon onset and development, monsoon mature and withdrawal and post-monsoon phases.

From the wavelet analysis of OLR averaged over eastern tropical South America from November 1982 to November 1995, we can clearly see the annual cycle was enhanced during El Niño years and the submonthly and the 1-3 month time-scale ISV activated only in summer half years. Being dynamically consistent, the similar features can also be found in VP850 of both GEOS and ECMWF reanalyses. Over eastern tropical South America, the temporal correlation between the 30-60 day band-pass filtered ECMWF 850-hPa velocity potential and OLR in the summer half-year is about 0.67. The summer half-year composite of VP850 spectrum, averaged over eastern tropical South America, shows more significant spectral peak at 45-day period in GEOS reanalysis.

The geographic distributions of the 30-60 day band averaged VP850 spectral density, are composited for the summer and the winter half-year, respectively. Due to short record for each half-year span, the spectral analysis of maximum entropy method (MEM) is used to sharpen the spectral features. Overall, the composites show the oscillation in ECMWF reanalysis is weaker than that in GEOS reanalysis. The intensity of the former is about 80% of the latter. Both reanalyses show two centers, one zonally elongated over the maritime continent of the western Pacific, which is consistent with the illustration of MJO by Madden and Julian (1972), and the other extending northwest-southeastward over tropical South America in alignment with the monsoon migration. The intensity of the later is about 60% of the former. The semiannual composites show that the oscillation is much stronger in the summer half-year than in the winter half-year (almost a factor of 3/2 seen over tropical South America in both reanalyses). More realistically, the ECMWF reanalysis demonstrates a seasonal preferred location of the oscillation center, which follows the seasonal migration of the convective activities associated with American monsoons over Central-South America.

4. Identification of SISA

Looking for the intrinsic 30-60 day oscillation over tropical South America, we conducted a rotated empirical orthogonal function (REOF) analysis for the 30-60 day bandpass filtered VP850 in summer half-years. The Varimax rotation, which removes the spatial but keeps the temporal orthogonality, is applied to identify regionally confined patterns (Nigam and Shen 1993). The result shows the first and the second modes, which display a 90-degree phase shift in both space and time, represent the propagating MJO. The third mode, though explaining less variance than the leading two modes (7% in GEOS and 14% in ECMWF), concentrates its most variance over eastern tropical South America. This feature is even more prominent in the ECMWF reanalysis.

To demonstrate whether the oscillation represented by the third mode is independent of MJO, lag-correlations between the third rotated principal component (RPC) and the 30-60 day bandpass filtered global VP850 are computed for a complete oscillation cycle. The result evidently shows the standing characteristics of SISA, which forms locally and not related to the eastward propagating MJO.

The importance of this tropical South American mode is further demonstrated by the reconstruction of VP850 using the leading three REOF modes for summer half-years. We can see that over tropical South America the third mode together with MJO can almost mimic the total variability by both reanalyses. The role played by individual oscillating component is also checked. For example, during 1991/92 summer half-year, the reconstruction shows weak MJO influence and strong local oscillation over tropical South America from austral spring to early summer of 1991. Afterwards, the eastward propagating MJO becomes dominant but distinct disturbances of SISA can still be seen when waves of MJO passing over tropical South America.

5. Oscillation regime and convective coupling

In association with the oscillations of OLR and VP850, distinct mass fluctuations are also found. The summer half-year composite of MEM spectral density of sea level pressure (SLP) averaged over eastern tropical South America shows consistent three spectral peaks at the periods of 36-60 day, 20 day and 12 day. The correlations of SLP with the three leading RPCs of VP850 shows that the areas highly correlated with MJO (greater than 0.4) are confined to the Pacific and the Indian Ocean. The stationary ISV over South America has high correlation with SLP variability over the area from tropical South America to the west coast of tropical Africa. The two strong impact regimes of MJO and SISA are well separated by the Andes, which blocked the low-level influences from the Pacific side. East of the Andes, the 30-60 day mass variability is more closely related to SISA. This can be further demonstrated by computing one-grid correlations of 30-60 day bandpass filtered SLP with the base grid at eastern Brazil and western central Africa, respectively. From the result we can see a well-defined spatial regime extending from tropical South America east of the Andes to central Africa, which is consistent with the area highly correlated with SISA. It shows evidently that the 30-60 day oscillation over South America can be locally manifested and does not necessarily depend on MJO.

Being convectively coupled with the oscillation, the rainfall variability over eastern tropical South America shows the same spectral characteristics as that of SLP in the summer half-year. To distinguish the geographic impact of each 30-60 day ISV mode, we compute the regression of each RPC of VP850 with rainfall and compare the result with the corresponding natural mode of rainfall variations represented by the independent EOF. For the first and the second modes, large amplitudes are found over the Indian Ocean and the western Pacific, where MJO prevails, and the patterns between the regression and EOFs are highly correlated. Over tropical South America a moderate rainfall signal associated with MJO moves from western to eastern tropical South America. For the third mode, the regression shows a similar pattern with the rainfall EOF3 over tropical South America but less coherent over the western Pacific.

The importance of the third mode to the South American regional rainfall variability is further investigated by computing the percentage of the local variance explained by the regression with each mode. We find the impact of each mode has distinct geographic preference. It shows that the MJO has large impact over northeastern Brazil and the nearby Atlantic Intertropical Convergence Zone (ITCZ). While the impact of SISA is concentrated on central Brazil, which extends southeastward and influences the South Atlantic Convergence Zone (SACZ), and the area over 10°N of the western Atlantic. As we will see in the next section, these two preferred SISA impact areas are located along the path of the monsoon flow, indicating close relationship between SISA and SASM variations.

6. Dynamical response and impact on SASM

The dynamical responses of the leading three modes of 30-60 day ISV are illustrated by regressing each RPC of VP850 with streamfunction at 200 and 850 hPa, respectively. In the upper troposphere, the responses of the first and the second modes show a pattern similar to the illustration of Matthews (1993) and Sperber *et al.* (1997), who depicted twin anticyclones (cyclones) over west (east) of the convection accompany MJO propagating eastward. This pattern is vertically out of phase in the tropics and in phase poleward, and can be explained by the counteraction between the streamfunction tendencies induced by the horizontal advection of planetary vorticity and the divergence of planetary vorticity flux (Chen and Chen 1997). The impact of the propagation of this pattern on the tropical easterlies can be clearly seen over equatorial South America.

Consistent with the summertime heating over tropical South American continent, the response of the third RPC shows two anomalous cyclonic (anticyclonic) circulations, which are symmetric about the equator, at east (west) of tropical South America in the upper troposphere. A small anticyclonic cell can be seen over southern Peruvian highland, where intense heating is found during the summertime. In the lower level, a large anticyclonic disturbance is over northwestern Africa and a cyclonic perturbation along the South Atlantic convergence zone (SACZ). As a result, anomalous flows, denoted by streamlines, follow the SASM flow pattern, indicating a close relationship between SISA and the intraseasonal variation of SASM. Recently, Jones and Carvalho (2002) identified two flow regimes in 10-70 day time-scale in association with SASM active and break phases, according to the phase of the low-level zonal flow over Rondonia State of Brazil. They showed that during the monsoon active phase, the anomalous flow traveled along the tropical north Atlantic, crossed the equator over the east of the Andes, ran toward Southeast Brazil and closed in a cyclonic anomalous circulation off the coast of Argentina and Uruguay. During the break phase, the flow reversed completely. By making composites of 850-hPa wind and OLR for two SISA extreme phases, of which the VP850 RPC3 amplitudes exceed 1.2 standard deviation, we find the anomalous low-level flow of SISA swings between the active and break monsoon flow regimes. The OLR anomaly, extending northwest-southeastward over tropical South America, flips the phase in association with the anomalous monsoon flow convergence. Evidently, the variation of SISA is related to the break and revival of SASM.

7. Concluding remarks

Using GEOS-1 and ECMWF reanalyses, NCEP OLR and CMAP rainfall data we have investigated the ISV source over tropical South America during austral summer half-year. Rotated EOF analysis of 30-60 day bandpass filtered VP850 reveals that the first two leading modes are closely related to MJO. The third mode, SISA, which shows standing oscillation characteristics and accounts for a large portion of ISV over tropical South America, suggests a local forcing mechanism. The total 30-60 day variability of VP850 over tropical South America can be reconstructed by the three leading REOF modes. Further investigation reveals a well-defined oscillation regime of SISA, which is separated from that of MJO by the Andes, extending from tropical-subtropical South America east of the Andes to central Africa. The dynamical impact of SISA on the upper tropospheric rotational flow shows a typical wave pattern of symmetric

variations in streamfunction, *i.e.*, a leading pair of cyclones and a trailing pair of anticyclones in association with localized heat sources and sinks. The impact of SISA on the regional climate shows a close relationship with SASM break and revival. Our results suggest that in the austral summer half-year the tropical South American region possesses a source of ISV that is distinct from that due to the MJO.

Acknowledgments. This research is supported by the Earth Observing System / Interdisciplinary Science investigation on hydrological processes and climate, and the Global Modeling and Analysis Program of NASA, Mission to Planet Earth Office.

Dynamical Seasonal Predictability of the Asian Summer Monsoon

K. R. Sperber, C. Brankovic, M. Deque, C. S. Frederiksen, R. Graham, A. Kitoh, C. Kobayashi, T. Palmer, K. Puri, W. Tennant, and E. Volodin

Ensemblesofhindcastsfromsevenmodelsareanalyzedtoevaluatedynamical seasonal predictability of 850hPa wind and rainfall for the Asian summer monsoon (ASM) during 1987, 1988, and 1993. These integrations were performed using ob-served sea surface temperatures and from observed initial conditions. The experiments were designed by the CLIVAR Working Group on Seasonal to Interannual Prediction as part of the Seasonal prediction Model Intercomparison Project (SMIP). Integrations from the European Union PROVOST (Prediction of climate Variations on Seasonal to interannual Timescales) experiment are also evaluated.

The National Centers for Environmental Prediction/National Center for Atmospheric Research and European Centre for Medium-Range Weather Forecasts reanalyses and observed pentad rainfall form the baseline against which the hindcasts are judged. Pattern correlations and root-mean-square differences indicate errors in the simulation of the time-mean low-level flow and the rainfall exceed observational uncertainty. Most models simulate the subseasonal EOF's that are associated with the dominant variations of the 850hPa flow during the ASM, but not with the fidelity exhibited by the reanalyses as determined using pattern correlations. Pattern correlations indicate that the first EOF, associated with the tropical convergence zone being located over the continental landmass, is best simulated. The higher order EOF's are less well simulated, and errors in the magnitude and location of their associated precipitation anomalies compromise dynamical seasonal predictability, and are related to errors of the mean state. In most instances the models fail to properly project the subseasonal EOF's/PC's onto the interannual variability with result that hindcasts of the 850hPa flow and rainfall are poor. In cases where the observed EOF's are known to be related to the boundary forcing, the failure of the models to properly project the EOF's onto the interannual variability indicates that the models are not setting up observed teleconnection patterns.

Sperber, K. R., C. Brankovic, M. Deque, C. S. Frederiksen, R. Graham, A. Kitoh, C. Kobayashi, T. N. Palmer, K. Puri, W. Tennent, and E. Volodin, 2001: Dynamical Seasonal Predictability of the Asian Summer Monsoon. Mon. Wea. Rev., 129, 2226-2248.

Experiments with a Data Assimilation System to Diagnose AGCM Hindcasts of the MJO

Man Li C. Wu, Siegfried D. Schubert, Derek Van Pelt
Data Assimilation Office
Goddard Laboratory for Atmospheres
and
Duane Waliser
Institute for Terrestrial and Planetary Atmospheres
State University of New York

I. Introduction

The objectives of this study are to (1) develop a better understanding of how observations constrain/impact the MJO in a data assimilation system with the aim of improving the representation of the MJO, and (2) to carry out AGCM predictability/forecast experiments under various observational constraints to assess model errors and sensitivity to initial conditions. Our current focus is on the second objective.

We use the NASA-NCAR AGCM to carry out this study. The model is based on the finite-volume dynamical core developed at the DAO (Lin and Rood 1998), with physical parameterizations from the NCAR CCM-3 (Kiehl et al. 1996). The data assimilation system is the finite volume Data Assimilation System (fvDAS) of the DAO (DAO Office Note, 1999).

The ability of the current version of the AGCM to simulate the MJO is highlighted in Figs. 90 through 94 in Chang et al, 2001. These figures show that the model generally reproduces the large-scale structure of the MJO variability. However, the model MJO is too weak and the period is too short (around 20 to 30 days) compared to that found in the NCEP/NCAR reanalysis (40 to 60 days). A major problem with the simulated mean climate is the lack of precipitation over much of the western Pacific warm pool and Indonesia region, and too much rainfall over the western Indian Ocean and East China (Figs. 26 and 27 of Chang et al, 2001).

In order to address the AGCM deficiencies above, we made the following experiments covering the period August and September of 2000: (a) a full assimilation run with the fvDAS, (b) an ensemble of 9 AGCM hindcasts with different atmospheric initial conditions, and (c) an assimilation run in which only atmospheric moisture observations where ingested (fvDAS_only_q) - the aim here was to examine the impact of correcting the moisture bias in the AGCM on both the climate and on the representation of the MJO. In the following discussion, the focus is on the impact of the moisture correction to the representation of the MJO.

II. Results

Figure 1 is a longitude-time diagram of velocity potential anomalies averaged over between 10S and 10N. Both the fvDAS and NCEP/NCAR reanalysis show a well defined eastward propagation associated with the MJO. The AGCM ensemble mean initially follows the observations, but loses skill in a matter of a few days. The simulated anomalies travel to the east too fast. Afterwards, the central Pacific is dominated by a sinking branch of the MJO for more than a month. The ensemble variance shows that the limit of predictability in the AGCM for this case is about 10 days to 2 weeks.

A diagnosis of the mean moisture field indicates a substantial bias. Specifically, in the tropics between 10S to 10N, the AGCM is too wet over the Indian Ocean and too dry over most of the western Pacific Ocean. Around the ITCZ (latitudes 12N to 16N), the dry area extends into the eastern Pacific and the dry situation is most severe.

In the assimilation with the moisture-only correction (fvDAS_only_q run), the moisture bias are largely corrected. In addition, the results show a better precipitation field. In particular, the insufficient precipitation over Indonesia and western Pacific warm pool region is corrected and the excessive rainfall over the western Indian Ocean is being reduced. Bias in the velocity potential over the corresponding regions is also improved.

The impact of the moisture correction on the representation of the MJO as it cycles around the globe is also positive. With the assimilation of moisture, the rising branch of the MJO in the Central Pacific is enhanced so as the eastward propagation. The results also improve the skill of MJO hindcasts (especially EOF2). EOF 2 has a dipole centered over the central Pacific and western Indian Ocean.

In the diagnoses of the moist heating of the fvDAS data, we found that the moist heating leads the rising branch of the MJO, and the rising branch of the MJO also enhances the moist heating. One of the apparent reasons for the failure of the AGCM to produce a reasonable MJO is that the AGCM is too dry over the western Pacific region and it cannot generate enough moist heating ahead of the rising branch of the MJO.

When we compare the fvDAS with the AGCM and the fvDAS_only_q results, we find that the AGCM heating over the central Pacific is too weak. When the moisture bias is corrected, the moist heating in the central Pacific is improved, which in turn enhances the rising branch of the MJO in the central Pacific and improves the eastward propagation of the MJO.

III. Conclusions

The MJO in the current version of the NASA/NCAR model is too weak and has dominant periods that are too short: these are problems that are common to many other AGCMs. On the other hand, the MJO is quit reasonable within an assimilation system that employs that AGCM. The AGCM problems are reflected in hindcasts of a strong MJO event where the model loses skill within a matter of days and loses predictability in about one month. Initial experiments

correcting only the moisture fields in the model appear to have positive effects on the precipitation climatology and improve the representation of the MJO. Follow-on experiments are needed to determine whether similar benefits of the MJO can be achieved with a simple moisture bias correction.

References

Chang, Y.-H., S. D. Schubert, S-.J Lin, S. Nebuda, and B. W. Shen, 2001:The Climate of the FCCM-3 Model - The Technical report series on global modeling and data assimilation, NASA/TM-2001-104606, Vol. 20, pp127.

da Silvar, A. and S-.J Lin, 1999, The DAO physical-space/finite-volume data assimilation system. Part I: Algorithm theoretical basis for the "violet' core system - Office Note series on global modeling and data assimilation, DAO Office Note 2000-nn, pp 27.

Lin, S.-J. and R. B. Rood, 1998: A flux-form semi-Lagrangian general circulation model with a Lagrangian control volume vertical coordinate. The Rossby-1000 symposium, Stockholm, Sweden.

Kiehl, J. T., J. J. Hack, and B. P. Briegleb, 1994: The simulated earth radiation budget of the NCAR CCM2 and comparisons with the Earth Radiation Budget Experiment (ERBE). J. Geophys. Res., 99, 20815-20827

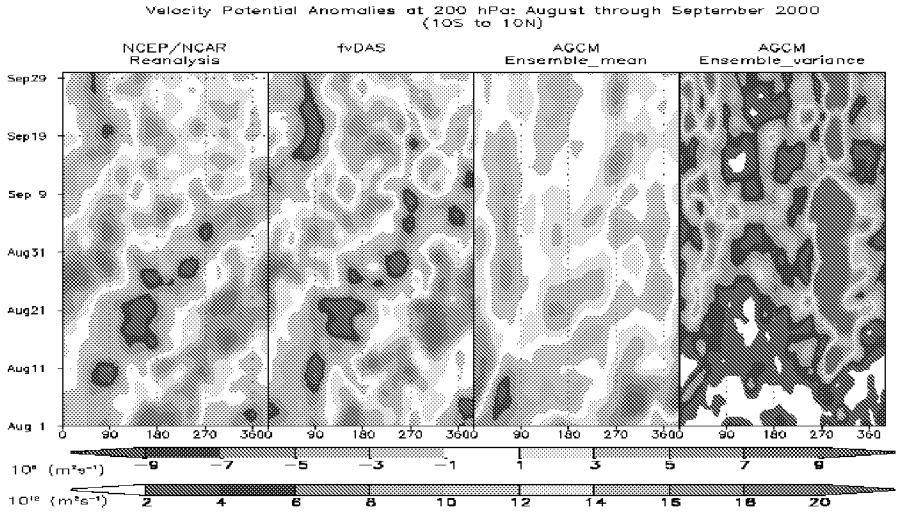
Velocity Potential Anomalies at 200 hPa: August through September 2000
(10S to 10N)
NCEP/NCAR Reanalysis
fvDAS
AGCM Ensemble_mean
AGCM Ensemble_variance
Sep29
Sep19
Sep 9
Aug31
Aug21
Aug11
Aug 1
0 90 180 270 360
10⁶ (m²s⁻¹)
−9 −7 −5 −3 −1 1 3 5 7 9
10¹⁰ (m²s⁻¹)
2 4 6 8 10 12 14 16 18 20

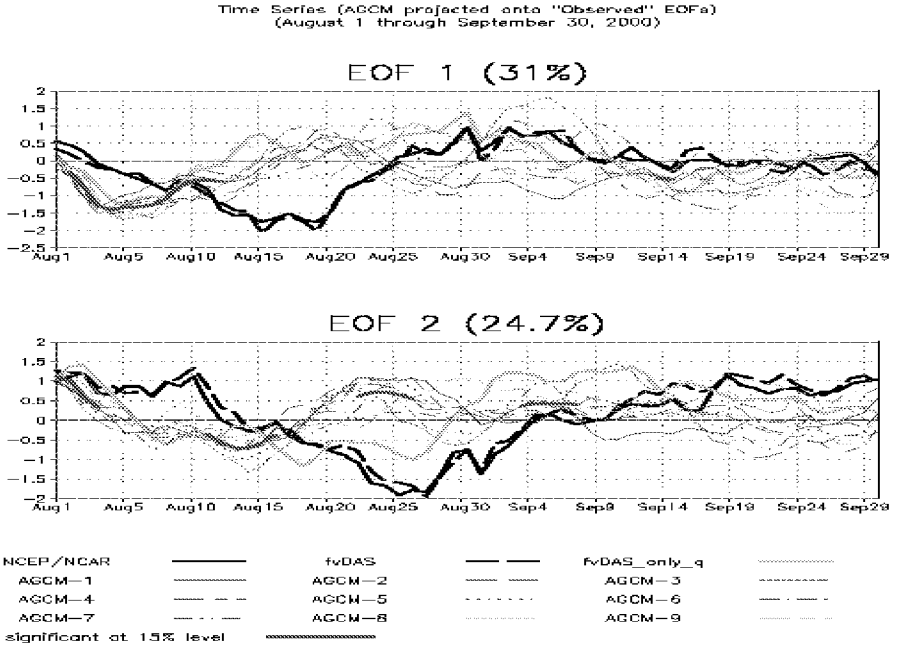
Time Series (AGCM projected onto "Observed" EOFs)
(August 1 through September 30, 2000)
EOF 1 (31%)
EOF 2 (24.7%)
Aug1 Aug5 Aug10 Aug15 Aug20 Aug25 Aug30 Sep4 Sep9 Sep14 Sep19 Sep24 Sep29
NCEP/NCAR
fvDAS
fvDAS_only_q
AGCM−1
AGCM−2
AGCM−3
AGCM−4
AGCM−5
AGCM−6
AGCM−7
AGCM−8
AGCM−9
significant at 15% level

Session IV

Tropical/Extratropical Interactions

Tropical Influences on Subseasonal Extratropical Variability and Predictability

Prashant D. Sardeshmukh
NOAA-CIRES Climate Diagnostics Center
Boulder, Colorado, USA

This talk emphasized three points: 1) A large fraction of the total power of extratropical tropospheric height variability resides in the intraseasonal band; 2) Much of the predictability on this time scale can be captured by simple multilinear Markov models; and 3) Tropical forcing is a major (though not the only) source of this predictability.

In support of point 1, it was shown that to a first approximation the average wintertime power spectrum of 500 mb heights for northern hemispheric gridpoints poleward of 20 N is well approximated by that of red noise with a 3-day correlation scale. The hemispherically averaged variances of daily, weekly, monthly and seasonal-average anomalies are also consistent with that of 3-day red noise. It was further emphasized that about 88% of the total power of a red noise time series lies between periods of 0.1 and 10 times the characteritic period, which for 3-day red noise is 2π x 3 ~ 18 days. Thus a large part of the total power lies in the intraseasonal band. Shorter-scale synoptic variability modifies this picture somewhat in the western ocean basins, but longer term interannual and interdecadal variability remains modest in comparison, even in the eastern ocean basins. Also consistent with this picture, one-point teleconnection maps of daily, weekly, monthly, and seasonal-average anomalies for base points in the north Pacific and Atlantic have a remarkably similar spatial structure across these time scales.

If simple univariate 3-day red noise captures so much of the structure of tropospheric variability, then multivariate red noise (with multiple time scales and patterns) should do even better. Such a model may be constructed directly from observed statistics through the process of Linear Inverse Modeling (Penland 1989; Penland and Sardeshmukh 1995) as follows. In any multidimensional statistically stationary system with components x_i, one may define a time-lag covariance matrix $C(\tau)$ with elements $C_{ij} = < x_i(t+\tau)\, x_j(t) >$, where angle brackets denote a long-term average. In linear inverse modeling, one assumes that the system satisfies $C(\tau) = G(\tau)C(0)$, where $G(\tau) = exp(L\tau)$ and L is a constant matrix, and uses this relationship to estimate L given observational estimates of $C(0)$ and $C(\tau_0)$ at some lag τ_0. In such a system any two states separated by a time interval τ are related as $x(t+\tau) = G(\tau)\, x(t) + \varepsilon$, where ε is a random error vector with covariance $E(\tau) = C(0) - G(\tau)C(0)G^T(\tau)$. Such a model may then be used to make forecasts. The vector $G(\tau)x(t)$ represents an "infinite-member ensemble-mean" forecast for $x(t+\tau)$ given $x(t)$, i.e the forecast signal, and $E(\tau)$ represents the expected covariance of its error, i.e the noise. As pointed out for example by by Sardeshmukh et al. (2000), the expected correlation ρ_∞ of such forecasts with observations is given by $\rho_\infty^2 = S^2/[1+ S^2]$, where S is the forecast signal to noise ratio. More generally, the predictability of any system component may be estimated by defining the average S^2 for that component as the appropriate diagonal element of the signal covariance matrix $G(\tau)C(0)G^T(\tau)$ divided by the corresponding diagonal element of the noise covariance matrix $E(\tau)$, and for the system as a whole as the ratio of either the traces or the determinants of these matrices.

We have constructed such "linear inverse models" (LIMs) of 7-day running mean circulation anomalies in the northern hemisphere and diabatic heating anomalies in the tropics from their observed simultaneous and time-lag correlation statistics (see Winkler et al. 2001; Newman et al. 2002). The state-vector x has 37 components representing the first 30 combined EOFs of 250 and 750 mb streamfunction and the first 7 EOFs of column-averaged tropical diabatic heating. In both winter and summer, the models' forecast skill at Week 2 (Days 8 to 14) is comparable to that of NCEP's medium range forecast (MRF) model. Their skill at Week 3 (Days 15 to 21) is actually higher, partly due to their better ability to forecast tropical heating variations and their influence on the extratropical circulation. Furthermore, the geographical and temporal variations of forecast skill are similar in the LIMs and the MRF model.

The simplicity of the LIM makes it an attractive tool for assessing and diagnosing atmospheric predictability on subseasonal time scales. The model assumes that the dynamics of weekly averages

are linear, asymptotically stable, and stochastically forced. The validity of these assumptions have important implications for understanding subseasonal variability and predictability. In a forecasting context, the predictable signal is associated with the deterministic linear dynamics and the forecast error with the unpredictable stochastic noise. In our low-order linear model of the high-order chaotic real system, this stochastic noise represents the effects of both chaotic nonlinear interactions and unresolved initial components on the evolution of the resolved components. We assume its statistics to be state-independent.

An average signal to noise ratio S is estimated at each grid point on the hemisphere in the manner outlined above, and is then used to estimate the potential predictability ρ_∞ of 7-day running mean anomalies as a function of forecast lead time. The day on which ρ_∞ drops below 0.5 in winter is plotted in the left panel of Figure 1. The right panel shows the contribution to this from tropical heating, obtained by performing similar calculations in which the effects of the heating are turned off. It is clear that predictable tropical heating variations play an important role in enhancing the potential predictability of weekly averages in the extratropics, especially over the Pacific ocean and north America. The *actual* LIM forecast skill ρ (not shown) has a similar geographical structure but weaker magnitude than the potential skill.

The LIM formalism is also useful for diagnosing variations of forecast skill from case to case. In this framework, the *predictable* variations of forecast skill from case to case are associated with the predictable variations of signal, rather than of noise. This contrasts with the traditional emphasis in studies of shorter-term predictability on flow-dependent instabilities, i.e. on the predictable variations of the noise statistics. In the LIM, the predictable variations of signal are associated with variations of the initial state projection on the growing singular vectors of the LIM's propagator G, which have relatively large amplitude in the tropics. As shown in Figure 2 for Week 3 forecasts in winter, at times of strong projection on the first 3 singular vectors, the signal to noise ratio S is high, and the northern hemispheric circulation is not only potentially (ρ_∞) but also actually (ρ) more predictable than at other times. The version of the NCEP MRF model examined here is much less able to discriminate between relatively high and low forecast skill cases in this way. This is partly due to its lesser ability to forecast tropical heating variations in regions where the initial heating component of the growing singular vectors is important. Our results thus suggest both that there is considerable predictability of Week 2 and Week 3 averages in some regions of the northern hemisphere, and that it may currently not be fully realized in some forecasting systems because of their error in predicting tropical heating variations in sensitive areas.

References

Winkler, C.R., M. Newman and P.D. Sardeshmukh, 2001: A linear model of wintertime low-f requency variability. Part I: Formulation and forecast skill. *J. Climate*, 14, 4474-4494.

Newman, M., P.D. Sardeshmukh, C.R. Winkler, and J.S. Whitaker, 2002: A study of subseasonal predictability. *Mon. Wea. Rev.*, submitted.

Penland, C., 1989: Random forcing and principal oscillation pattern analysis. *Mon. Wea. Rev.*, 117, 2165-2185.

Penland, C., and P.D. Sardeshmukh, 1995: The optimal growth of tropical sea surface temperature anomalies. *J. Climate*, 8, 1999—2024.

Sardeshmukh, P.D., G.P. Compo and C. Penland, 2000: Changes of probability associated with El Nino. *J. Climate*, 13, 4268-4296.

Potential Predictability of 7-day running means

(Defined as Day on which Anomaly Correlation drops below 0.5)

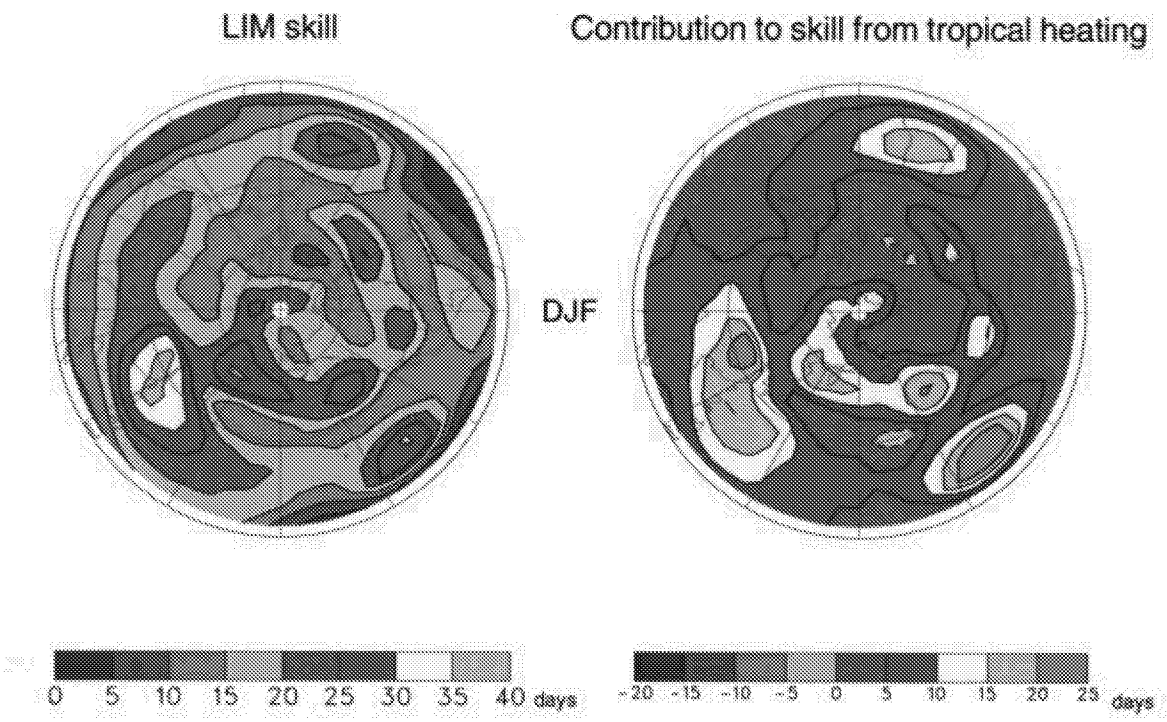

Figure 1

Winter

Week 3

(Days 15-21)

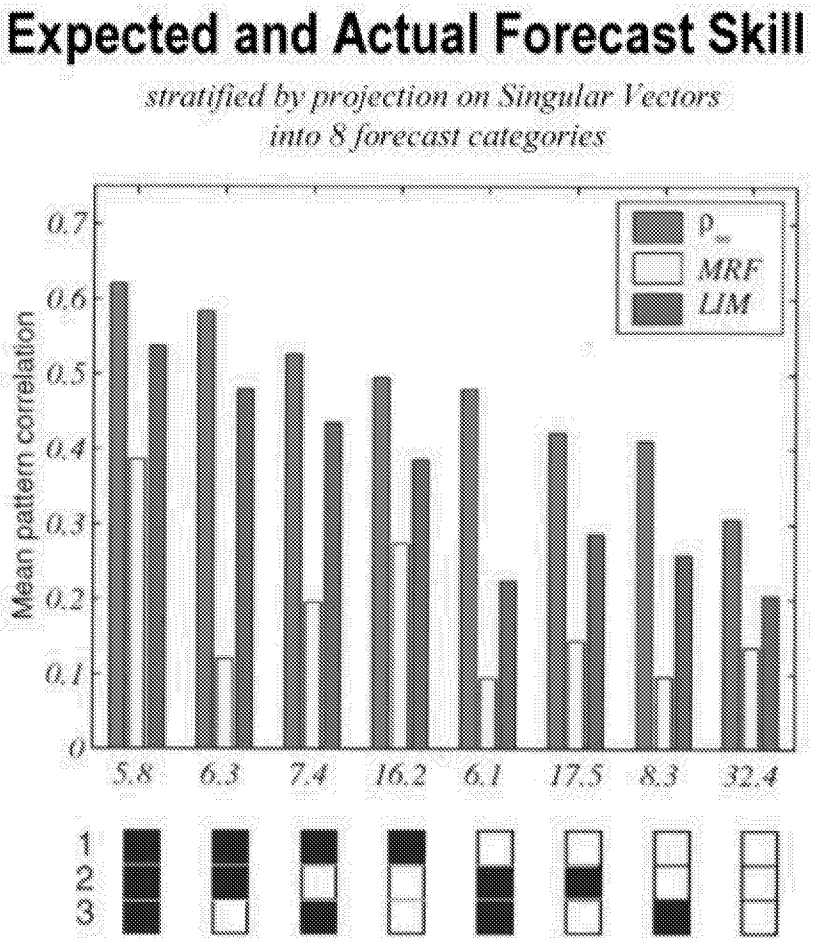

Figure 2

Mid-latitude Mountains and the MJO: A Prototype for Tropical-Extratropical Interaction?

Klaus M. Weickmann
NOAA-CIRES Climate Diagnostics Center
Boulder, Colorado 80303

The Madden-Julian oscillation produces a robust, repeatable signal in global and zonal atmospheric angular momentum (AAM). During northern winter, the MJO zonal wind anomalies appear first on the equator in the western hemisphere and then shift to the eastern hemisphere, stretching from the north Indian Ocean to the central Pacific Ocean. Global AAM anomalies increase and reach a maximum during this evolution. Studies of the torques that produce the AAM variations show Asian and North American mountains contribute to the mountain torque anomalies when analyzing 30-70 day filtered data but not when analyzing data based on a MJO index. The Andes and African Highlands make a larger contribution during an MJO. Subsequent observational studies of the mountain and frictional torque reveal an independent coherent evolution of the mid-latitude circulation that involves the adjustment by the atmosphere to stochastically-varying flow over the mid-latitude mountains. In this case, the frictional torque responds to strong or persistent mountain torque events in a matter of days and the response includes the PNA teleconnection pattern. The intraseasonal AAM variations thus involve the interaction of mostly independent processes in the tropics and mid-latitudes. Some recent cases are presented.

A Workshop on Prospects for Improved Forecasts of Weather and Short-term Climate Variability on Subseasonal (2 week to 2 month) Time Scales, NASA/Goddard Space Flight Center, April 16-18, 2002

Influences of the Madden Julian Oscillations on Temperature and Precipitation in North America during ENSO-Neutral and Weak ENSO Winters

Yan Xue*, Climate Prediction Center, Yan.Xue@noaa.gov
Wayne Higgins, Climate Prediction Center, Wayne.Higgins@noaa.gov
Vernon Kousky, Climate Prediction Center, Vernon.Kousky@noaa.gov

1. Introduction

A number of studies have shown that the Madden-Julian Oscillation (MJO) have a strong influence on the atmospheric circulation and precipitation patterns in the tropical and extratropics (Madden and Julian 1971; Lau and Chan 1985; Knutson and Weickmann 1987; Kayano and Kousky 1999). Recent studies also suggest that the MJO-related tropical forcing is linked to precipitation events along the west coast of the United State during the winter season (Mo and Higgins 1998; Higgins et al. 2000).

Dynamical models generally simulate the MJO quite poorly, partly because of inherent difficulties in parameterizing tropical convection. Statistical prediction models have shown a modest skill relating subseasonal variations in tropical convection to week-2 prediction of wintertime rainfall in western North America (Whitaker and Weickmann 2001). Operational week two ensemble predictions show levels of skill that are comparable to the statistical forecasts. However, neither statistical or dynamical prediction models have demonstrated useful levels of skill in forecasting MJO-related impacts beyond week 2.

We believe that improved monitoring and assessment of the MJO and its impacts on the atmospheric circulation and precipitation patterns will lead to better prediction. In this work we focus on ENSO-neutral and weak ENSO winters since the MJO is known to be quite active during those times. Velocity potential at 200-hPa has been used to construct a composite index for life cycles of the MJO (Knutson and Weickmann 1987). A similar approach is taken here. An extended Empirical Orthogonal Function (EEOF) analysis is applied to the bandpass filtered (25-87 days) pentad velocity potential at 200-hPa for ENSO-neutral and weak ENSO winters (November-April) during 1979-2000. The first EEOF is composed of ten time-lagged patterns. We construct ten MJO indices by regressing the filtered pentad data onto the ten patterns of the first EEOF. Keyed on the ten MJO indices, ten composites for the major MJO events are derived for various fields, including surface air temperature and precipitation. Our composites are constructed with unfiltered pentad data in which the winter season mean is removed.

Significant MJO-related influences on surface air temperature and precipitation in North America are found. The potential predictability for those fields derived from the tropical MJO-related forcing is discussed.

*Corresponding author address: Dr. Yan Xue, NOAA/Climate Prediction Center, 5200 Auth Road #605, Camp Springs, MD 20746.

2. Data

The data set used in this study consists of nonoverlapping five-day (pentad) means for 200-hPa velocity potential, 200-hPa zonal wind and 500-hPa geopotential height derived from the NCEP/NCAR CDAS/Reanalysis data (Kalnay et al. 1996). As a proxy for deep tropical convection we use pentad OLR data derived from measurements made by the NOAA operational polar-orbiting satellites for the 1979-2000 period. We also use the GPCP pentad precipitation analysis for its global coverage (Xie et al. 2002). The pentad global surface air temperature is based on GTS data (Ping-Ping Xie, personal communication).

3. MJO indices

The ENSO-neutral and weak ENSO winters during 1979-2000 are selected according to the CPC ENSO classification (http://www.cpc.ncep.noaa.gov/research_papers/ncep_cpc_atlas/8/ensoyrs.txt). Based on this, 15 winters are selected and used to calculate the EEOF of velocity potential at 200-hPa (referred to as CHI200 hereafter). The first EEOF, composed of ten time-lagged patterns, describes an eastward propagation of the MJO with a timescale of about 45 days (Fig. 1). We construct ten MJO indices by regressing the filtered pentad CHI200 onto each of the ten patterns. So positive indices correspond to the convectively active phase of the MJO at different longitudes. Those MJO indices have been implemented for the real time monitoring of the MJO at CPC: http://www.cpc.ncep.noaa.gov/

products/precip/Cwlink/daily_mjo_index/mjo_index.html.

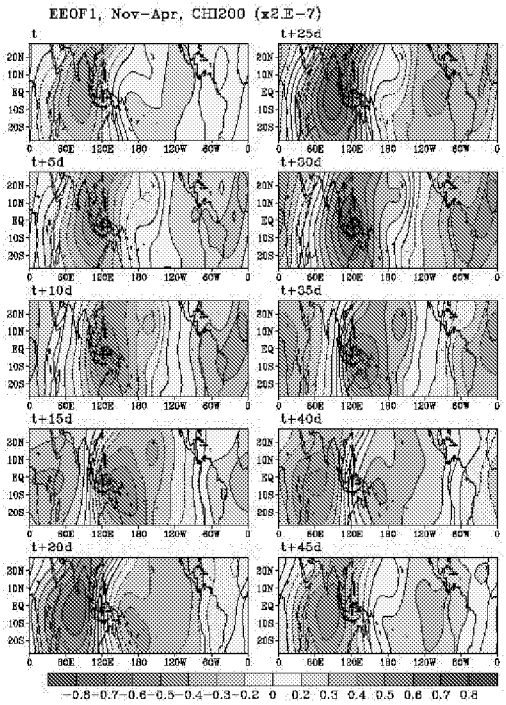

Fig. 1. The first EEOF of the pentad velocity potential at 200-hPa for the ENSO-neutral and weak ENSO winters (November-April) during 1979-2000.

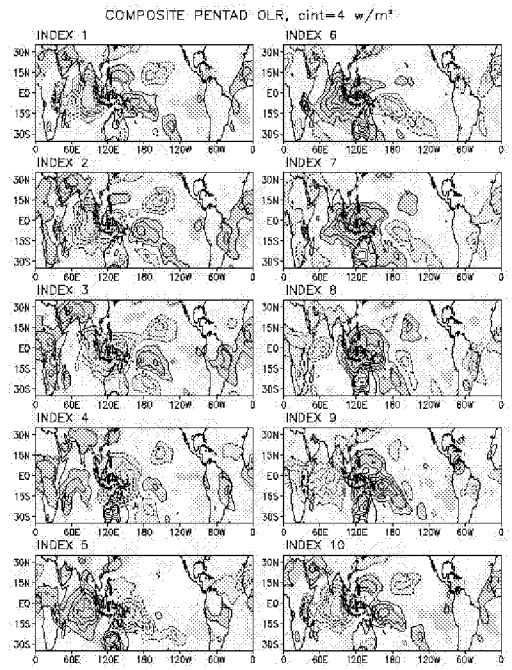

Fig. 2. OLR composites keyed on the ten MJO indices. The contour interval is 4 w/m2, and the zero contour is omitted. The blue (yellow) shading denotes negative (positive) anomalies significant at the 95% level.

4. MJO composites

We identify MJO events when the maxima of the standardized MJO indices exceed 0.8 standard deviations. To increase the sample size, one to four pentads centered on the maxima are used in composites, depending on the amplitudes of the indices. So the stronger events are weighted more in composites than the weaker ones are. We restrict our cases to the extended cold season (December to April). Based on this, about 25 to 29 MJO events are selected for each of the ten MJO indices. The number of pentads included in each composite varies from 67 to 83 since more than one pentads are used for each MJO event. The statistical significance of the composites at each grid point is evaluated by comparing selected MJO pentads to the remaining non-MJO pentads in the ENSO-neutral and weak ENSO winters via a two-tailed student's t test.

The life cycle of the MJO and its influences on the upper-tropospheric circulation are described by the composites of OLR and 200-hPa zonal wind (Fig. 2 and 3). The initial phase of the cycle is characterized by enhanced convection in far eastern Africa and the Indian Ocean, and suppressed convection in the western Pacific and the South Atlantic Convergence Zone (SACZ) (index 1 and 2). There are twin anticyclones located to the west and twin cyclones to the east of the tropical forcing, which in turn retracts the East Asian Jet (Fig. 3). When the enhanced convection shifts eastward towards Indonesia, westerly wind anomalies prevail in the upper troposphere over the gulf of Alaska and the Pacific North West (PNW), which brings wet condition there (Fig. 4). As the enhanced convection moves out of Indonesia and suppressed convection sets up over the Indian Ocean, the East Asian Jet extends eastward (index 5). This circulation pattern remains quisi-stationary for about three pentads (index 6-8 in Fig. 3). When the enhanced convection moves to northern South America and Africa, a new cycle begins (index 9-10 in Fig. 2).

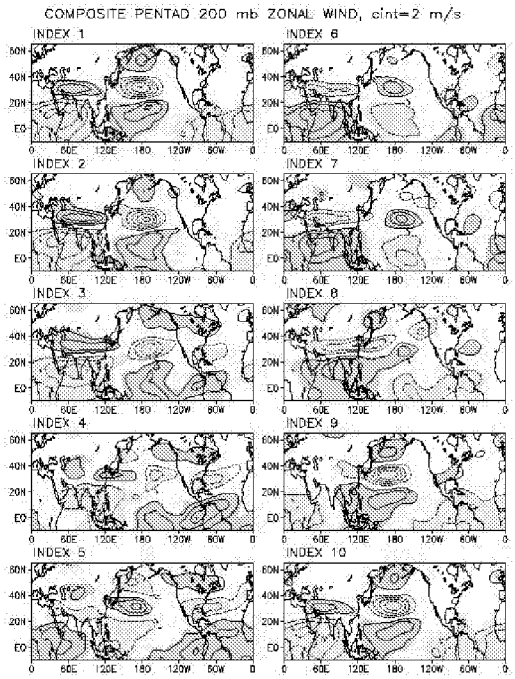

Fig. 3. Same as Fig. 2 except for the 200-hPa zonal wind. The contour interval is 2 m/s.

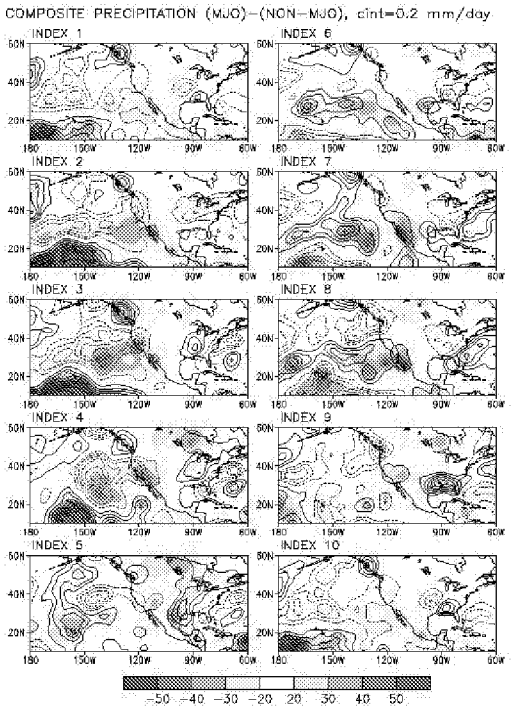

Fig. 4. Differences of composites of MJO pentads and non-MJO pentads. The contour interval is 0.2 mm/day, and the zero contour is omitted. The shading denotes the percentage departure relative to the climatological pentad precipitation based on te Dec-Apr period.

Concurrent with the tropical MJO-related forcing, significant precipitation signals are found in the U.S. (Fig. 4). The MJO-related precipitation signal is most pronounced along the west coast, which is consistent with previous studies (Mo and Higgins 1998; Higgins et al. 2000). During index 3 and 4, the PNW is wet and California is dry. However, the wet signal in the PNW is negligible compared to the local climatology because most MJO events happen during later winter and early spring, while the PNW receives its peak precipitation in Dec-Jan. The California precipitation begins as the enhanced convection moves to the date line (index 7) and persists for two to three pentads. This is probably associated with the upper-tropospheric westerly wind anomalies that act to steer weather systems into this region (Whitaker and Weickmann 2001, hereafter WW). We noticed that the OLR pattern of index 8 agrees very well with the canonical predictor OLR pattern (at a 2-week lag) for the week-2 prediction of the western north American rainfall of WW. It appears that the precursor OLR signal for the week-2 prediction of California precipitation in WW is that around index 5.

Significant MJO-related influences on surface air temperature in North America are found (Fig. 6), that are consistent with the MJO-related influences on 500-hPa geopotential height (Fig. 5). When the enhanced convection is in the Indian Ocean (index 1 and 2), strong blocking activity occurs in the northwestern Pacific and a deep trough is located over the gulf of Alaska. As the enhanced convection moves eastward toward Indonesia (index 3 and 4), the composite 500-hPa geopotential height resembles a negative PNA pattern, that is characterized by a ridge in the northeastern Pacific, a trough in the northwestern U.S. and a ridge in the southeastern U.S.. This quisi-negative PNA pattern lasts 2-3 pentads, producing warm anomalies in the eastern U.S. and cold anomalies in the western Canada (Fig. 6). As the enhanced convection moves toward dateline, a weak positive PNA pattern forms, causing warm anomalies in the western Canada (index 8 in Fig. 5 and 6). As the enhanced convection returns to Africa and the

Indian Ocean, anomalous trough covers the western U.S., producing cold anomalies in the west (index 9). Averaged over the cycle, the U.S. tends to be warm-than-normal in the east and cold-than-normal in the west. These long lasting warm anomalies (2-3 pentads) in the east will undoubtably contribute significantly to monthly forecasts issued regularly at the CPC when the MJO is active ("forecasts of opportunity").

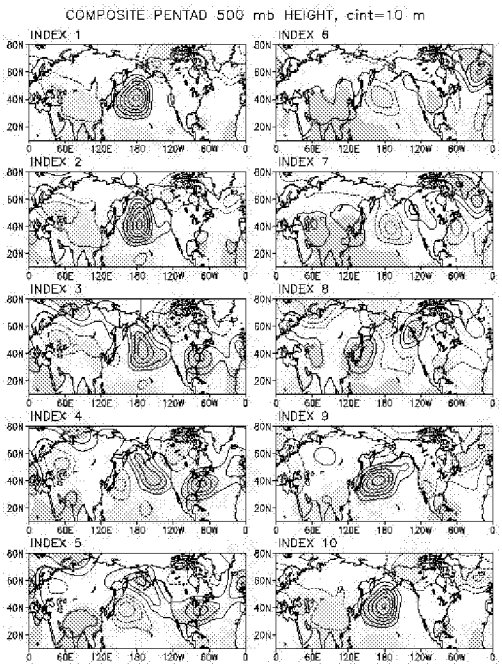

Fig. 5. Same as Fig. 2 except for the 500-hPa geopotential height. The contour interval is 10m.

REFERENCES

Higgins, R. W., J.-K. E. Schemm, W. Shi, and A. Leetmaa, 2000: Extreme precipitation events in the western united states related to tropical forcing. *J. Climate*, **13**, 793-820.

Kalnay, E., and Coauthors, 1996: The NCEP/NCAR 40-year reanalysis project. *Bull. Amer. Meteor. Soc.*, **77**, 437-471.

Kayano, M. T., and V. E. Kousky, 1999: Intraseasonal (30-60 day) variability in the global tropics: principal modes and their evolution. *Tellus*, **51A**, 373-386.

Knutson, T. R., and K. M. Weickmann, 1987: 30-60 day atmopsheric osciallations: composite life cycles of convection and circulation anomalies. *Mon. Wea. Rev.*, **115**, 1407-1436.

Lau, K.-M., and P. H. Chan, 1985: Aspects of the 40-50 day oscillation during the northern winter as inferred from outgoing longwave radiation. *Mon. Wea. Rev.*, **113**, 1889-1909.

Madden, R. A., and P. R. Julian, 1972: Description of global scale circulation cells in the tropics with 40-50 day period. *J. Atmos. Sci.*, **29**, 1109-1123.

Mo, K. C. and R. W. Higgins, 1998: Tropical influences on California precipitation. *J. Climate*, **11**, 412-430.

Whitaker, J. S., and K. M. Weickmann, 2001: Subseasonal variations of tropical convection and week-2 prediction of wintertime western north american rainfall. *J. Climate*, **14**, 3279-3288.

Xie, P., J.E. Janowiak, P.A. Arkin, R. Adler, A. Gruber, R. Ferraro, G. J. Huffman, and S. Curtis, 2002: GPCP pentad precipitation analysis: An experimental data set based on gauge observations and satellite estimates. (Summitted to J. Climate).

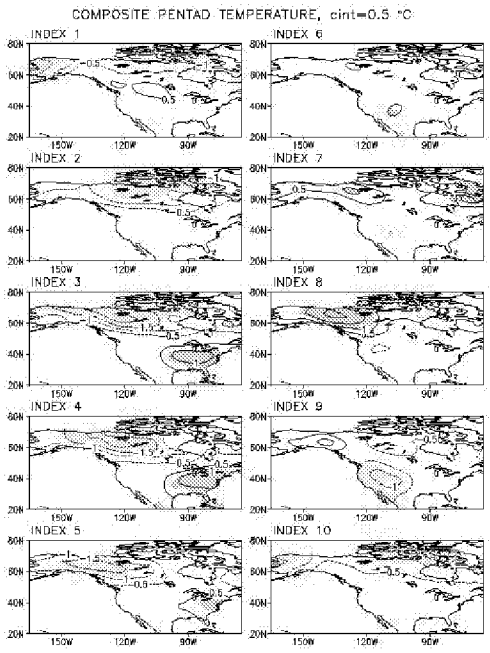

Fig. 6. Same as Fig. 2 except for surface air temperature. The contour interval is 0.5 degree.

The Role of MJO Activity Modulating the SACZ Persistence, Intensity and Form, and Regional Impacts on Extreme Precipitation Events

Leila M. V. Carvalho, Charles Jones and Brant Liebmann
Institute for Computational Earth System Science (ICESS)
University of California
Santa Barbara, CA 93106-3060

The tropical atmosphere exhibits significant amounts of variance on time scales of 20-90 days. In particular, the Madden-Julian Oscillation (MJO) is the main mode of tropical intraseasonal variation with large influences on the Asian-Australian Monsoons and mid-latitude teleconnections. Previous works have shown that intraseasonal variations play an important role on the variability of the South American Monsoon System (SAMS). The South Atlantic Convergence Zone is part of the SAMS and its variability affects large areas of tropical and subtropical South America.

This study examines the influence of the MJO on the intensity, persistence, and form of the SACZ and regional implications for the occurrence of extreme precipitation over Brazil. Daily Outgoing Longwave Radiation (OLR) is examined during 22 years to characterize convective activity in the SACZ. An objective algorithm is applied to identify OLR properties related to intensity and form of the SACZ such as area, minimum OLR, fraction with minimum OLR, eccentricity, and extent to the Atlantic Ocean and the Amazon. Factor analysis is then applied to time series of OLR properties to characterize the SACZ features. Two factors explain ~ 65% of the total variance of the convective activity patterns in the SACZ and characterize events according to the intensity (Factor-1) and extent of the OLR features to the Atlantic Ocean (Factor-2). Factor-1 is then used as an index to infer persistence of intense SACZ episodes. Factor-2 characterizes distinct situations when convection is displaced to the Atlantic Ocean or more continental.

The MJO episodes are characterized independently using filtered OLR (10-90 days) data and principal components analysis. The propagation of midlatitudes wave train is also investigated using filtered OLR (10-90 days) data but with a distinct procedure. Precipitation over Brazil is examined with data from stations interpolated in a grid of 2x2° of latitude and longitude. It is shown that MJO events modulate approximately 30% of the total SACZ episodes with persistence greater than 3 days. The midlatitude wave trains modulate the SACZ extent to the Atlantic Ocean. It is shown that there are significant regional impacts in the occurrence of extreme precipitation over Brazil related to MJO occurrences and to the midlatitude wave train. The relationships between the occurrence of MJO and the wave train are also investigated.

Modulation of the North Pacific-Pacific Northwest Storm Activity by MJO

T. C. (Mike) Chen, David Li,
Peter Hsieh, and Jordan Alpert
Iowa State University

The x-t diagram of precipitation along 45°N were constructed over the North Pacific-Pacific Northwest region for the last twenty years, with different data sources: precipitation generated by the GEOS-1 and NCEP/NCAR reanalysis, Goddard precipitation estimates, and OLR. A clear 30-60 day modulation of the eastward migration of storm tracks emerges from these x-t diagrams. Storm tracks migrates eastward when the MJO deepens the Aleutian low. It was shown by our previous study (Chen and Alpert 1990 MWR) that the descent forecast skill of the planetary-scale divergent circulation can reach five days by the NMC medium-range forecasts (MRF). Thus, an effort is undertaking to explore how many days the modulation of the North Pacific-Pacific Northwest storm track activity by the MJO can properly predicted by the NCEP MRF. Preliminary results show that the five-day forecast skill generally can be obtained. However, the forecast skill may exceed this limit when the MJO is strong and well-organized.

Monthly Variability of ENSO Signals and the Relevance for Monthly Predictions

Martin P. Hoerling
NOAA-CIRES Climate Diagnostics Center
Boulder, CO

The role of ENSO in the predictability of monthly averages (monthly prediction) is explored. The simplest approach, and one commonly used, is to specify the seasonal mean atmospheric signal related to ENSO. An effective "monthly resolution" to such signals is rendered by calculating overlapping, seasonal averages. Yet, these could underestimate true monthly ENSO-related predictability to the extent that distinct monthly signals exist, and vary within a season. It is well established that the potentially predictable ENSO signal varies from one season to another, and it is thus reasonable to expect that some variation occurs even within a season. This could occur due to a strong sensitivity of tropical-extratropical interactions to modest changes in the atmospheric base state. It could also be due to sub-seasonal changes in the tropical forcing accompanying the ENSO cycle itself.

The focus of this study is to provide evidence for the existence of sub-seasonal variations in the ENSO signal, and the analysis uses NSIPP climate simulations and observed data for 1950-2000. Results are presented for the late boreal Fall season (October-November-December, OND), during which the seasonal mean 500-mb ENSO signal is compared to the individual monthly signals. Distinct atmospheric signals occur in each month. A striking feature of the sub-seasonal variation in the ENSO signal is that the October and December responses over the Pacific-North American region are anti-correlated, and as such the associated seasonal mean signal is a smeared residual of sharper patterns. The practical importance for monthly predictions is discussed within a "signal-to-noise ratio" framework for predictability assessment.

The Influence of El Niño on the circulation over the North Pacific and North America

Hilary Spencer Julia M. Slingo

April 2002

1 Motivation

Simulating ENSO teleconnections with an atmospheric GCM (AGCM) is normally considered to be of interest to seasonal forecasting. A long AGCM ensemble with observed SSTs is studied and shows that there are significant systematic errors of seasonal means over the North Pacific during the peak of El Niño in DJF and after the peak in MAM. It has been shown by other contributors that improved subseasonal forecasting (2 weeks to 2 months) requires reduced systematic model errors. Therefore, reducing the sources of the seasonal mean systematic error should be beneficial to shorter timescales. It is shown that these systematic errors can be dramatically reduced with a small increase in the vertical model resolution.

2 Method

An ensemble of six integrations of the UK Met. Office model, HadAM3 (Rodwell and Folland, 2001), with observed SSTs (GISST, version 2.3b, Parker *et al.*, 1995) was run at the Hadley centre and is studied here. The model resolution is 2.5° latitude by 3.75° longitude and 19 vertical levels. The model is described further by Pope *et al.* (2000). HadAM3 has also been integrated with observed SSTs from 1979-1996 at the Hadley centre with 30 vertical levels and various horizontal resolutions (Pope and Stratton, 2001). This is an AMIPII integration and so has slightly different SSTs from the 19 level integration. The El Niño event of 1982/83 is compared with NCEP reanalysis data (Kalnay *et al.*, 1996) and with CMAP precipitation (Xie and Arkin, 1996). The 1982/83 event is common to all four datasets. Other events have also been studied with the same conclusions but not included here. A fuller discussion of the results can be found in Spencer and Slingo (2002).

3 Results

The climatological, DJF SSTs from GISST and the DJF SSTs from 1982/83 from GISST and the AMIPII SSTs are shown in figure 1. The two datasets are slightly different in the tropical Pacific but the main differences between the HadAM3 integration with 19 levels (GISST SSTs imposed) and that with 30 levels (AMIPII SSTs imposed) are thought to be due to the different vertical resolutions.

The mean sea level pressure anomalies during DJF of the El Niño of 1982/83 for the HadAM3 integrations with both 19 and 30 levels and for the NCEP reanalysis are shown in

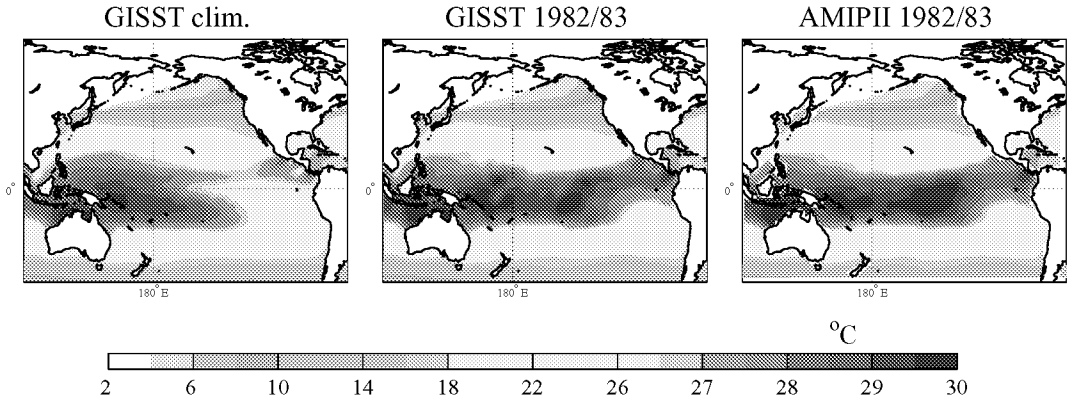

Figure 1: Sea surface temperature during DJF, climatology and El Niño

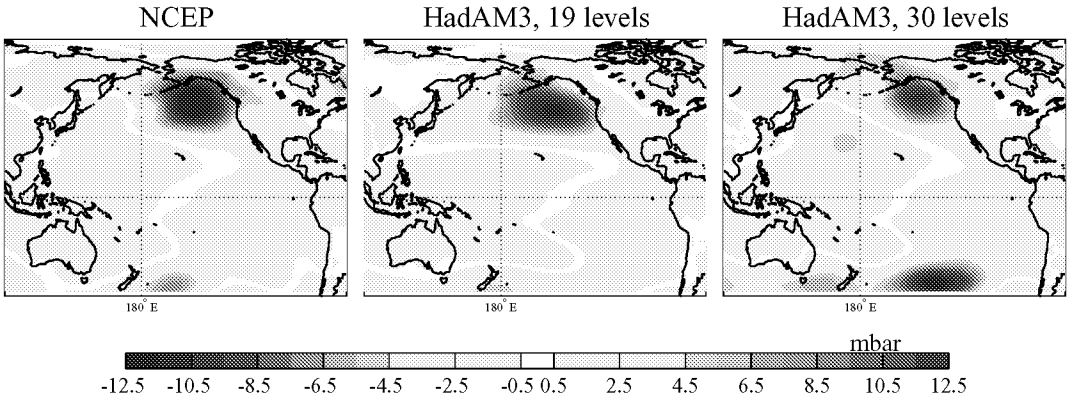

Figure 2: Mean sea level pressure anomalies during DJF of the El Niño of 1982/83 for NCEP reanalysis data and one member seasonal means of HadAM3 with observed SSTs

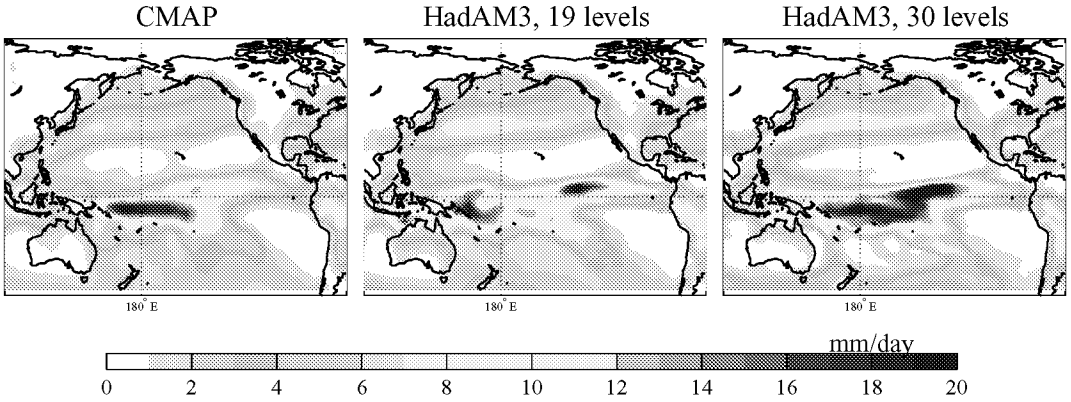

Figure 3: Total precipitation during DJF of the El Niño of 1982/83 for CMAP and one member seasonal means of HadAM3 with observed SSTs

figure 2. This shows the tropical Pacific to be simulated accurately by both models but there are large and highly significant errors in the 19 level model in the North Pacific region. Both the reanalysis and HadAM3 with 30 vertical levels show low pressure in the central and east of the North Pacific with high pressure to the west, whereas HadAM3 with 19 levels simulates a very deep Aleutian low across the whole of the North Pacific. Although only one realisation for each dataset is plotted, every member of the six with 19 vertical levels show very similar behaviour and none have high pressure in the west of the North Pacific. However, whenever a deepening of the Aluetian low is observed during a strong El Niño in DJF, it is accompanied by a high pressure anomaly in the west of the North Pacific. Therefore, HadAM3 with 19 levels never captures the observed response but one integration of one event with 30 vertical levels captures this observed response well, with low pressure across the centre and east of the North Pacific and high pressure in the west.

The reason for this improved simulation with 30 vertical levels can be traced to the tropical Pacific precipitation. The 19 level model simulates the precipitation climatology very well (not shown) and also simulates the approximate locations of reduced and enhanced precipitation during El Niño (also not shown). However, if the total precipitation during El Niño is plotted (figure 3), it can be seen that the enhanced precipitation simulated with 19 levels in the central tropical Pacific is not sufficient to shift the peak of the total precipitation into the central tropical Pacific as is observed. The CMAP observations show a broad peak in total precipitation across the west and centre of the tropical Pacific. This is not identical to that simulated with 30 vertical levels but the broad features south of the equator are similar. However, when simulated with 19 vertical levels, the peak precipitation remains in the west of the tropical Pacific and a separate, smaller peak is simulated towards the east. This implies that the divergent circulation at upper levels will be in a different longitudinal position in the simulation with 19 levels. It is this divergent circulation which forces the extratropical response.

This is confirmed by plotting the total velocity potential at 200mb for DJF of 1982/83 for the three datasets in figure 4. For each dataset, the velocity potential minimum, indicating the centre of the divergence, is situated over the maximum precipitation in the tropical Pacific. Hence the NCEP reanalysis and 30 level HadAM3 North Pacific are forced from the central tropical Pacific whereas the 19 level HadAM3 North Pacific is forced from the western tropical Pacific, in a similar manner to non-El Niño conditions. This explains the different longitudinal positions of the extratropical responses of the three datasets.

In order to trace the source of the precipitation errors in the tropical Pacific, probability density functions (p.d.f.s) of precipitation as a function of SST are calculated for each January between 1979 and 1998 and for each grid box in the western and central tropical Pacific (160°E to 120°W and 10°S to 5°N) for CMAP and the HadAM3 integrations. The p.d.f.s are calculated using a two dimensional Gaussian kernel estimator (Marshall and Molteni, 1993). All three datasets show suppressed precipitation over the cooler SSTs and more high precipitation as SST increases. However, HadAM3 with 19 levels simulates the highest precipitation over the warmest SSTs and few instances with low precipitation over the warmest SSTs, unlike CMAP. HadAM3 with 19 levels shows least variability of precipitation for any SST value which leads to the precipitation distribution matching closely the observed SST distribution (figure 1). This leads to the localised spikes of precipitation seen in figure 3 rather than the more smeared out distribution of the other datasets.

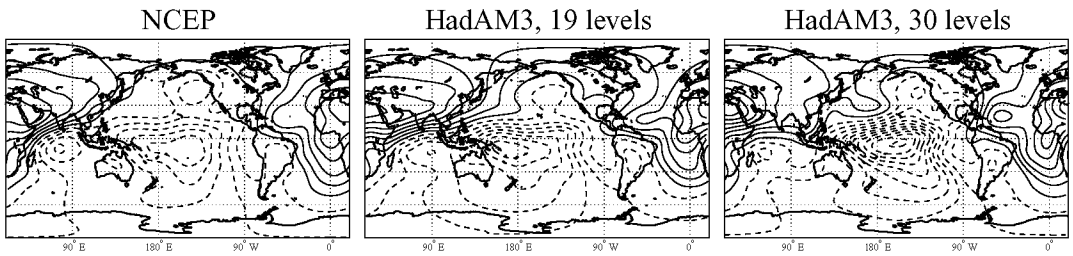

Figure 4: Total 200mb velocity potential during DJF of the El Niño of 1982/83 for NCEP reanalysis data and one member seasonal means of HadAM3 with observed SSTs The contour interval is $2 \times 10^6 m^2 s^{-1}$ and negative contours are dashed and start at $-1 \times 10^6 m^2 s^{-1}$

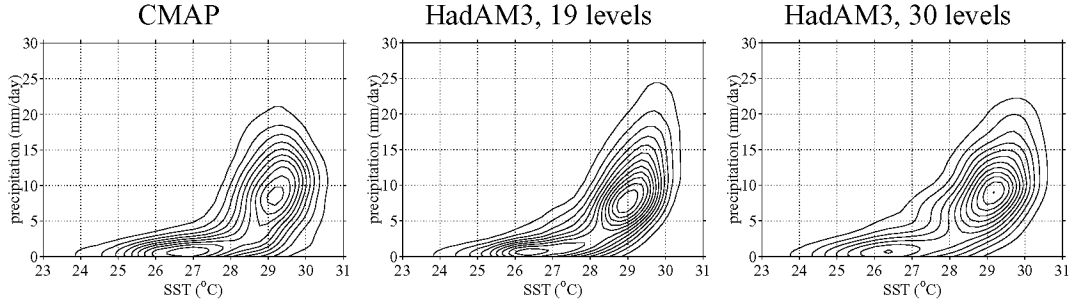

Figure 5: The probability density function of precipitation as a function of SST for each January between 1979 and 1998 and for each grid box in the western and central tropical Pacific (160°E to 120°W and 10°S to 5°N) for CMAP and HadAM3.

4 Discussion

The close relationship between precipitation and SST for the simulation with 19 levels, is probably due to a lack of convective inhibition. Inness *et al.* (2001) found that using 30 model layers with HadAM3, with enhanced vertical resolution around the freezing layer of convection, improved the simulation of the MJO. Deep convection is inhibited due to the convection being capped by the inversion created by the freezing layer. Without this inversion being adequately resolved, as is the case with 19 levels, deep convection can form too readily over a warm SST anomaly. This leads to the close relationship between SST and precipitation modelled with 19 levels.

Many authors have shown that the position of the North Pacific response to El Niño is relatively insensitive to the longitudinal location of the tropical heating anomaly (eg. Geisler *et al.*, 1985; Sardeshmuckh and Hoskins, 1988). The latter argue that the longitudinal location of the forcing is dependent on the location of strong meridional gradients of vorticity. However, for the case of a very strong El Niño event such as 1982/83, the tropical heating anomaly is sufficiently large to alter the basic state, shifting the location of maximum meridional gradients. This emphasises the importance of studying absolute fields as well as anomalies.

References

Geisler, J., Brown, M., Bates, G., and Muñoz, S. (1985). Sensitivity of January climate response to the magnitude and position of equatorial pacific sea surface temperature amomalies. *Journal of Atmospheric Science*, **42**(10), 1037–1049.

Inness, P., Slingo, J., Woolnough, S., Neale, R., and Pope, V. (2001). Organization of tropical convection in a GCM with varying vertical resolution; implications of the Madden-Julian Oscillation. *Climate Dynamics*, **17**(10), 777–793.

Kalnay, E., Kanamitsu, M., Kistler, R., Collins, W., Deaven, D., Gandin, L., Iredell, M., Saha, S., White, G., Woollen, J., Zhu, Y., Leetmaa, A., Reynolds, B., Chelliah, M., Ebisuzaki, W., Higgins, W., Janowiak, J., Mo, K., Ropelewski, C., Wang, J., Jenne, R., and Joseph, D. (1996). The NCEP/NCAR Reanalysis 40-year Project. *Bulletine of the American Meteorological Society*, **77**, 437–471. Web site http://www.cdc.noaa.gov.

Marshall, J. and Molteni, F. (1993). Toward a dynamical understanding of planetary-scale flow regimes. *Journal of Atmospheric Science*, **50**(12), 1792 –1818.

Parker, D. E., Folland, C. K., and Jackson, M. (1995). Marine surface temperature: observed variations and data requirements. *Climatic Change*, **31**, 559–600.

Pope, V. and Stratton, R. (2001). The processes governing horizontal resolution sensitivity in a climate model. *Submitted to Climate Dynamics*.

Pope, V., Gallani, M., Rowntree, P., and Stratton, R. (2000). The impact of new physical parameterisations in the Hadley Centre climate model: HadAM3. *Climate Dynamics*, **16**, 123–146.

Rodwell, M. and Folland, C. (2001). Atlantic air-sea interaction and seasonal predictability. *Quarterly Journal of the Royal Meteorological Society*, **127**, 1–33.

Sardeshmuckh, P. and Hoskins, B. (1988). The generation of global rotational flow by steady idealized tropical divergence. *Journal of Atmospheric Science*, **45**(7), 1228–1251.

Spencer, H. and Slingo (2002). The simulation of the seasonal evolution of ENSO by an atmospheric general circulation model. *submitted to J. Clim.*

Xie and Arkin (1996). Analyses of global monthly precipitation using gauge observations, satellite estimates, and numerical model predictions. *Journal of Climate*, **9**, 840 –858.

The Impact of Sub-seasonal Sea Surface Temperature Variability on the Simulation of the Seasonal Mean Extra-tropical Circulation

Ben Kirtman
Center for Ocean-Land-Atmosphere Studies

The purpose of this study is to examine the impact of sub-seasonal sea surface temperature (SST) variability on the simulation of the seasonal mean extra-tropical circulation using a state-of-the-art high resolution atmospheric general circulation model (AGCM). The format is a case study for January through March 1989 (JFM89) and the primary emphasis is on regional scales over North America. The SST boundary conditions in the AGCM simulations were prescribed using observed weekly data. Experiments were made in which the week-to-week (sub-seasonal) SST variability was suppressed. In terms of the largest spatial scales, the sub-seasonal SST variability has only a modest impact; however, statistically significant modifications to the 500 mb height anomalies over North America were detected. Consistent with these changes in the height field, the seasonal mean North American rainfall anomalies were particularly sensitive to the sub-seasonal SST variations, especially over the Pacific Northwest.

Two possible mechanisms for this sensitivity were investigated with additional AGCM experiments and model diagnostics. The first mechanism, referred to as a "stochastic" effect, is defined by the hypothesis that the week-to-week SST variability only serves to enhance the amplitude of tropical precipitation variability, which, in turn, modifies the mid-latitude response. With this "stochastic" effect, the details of the sub-seasonal SST evolution do not matter. In contrast, the second mechanism is a "deterministic" effect in that the details of the evolution of the sub-seasonal SST matter. The experiments presented here indicate that the "stochastic" effect is small and that the details of the sub-seasonal SST produce significant differences. This conclusion is supported by experiments with very large ensembles using a somewhat lower resolution AGCM and a non-linear barotropic model. Finally, some implications of these results for real time forecasting are discussed.

Simulation of Time Mean Tropical Circulation and Its Variations in AMIP Runs Using Different Versions of the Operational NCEP Global Model

Suranjana Saha
Environmental Modeling Center (EMC)
National Centers for Environmental Prediction (NCEP)
Washington, D.C.
Suranjana.Saha@noaa.gov

A primary reason to believe there could be predictability beyond week-2 would be skill in forecasting organized transient tropical convection, such as the MJO which has time scales of 20-70 days. Assuming that the forecast should be made by a model (GCM), it has been a perennial frustration to modelers that GCM's do not simulate, let alone predict, phenomena like the MJO very well at long leads. At NCEP we are revisiting this topic anew, and have made many 1 year (2001) AMIP style model integrations. Three different horizontal resolutions (T62, T126 and T170), as well as three different vertical resolutions (L28, L42 and L64) have been combined with two different convective parameterization schemes (SAS and RAS). In all 9 such runs have been made. All experiments start on 15 Dec 2000 and end on 31 Dec 2001 ... 382 days. The timeseries for most fields have been saved for 0Z, 6Z, 12Z and 18Z....total of 382 x 4 =1528 time levels. Monthly means for all diabatic heating components as well as other important 3_D quantities have been saved and is available to the community. For a reality check we used three operational NCEP analyses for the same 1 year period, specifically the high resolution T170L42 GDAS, the low resolution T62L28 GDAS, and the T62L28 CDAS.

The question is how well do we simulate upper level divergence or tropical velocity potential anomalies and how do they depend on the convection scheme, horizontal or vertical resolution. Fortunately, the year 2001 had strong MJO activity. Leaving aside questions of short range forecast skill (first 2 weeks), we studied the amplitude of the anomalies, and the phase speed or period in the extended integration. We found that most model versions had an acceptable strength of velocity potential anomalies, but the westerly phase speed of the MJO appear to be too low in nearly all model versions, except in a few. Study of the diabatic heating fields has yet to establish whether the results are merely fortuitous, or correct for the right reason.

An Empirical Estimate of Subseasonal Predictability

Matt Newman
NOAA-CIRES Climate Diagnostics Center
Boulder, Colorado

Linear inverse models (LIMs) suitable for studies of atmospheric extratropical variability and predictability on longer than weekly time scales have been constructed for each season of the year, using atmospheric observations of the past 30 years. Notably, these empirical-dynamical models include tropical diabatic heating as a predicted model variable rather than as a forcing, and also include, in effect, the feedback of the extratropical weather systems on the more slowly varying circulation. The models are capable of reproducing both lagged covariance statistics from independent data and the development of individual streamfunction and tropical heating anomalies. In fact, week 2 predictions by the models have skill comparable to that of the NCEP MRF ensemble mean forecasts (forecasts are available at http://www.cdc.noaa.gov/lim). Comparison to a 20-year dataset of "reforecasts" using the early 1998 operational version of the MRF further shows that the LIM has notably higher week 3 skill year-round, and may even have higher week 2 skill during spring. The LIM also has much greater skill than the MRF for forecasts of tropical diabatic heating.

Theoretical predictability limits derived for the LIM suggest that the model has useful mean forecast skill at forecast lead times of between three and five weeks, depending upon both season and geographical region. Some initial atmospheric states which result in strong deterministic growth are associated with greater predictability because of a relatively high signal to noise ratio, although these states too have strong seasonal dependence. Our analysis further suggests that without inclusion of tropical heating, weekly averages may be predictable between about 1-2 weeks in the extratropics, but with tropical heating included, they may be predictable as far as 5-7 weeks ahead.

Sensitivity of streamfunction anomaly growth to both the strength and location of tropical diabatic heating anomalies is shown to shift from the central Pacific in winter to the West Pacific and Indian oceans in summer. Such optimal anomaly growth is related not only to ENSO but also to tropical intraseasonal variability. These results also have important implications for the development of persistent anomalies, such as North American heat waves and droughts.

Role of Satellite Rainfall Information in Improving Understanding of the Dynamical Link Between the Tropics and Extratropoics Prospects of Improved Forecasts of Weather and Short-Term Climate Variability on Sub-Seasonal Time Scales

Arthur Y. Hou
Data Assimilation Office
NASA Goddard Space Flight Center, Greenbelt, MD USA 20771
E-mail: arthur.hou@gsfc.nasa.gov

Abstract

The tropics and extratropics are two dynamically distinct regimes. The coupling between these two regimes often defies simple analytical treatment. Progress in understanding of the dynamical interaction between the tropics and extratropics relies on better observational descriptions to guide theoretical development. However, global analyses currently contain significant errors in primary hydrological variables such as precipitation, evaporation, moisture, and clouds, especially in the tropics. Tropical analyses have been shown to be sensitive to parameterized precipitation processes, which are less than perfect, leading to order-one discrepancies between estimates produced by different data assimilation systems.

One strategy for improvement is to assimilate rainfall observations to constrain the analysis and reduce uncertainties in variables physically linked to precipitation. At the Data Assimilation Office at the NASA Goddard Space Flight Center, we have been exploring the use of tropical rain rates derived from the TRMM Microwave Imager (TMI) and the Special Sensor Microwave/ Imager (SSM/I) instruments in global data assimilation. Results show that assimilating these data improves not only rainfall and moisture fields but also related climate parameters such as clouds and radiation (Fig. 1), as well as the large-scale circulation and short-range forecasts (Fig. 2). These studies suggest that assimilation of microwave rainfall observations from space has the potential to significantly improve the quality of 4-D assimilated datasets for climate investigations (Hou et al. 2001).

In the next few years, there will be a gradual increase in microwave rain products available from operational and research satellites, culminating to a target constellation of 9 satellites to provide global rain measurements every 3 hours with the proposed Global Precipitation Measurement (GPM) mission in 2007. Continued improvements in assimilation methodology, rainfall error estimates, and model parameterizations are needed to ensure that we derive maximum benefits from these observations.

References

Hou, A. Y., S. Zhang, A. da Silva, W. Olson, C. Kummerow, J. Simpson, 2001: Improving global analysis and short-range forecast using rainfall and moisture observations derived from TRMM and SSM/I passive microwave instruments. *Bulletin of Amer. Meteor. Soc.*, **82**, 659-679.

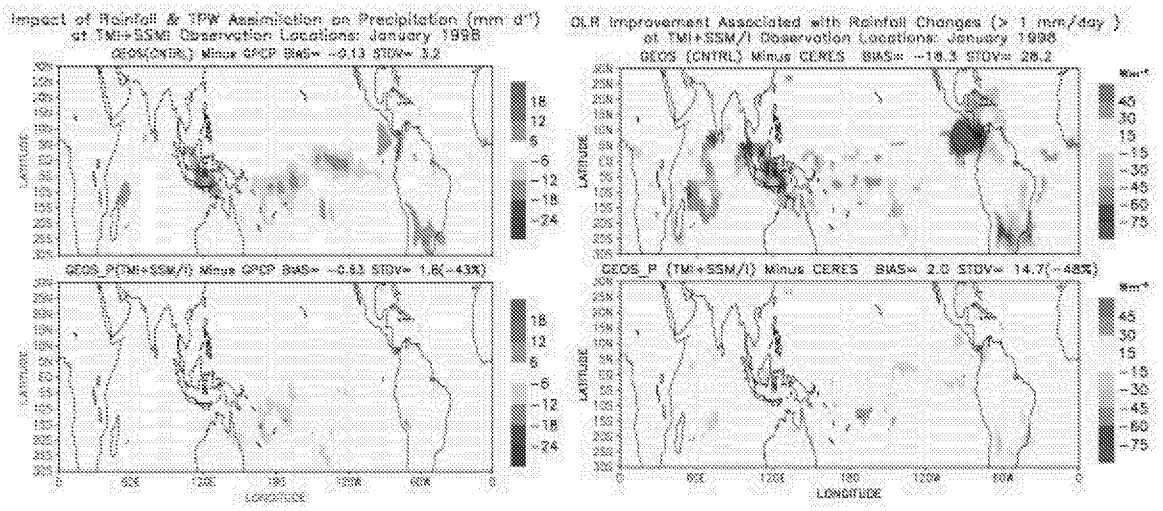

Figure 1. GEOS assimilation results with and without TMI and SSM/I observations for January 1998. Left panels show errors in the monthly-mean tropical precipitation fields verified against GPCP combined Satellite-gauge estimate: Top is the difference between the GEOS control (without rainfall and TPW data) and GPCP. Bottom is the corresponding error in GEOS assimilation with rainfall and TPW data. Right panels show the impact on the outgoing longwave radiation (OLR) verified against CIRES/TRMM measurements. Percentage changes in the tropical-mean error standard deviation relative to the GEOS control are given in parentheses.

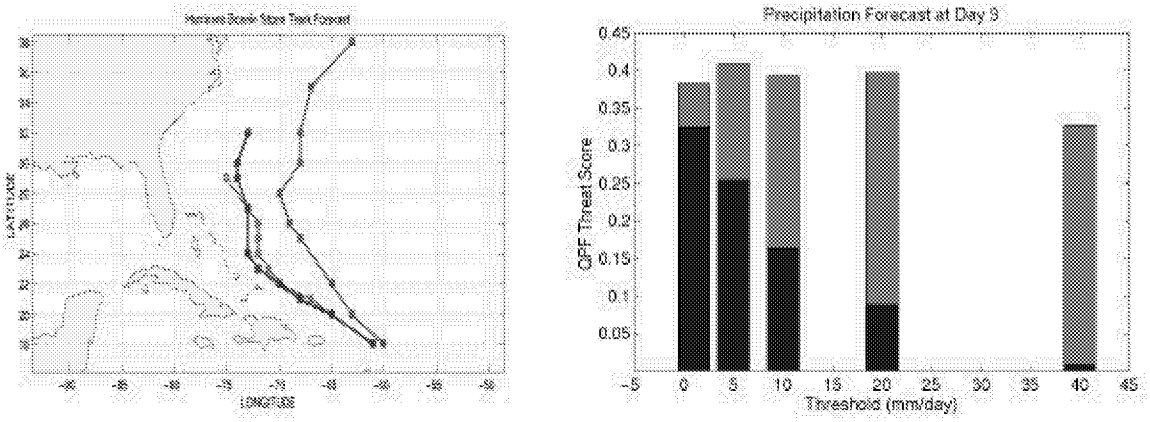

Figure 2. Improved storm track forecasts and QPF Equitable Threat Scores for Hurricane Bonnie. The left panel shows that the 5-day storm track forecast initialized with 1° x 1° GEOS analysis containing TMI and SSM/I rainfall data (blue) is in close agreement with the best track analysis from NOAA. The track from the control experiment is shown in green. The forecasts are initialized at 12:00 on 20 August 1998. The right panel shows the consistently higher Equitable Threat Scores for Day 3 precipitation forecast (red) initialized by the analysis with rainfall data. Results for the control experiment are shown in blue. A higher Threat Score corresponds to greater forecast skills.

Session V

Role of Land Surface Processes

Predictability Associated with Land Surface Moisture States – Studies with the NSIPP System

R. D. Koster and M. J. Suarez

1. Introduction

Hydrologists have long speculated that soil moisture information can be used to increase skill in monthly to seasonal forecast systems. For this to be true, though, three conditions must be satisfied: (1) an imposed initial soil moisture anomaly in the forecast system must have some memory, so that it persists into the forecast period; (2) the modeled atmosphere must respond in a predictable way to the persisted anomaly; and (3) the forecast model must correctly represent both the soil moisture memory and the atmospheric response as they occur in nature. In this short paper, we review some recent work at NSIPP (NASA Seasonal-to-Interannual Prediction Project) that addresses all three conditions.

2. Analysis of Requirement 1: Soil Moisture Memory

Koster and Suarez (2001) manipulated the water balance equation into an equation that relates the autocorrelation of soil moisture – soil moisture memory – to four separate controls: (1) a restoring force due to evaporation's sensitivity to soil moisture, (2) a restoring force due to runoff's sensitivity to soil moisture, (3) seasonal variability in climatic forcing, and (4) any correlation that may exist (through feedback or otherwise) between soil moisture at the beginning of the time period and subsequent forcing. The equation was found to reproduce well the autocorrelations that were actually simulated by the GCM. Thus, it can be used to analyze the controls over soil moisture memory at any given grid cell. Koster and Suarez (2001) found, for example, that the runoff sensitivity provides the main control over soil moisture memory in the eastern U.S., whereas the evaporation sensitivity provides the main control in the west. In the central U.S., the evaporation effect is counteracted somewhat by a nonzero soil-moisture/forcing correlation.

3. Analysis of Requirement 2: Atmospheric Response to Land Moisture Anomalies

The response of the atmosphere to soil moisture anomalies was investigated by Koster et al. (2000) with two parallel 16-member ensembles of 45-year simulations. In the first ensemble, the land surface was allowed to evolve freely with the atmosphere. In the second, it was not – instead, an interannually-varying time series of evaporation efficiency (as derived from one of the simulations in the first ensemble) was prescribed at each grid cell. Thus, every member of the second ensemble was effectively given the same time series of land surface moisture boundary conditions. Also, interannually-varying SSTs were prescribed in both ensembles. Thus, the first ensemble addresses the question, "What is the impact of a perfect knowledge (now and into the future) of SSTs on precipitation", whereas the second addresses the question, "What is the impact of a perfect knowledge (now and into the future) of both SSTs and soil moisture on precipitation?"

By determining the degree to which the precipitation amounts within each ensemble agree with each other, we obtain a quantitative estimate of the impact of SSTs and soil moisture on precipitation. This is illustrated in Figure 1, which shows, for North America, an index that

effectively describes the fraction of region's precipitation variance that is explained by the noted boundary condition.

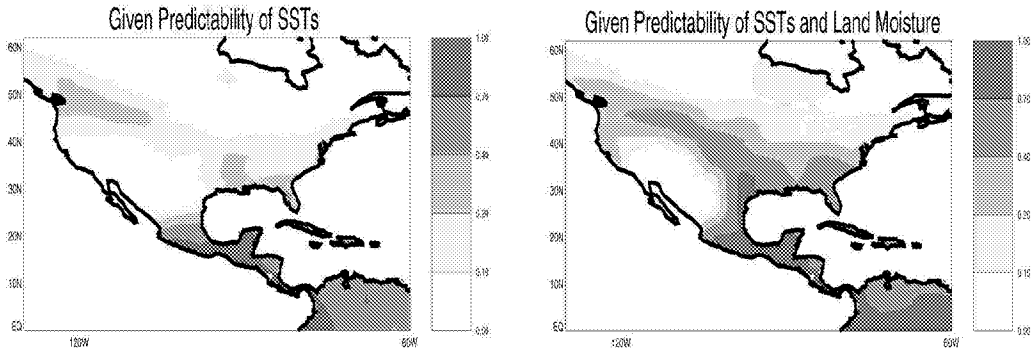

Figure 1. (left) Index of precipitation predictability given predictability of SSTs. (right) Index of precipitation predictability given predictability of SSTs and land moisture.

The figure shows, in essence, that foreknowledge of soil moisture could have a tremendous impact on our ability to predict precipitation in a swath that extends from the Gulf of Mexico to the northeast United States.

4. Combined Study: Impact of Land Moisture Initialization in the NSIPP system

In a recently submitted paper, Koster and Suarez (2002) describe a series of numerical experiments that effectively combine the two requirements examined above. The experiments consist of ensembles of 3-month precipitation forecasts that utilize "realistic" initial soil moisture conditions, as obtained through the previous application of observed daily precipitation to the GCM's land surface. The GCM's land and atmosphere are allowed to evolve together during each forecast period. Thus, for the forecasted precipitation to be influenced by the initialization, soil moisture memory must be significant *and* the atmosphere must be responsive to soil moisture anomalies.

The index plotted in Figure 2 (top) shows where soil moisture initialization had a significant impact on forecasted JJA precipitation at least once during the 5 boreal summers of study. The salient feature of the plot is the relatively small influence the initialization had over much of the globe. The influence is essentially limited to swaths in central North America, below the Amazon, in central Africa, and in western Asia. The bottom plot of Figure 2 shows where we might predict a significant impact based on: (1) a significant degree of interannual soil moisture variability on day 1, as measured by the standard deviation of initial soil moisture (in essence, it turns out, a surrogate for soil moisture memory); (2) an adequate sensitivity of evaporation to soil moisture, as measured by the product of the mean net radiation and the fitted slope of the evaporation ratio - soil moisture relationship; and (3) an adequate sensitivity of precipitation to evaporation, as measured by the convective fraction. The predicted locations agree well with the actual locations of impact, suggesting that we have correctly identified the controls of relevance.

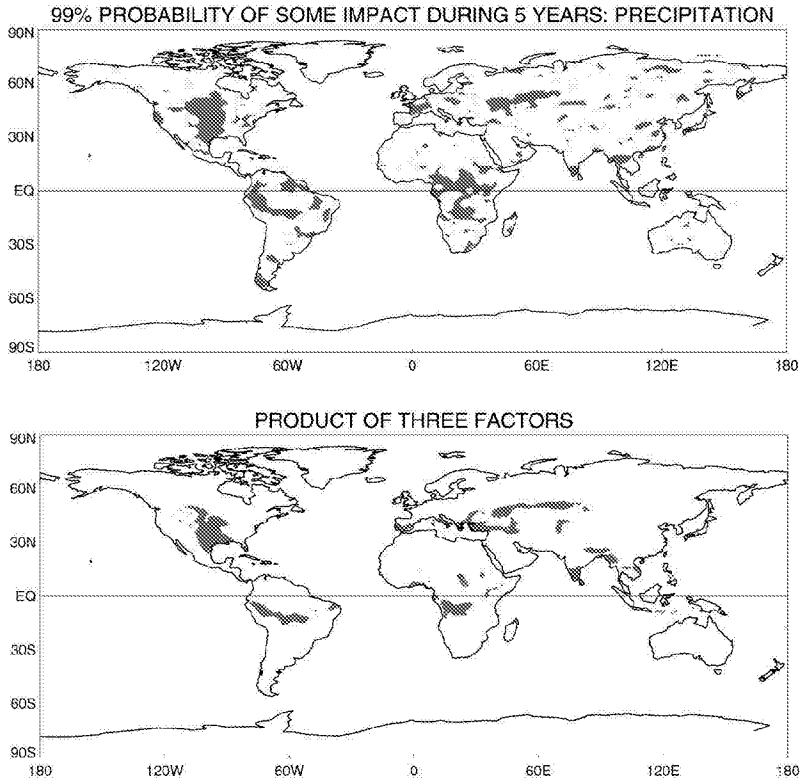

Figure 2. (top) Indication of where soil moisture initialization had some impact on forecasted precipitation during 5 years of experiment. (bottom) Indication of where the three factors mentioned in the text are all simultaneously large.

5. Analysis of Requirement 3: Realism of Model Results

Unfortunately, global observations of soil moisture and/or land-atmosphere feedback are non-existent, so we cannot verify many of our model results. The best we can do is demonstrate indirectly that they are consistent with available observations.

A signature of land-atmosphere feedback over the United States was sought in the 50-year "Unified Precipitation Database" generated by NCEP (Wayne Higgins, pers. comm.). Specifically, the data were analyzed to determine if a band of high precipitation autocorrelation (between pentads at lag 2) appears down the center of the U.S., as it does in the GCM due to feedback. The observations do indeed show this band in July, when it is also strongest in the GCM. This result is not conclusive, however, since the band of nonzero autocorrelations may also reflect monsoon dynamics, long-term precipitation trends, or other external influences. In any case, the magnitudes of the autocorrelations are much reduced in the observational data, suggesting that the GCM overestimates the feedback.

In one recent study of model dependence (Koster et al., 2002), four different GCMs performed the same highly controlled numerical experiment. The experiment was specifically designed to isolate the strength of land-atmosphere coupling in each host model. The variations between the models were surprisingly large, with the NSIPP model showing the largest coupling strength. Due to the non-existence of relevant observations, the models could not be ranked in terms of realism. Rather, the experiment served to showcase the uncertainty with which modelers understand the coupling.

6. Summary

The NSIPP coupled land-atmosphere modeling system has been used to investigate many aspects of land-atmosphere interaction. The overarching goal is to determine the value of soil moisture initialization for long-term forecasts.

7. References

Koster, R. D., M. J. Suarez, and M. Heiser, 2000: Variance and predictability of precipitation at seasonal-to-interannual timescales. *J. Hydrometeorology*, **1**, 26-46.

Koster, R. D. and M. J. Suarez, 2001: Soil moisture memory in climate models. *J. Hydrometeorology*, **2**, 558-570.

Koster, R. D., P. A. Dirmeyer, A. N. Hahmann, R. Ijpelaar, L. Tyahla, P. Cox, and M. J. Suarez, 2002: Comparing the degree of land-atmosphere interaction in four atmospheric general circulation models. *J. Hydrometeorology*, **3**, 363-375.

Koster, R. D. and M. J. Suarez, 2001: Impact of soil moisture initialization on seasonal weather prediction, submitted to *J. Hydrometeorology.*

The Predictability of Soil Moisture and Near Surface Temperature Based on the Hindcasts of NCEP Seasonal Forecast Model

By

Masao Kanamitsu (CRD/SIO, University of California, San Diego)
Cheng-Hsuan Lu (EMC/NCEP/NOAA)

Wesley Ebisuzaki (CPC/NCEP/NOAA) and
Jae Schemm (CPC/NCVEP/NOAA)

(Accepted in Journal of Climate after minor revision, Aug. 2002)

Using the NCEP/DOE Reanalysis soil moisture analysis and the NCEP Seasonal Forecast System, the seasonal predictability of the soil moisture, and near surface temperature over the globe were examined. It is shown that the NCEP/DOE Reanalysis soil moisture is reasonably good over the United States compared to an independent soil moisture observation. This means that the current experiments are conducted under more realistic conditions in contrast to model-based studies performed in the past.

Two sets of forecasts were made, one starting from climatological soil moisture as initial condition and the other starting from NCEP/DOE Reanalysis soil moisture. Each set is made of 10-member ensemble, 7-month integrations, 16 early Aprils as initial conditions for the 1979-1996 period.

The predictability of the soil moisture was examined over several regions over the globe with different climatological characteristics (Fig. 1), and the results are presented in Fig.2. It is found that the prediction skill of soil moisture is very high over regions where there is little or less precipitation. Over these areas, the soil moisture evolution is largely determined by the evaporation process, and the model does an excellent job in predicting this process. In many of these relatively dry or low precipitation areas, model prediction surpasses the anomaly persistency forecast. Over temperate zones with more precipitation, and over tropical monsoon regions, the prediction skill of the soil moisture drops quickly in the first 3-4 months. Over these regions, the soil moisture evolves following the Markov process in which precipitation acts as a white noise forcing and the soil moisture decays exponentially. The time scale of this Markov process computed as a ratio between precipitation and potential evaporation showed that the time scale is particularly short over the monsoon regions and some temperate zones. Over all the regions noted above, the forecast starting from climatological soil moisture is very poor, indicating that the soil moisture anomalies cannot be generated by model precipitation or by the model evaporation. From a practical point of view, the soil moisture initial condition is essential in making seasonal prediction over these areas. In contrast, the characteristics are very different over tropical South America. The forecast starting from climatological soil moisture quickly catches up to the forecast skill of initial soil moisture as well as the anomaly persistency. Particularly in the Northeast region of South America, the anomaly persistency becomes the worst forecast after 4 months. Over these areas, SST forcing determines the precipitation anomaly over land, and subsequently forces the soil moisture evolution. The effect of initial soil

moisture information tends to disappear after 3-4 months over these areas.

The near surface temperature anomaly forecast is closely related to the soil moisture anomaly forecast. The correlation, however, is not perfect. Thus the near surface temperature forecast skill is lower than the soil moisture forecast skill. Our analysis shows that the skill of predicting latent heat flux is lower than that of the soil moisture, and that of the surface temperature is even lower. This is because additional physical processes, such as cloudiness and near surface atmospheric conditions are also involved in determining the near surface air temperature.

The abundance of near surface temperature observation allows us to verify our hindcasts with independent data that are not used in the NCEP/DOE Reanalysis. The verification of temperature made against CD433 data clearly indicated that the use of the NCEP/DOE reanalysis soil moisture initial condition truly improved the forecasts.

For better prediction of soil moisture and near surface temperature during summer, it is important that the soil moisture initial condition is accurately specified and the model produces better precipitation forecast. Unfortunately, these two requirements are very difficult to satisfy, and further advances in observational and modeling studies are needed. Independent measure of the soil moisture is also extremely important to eliminate any model dependent result. In this regard, satellite observation that provides soil moisture measurement is becoming available, and the use of such data is strongly encouraged.

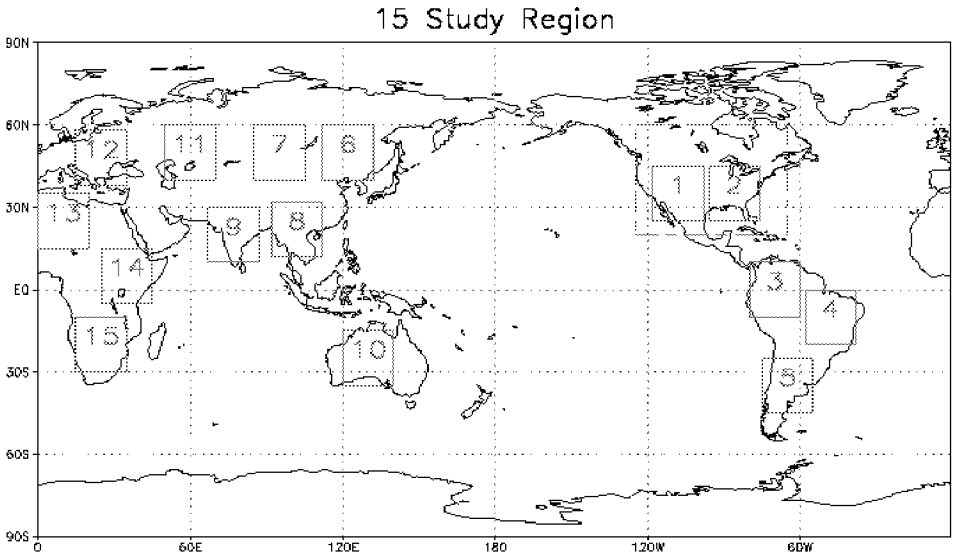

Figure 1. Areas selected for the verification of soil moisture.

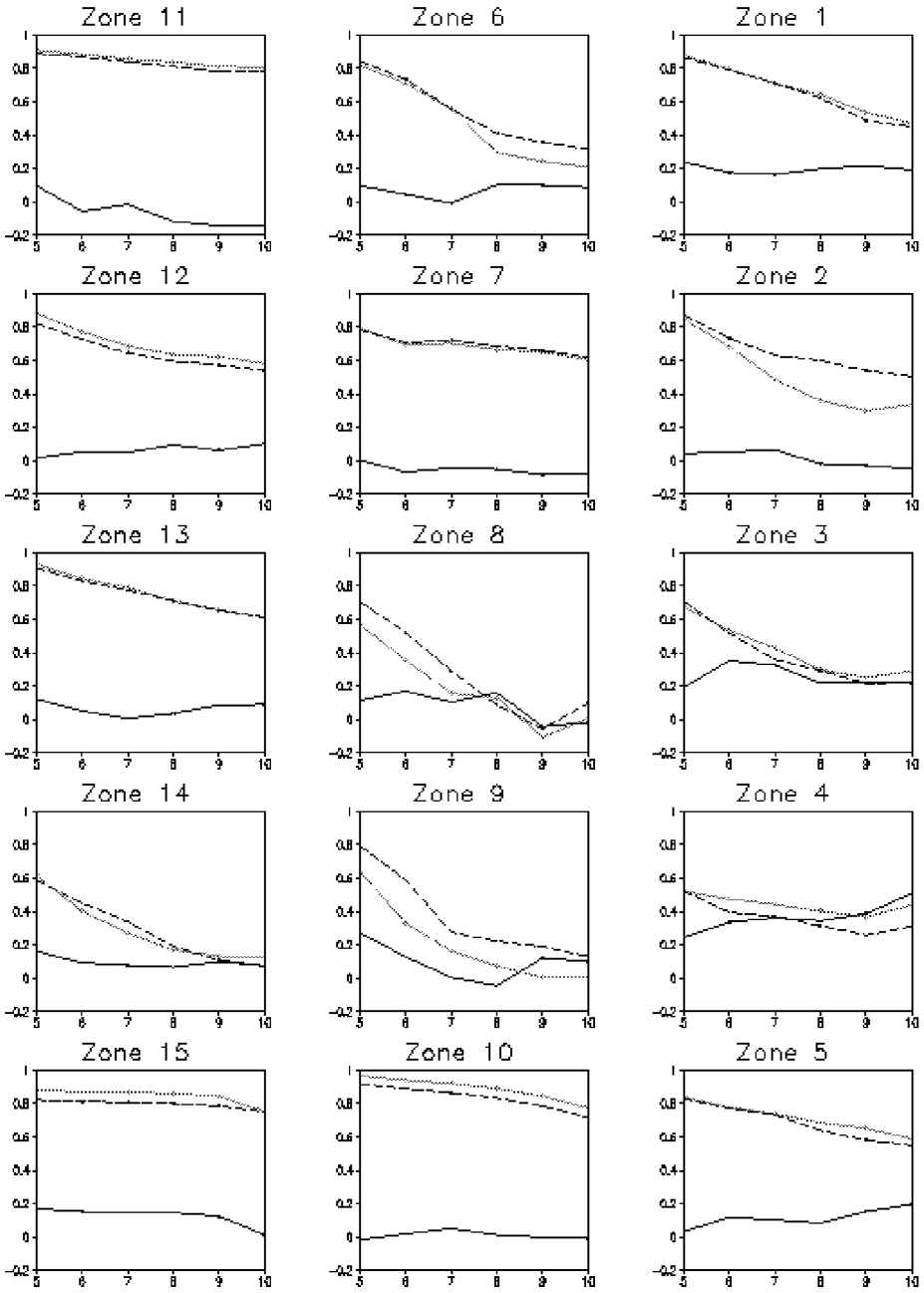

Figure 2. Soil moisture prediction skill decay curve for the 15 regions selected in Figure 2. Anomaly pattern correlation in abscissa and lead-time (month) in ordinate. The first month score is not plotted. Forecast from climatological soil moisture (dark solid), forecast from analysis soil moisture (light solid) and anomaly persistency (dashed) are plotted.

The Impact of Land Initialization and Assimilation on Climate Predictability and Prediction

C. Adam Schlosser (GEST/UBMC/NASA),
P. C. D. Milly (USGS/GFDL),
Paul A. Dirmeyer (COLA),
and David Mocko (SAIC/GSC)

Analysis will be presented which explores the impact of land conditions on monthly to seasonal climate simulations in a variety of atmospheric general circulation models (AGCMs). In one set of experiments, the Geophysical Fluid Dynamics Laboratory (GDFL) AGCM is used to explore the nature of soil-moisture predictability and associated climate predictability as an initial value problem. For another set of experiments, the Center for Ocean Land Atmosphere (COLA) and the Goddard Earth Observing System 2 (GEOS-2) AGCMs are used to investigate the impact of realistic snow initialization and assimilation in retrospective climate forecasts for the northern hemisphere spring (March-June).

In the GFDL AGCM experiments, soil-moisture predictability can be characterized by a first-order Markov process, and thus directly linked to soil-moisture persistence. As such predictability timescales of soil moisture are found to range from as little as a week (mid-latitude summer, tropics, and subtropics) to 2-6 months (middle to high latitude fall and winter). The degree of translation of soil-moisture predictability to atmospheric predictability is characterized by the ratio of the fraction of explained variance of an atmospheric variable to that of soil moisture. By this measure, high associated predictability (ratio greater than 0.5) of near-surface air temperature is found in the tropics, subtropics, and mid-latitude summers. In contrast, no widespread, appreciable associated precipitation predictability is found. Other recent climate-model experiments (e.g. Koster *et al.* 2001) that quantify the land's impact on precipitation suggest that a significant range in the magnitude of the simulated precipitation response exists. This poses a compelling task to quantify what the true magnitude of atmospheric response to land conditions is in nature, and how this will guide future activities in land-data assimilation and climate studies/prediction.

The diagnosis of the COLA AGCM snow initialization/assimilation experiments suggest that the most notable and widespread impact (focusing on near-surface air temperature skill) occurs during the month of April, and a weak impact is seen in the remaining months of the simulations (i.e. March, May, and June). The result is consistent with the intuitive expectation that (realistic) snow-cover anomalies will support strong (and skillful) temperature responses when coincident with relatively high incident solar radiation (i.e., when the impact of albedo modulation from the snow anomalies would be maximal). Results from the GEOS-2 AGCM, using a similar land surface model as in the COLA AGCM but with an improved snow-physics scheme, will also be analyzed and compared to the COLA AGCM results. The strength of the two AGCMs' responses to the snow assimilation are assessed accordingly against the errors of simulated snow in the control runs, as well as the representation of snow processes (and their functional link to the surface energy budget) between the AGCMs.

Three Modes of Climate Drift in Coupled Land-Atmosphere Systems

Paul A. Dirmeyer
Center for Ocean-Land-Atmosphere Studies

Three different modes of climate drift have been identified in a coupled land-atmosphere climate model. The fastest growing error modes are those associated with errors in the atmospheric initial conditions. The signature of these modes are evident as drift in the time series of land surface state variables. Second is the climate drift associated with systematic errors on the scale from weeks to seasons. This drift is dominated by the error modes with the largest saturation amplitude. This drift tends to erase the "information" in the anomalies in the land surface initial conditions, that would be expected to provide added predictability to medium-range to seasonal forecasts. Third, there is drift due to the coupled error mode, where systematic errors in the atmospheric physics can push the land surface state beyond its "observed" range or variability over seasons-years. This mode is evident in the clear stratification of skill (both in simulation of mean states, and prediction of anomalies) between DSP-type experiments (1-4 month simulations), and corresponding AMIP or C20C experiments (multi-decadal simulations). The coupled drift mode is relatively weak during winter, but evident during all other seasons. Examples of the three kinds of drift will be shown in global climate simulations, and methods for ameliorating these types of drift will be discussed.

GCM Simulation of the Large-scale North American Monsoon Including Water Vapor Tracer Diagnostics

Michael G. Bosilovich, Siegfried D. Schubert,
Yogesh Sud and Gregory K. Walker
NASA/Data Assimilation Office and Climate
and Radiation Branch
Goddard Space Flight Center
Greenbelt MD
Corresponding Email: mikeb@dao.gsfc.nasa.gov

Introduction

In this study, we have applied GCM water vapor tracers (WVT) to simulate the North American water cycle. WVTs allow quantitative computation of the geographical source of water for precipitation that occurs anywhere in the model simulation. This can be used to isolate the impact that local surface evaporation has on precipitation, compared to advection and convection.

A 15 year 1°? 1.25° simulation has been performed with 11 global and 11 North American regional WVTs. Figure 1 shows the source regions of the North American WVTs. When water evaporates from one of these predefined regions, its mass is used as the source for a distinct prognostic variable in the model. This prognostic variable allows the water to be transported and removed (precipitated) from the system in an identical way that occurs to the prognostic specific humidity. Details of the model are outlined by Bosilovich and Schubert (2002) and Bosilovich (2002). Here, we present results pertaining to the onset of the simulated North American monsoon.

Model and Methodology

The model used is the Finite Volume General Circulation Model (FVGCM) developed at NASA/DAO. The dynamical core is the Lin-Rood semi-Lagrangian dynamics (Lin and Rood, 1996). This dynamical core conserves mass and has been shown to be very good at handling atmospheric tracers. The physical parameterizations are taken from the NCAR Community Climate Model version 3.

Reynolds SST observation data set provides the surface boundary conditions over the oceans. Land data are derived from NCAR data sets. The land model includes prognostic soil temperature and moisture, as well as vegetation temperature, which determines land evaporation. The model was initialized in January 1982, and allowed to spin up for 4 years. WVTs were initialized at zero. Here we analyze the last 15 years (1986 – 2000).

Generally, the model simulates the dynamical circulation satisfactorily (S.-J. Lin, Personal Communication, figures not shown for brevity). The atmospheric moisture over North America is generally well represented, though the model may be drier than NVAP over the western third of the United States and also Mexico (Figure 2). The model does seem to produce too much mean summertime precipitation over land, including the maximum that extends too far to the western states (Figure 2).

NA Monsoon Onset

The onset of monsoon precipitation is generally characterized by a decrease in precipitation in Texas and increase in precipitation in Mexico (Barlow et al. 1998). Figure 3 shows the CPC precipitation difference of July minus June averaged from 1986-1998. The model simulated precipitation shows a signature comparable to the observations. This gives us confidence that the model is able to simulate the large-scale dynamics associated with the monsoon. Note that the model does not resolve the Gulf of California very well, which likely affects the models ability to initiate the monsoon in Arizona. Further, the model evaporation differences seems to show some correlation to the precipitation differences over land, but there seems to be little correlation over the Gulf of Mexico and tropical Atlantic Ocean. It appears that the increase of surface evaporation over the oceanic regions is being transported to the continent.

We next evaluate the geographical sources (Figure 1) of water contributing to the precipitation. Figure 4 shows the percent contribution from each North American source region to precipitation in Texas and western Mexico. June to July shows a jump in the fraction of water supplied from the Gulf of Mexico to Texas, while the total precipitation is decreasing. Corresponding to the decrease in total Texas precipitation is the decrease in local continental sources of water (MX and SP). This is related to the decrease in land evaporation. The increase of the fraction of precipitation from tropical Atlantic Ocean is likely related to the monsoon, and is certainly important, but it seems to be part of the large-scale evolution of the annual cycle. In western Mexico, the increase in July precipitation is related to a shift in the circulation, as Easterlies from the tropical Atlantic replace the contribution from the Pacific, especially the region named Baja Oceanic. One cannot overlook the contribution of water from continental Mexico. The fraction of precipitation from MX (figure 1) is the dominant source in May-July in western Mexico.

Summary and conclusions

There certainly appears to be a connection between the surface evaporation and precipitation over land. WVTs have helped to quantify this connection. Since the ratios of continental precipitation drop over land along with the precipitation, we expect that the decrease of surface evaporation is driving the decrease in precipitation in Texas. The surface evaporation drops, which reduces the water available for convection and decreases the convective instability of the region. Pentad and daily time series are being analyzed to verify this statement.

References

Barlow, M., S. Nigam and E. H. Berbery, 1998: Evolution of the North American monsoon system. *J. Climate*, **11**, 2238 – 2257.

Bosilovich M. G. and S. D. Schubert, 2002: Water vapor tracers as diagnostics of the regional hydrologic cycle, *J. Hydromet.*, **3**, 149-165.

Bosilovich, M. G., 2002: On the Vertical Distribution of Local and Remote Sources of Water for Precipitation. *Accepted* to Meteorology and Atmospheric Physics.

Lin, S.-J., and R. B. Rood, 1996: Multidimensional flux form semi-lagrangian transport schemes. *Mon. Wea. Rev.*, **124**, 2046 – 2070.

Figures

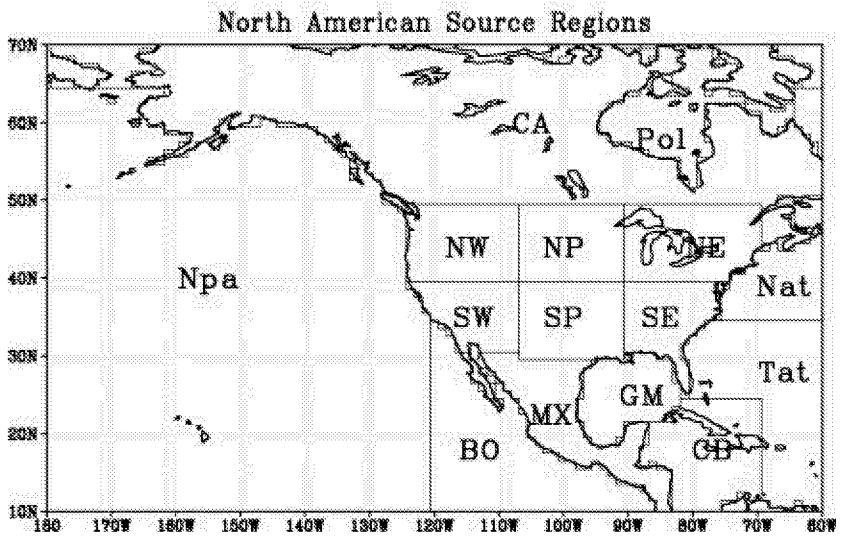

Figure 1 Geographical source regions of water vapor tracers in the model simulation. SE – Southeast; SP – Southern Plains; SW – Southwest; NW – Northwest; NP – Northern Plains; NE – Northeast; CA – Canada; MX – Mexico; Nat – North Atlantic; Tat – Tropical Atlantic; CB – Caribbean; GM – Gulf of Mexico; BO – Baja Oceanic and NP – North Pacific. (Global tracer sources not shown).

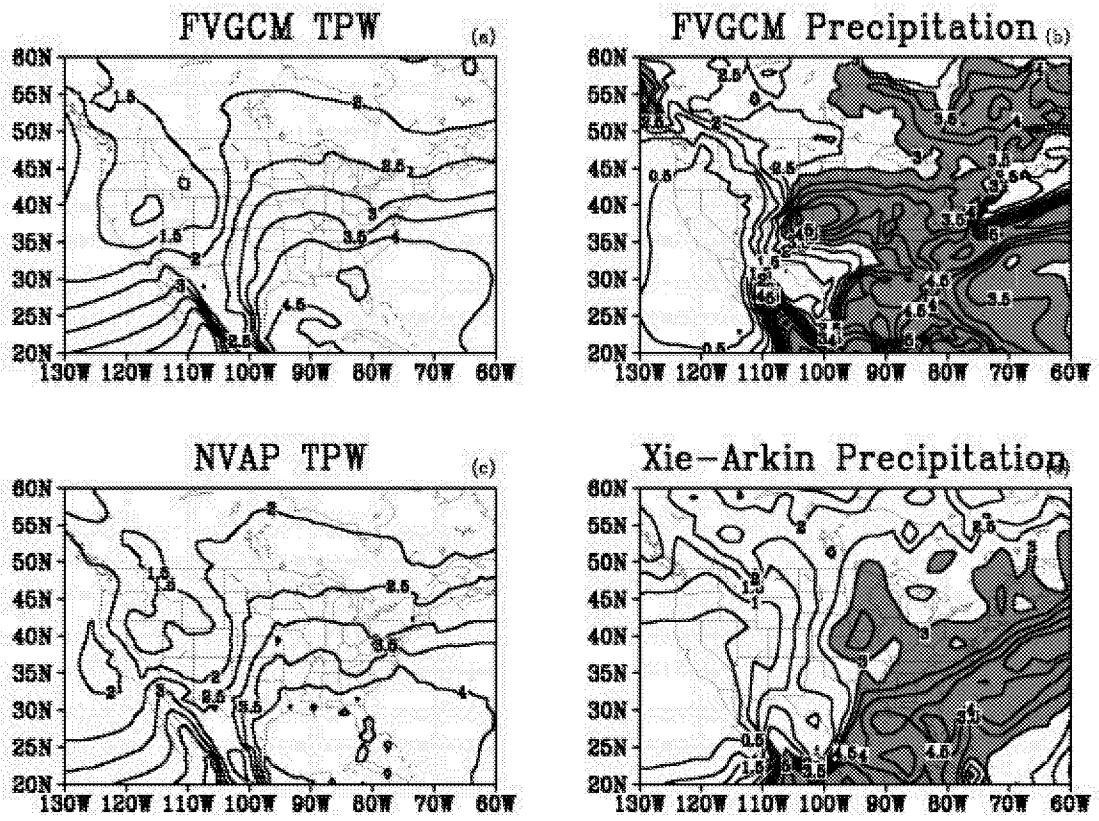

Figure 2 Model validations of precipitation and TPW. Gauge precipitation is averaged over JJA 1986 - 1998 (Wayne Higgins data set, there is no data in Canada or over the ocean). TPW is averaged over the NVAP period (1988-1994). Contours of respective fields are the same, and precipitation greater than 3 mm day^{-1} are shaded.

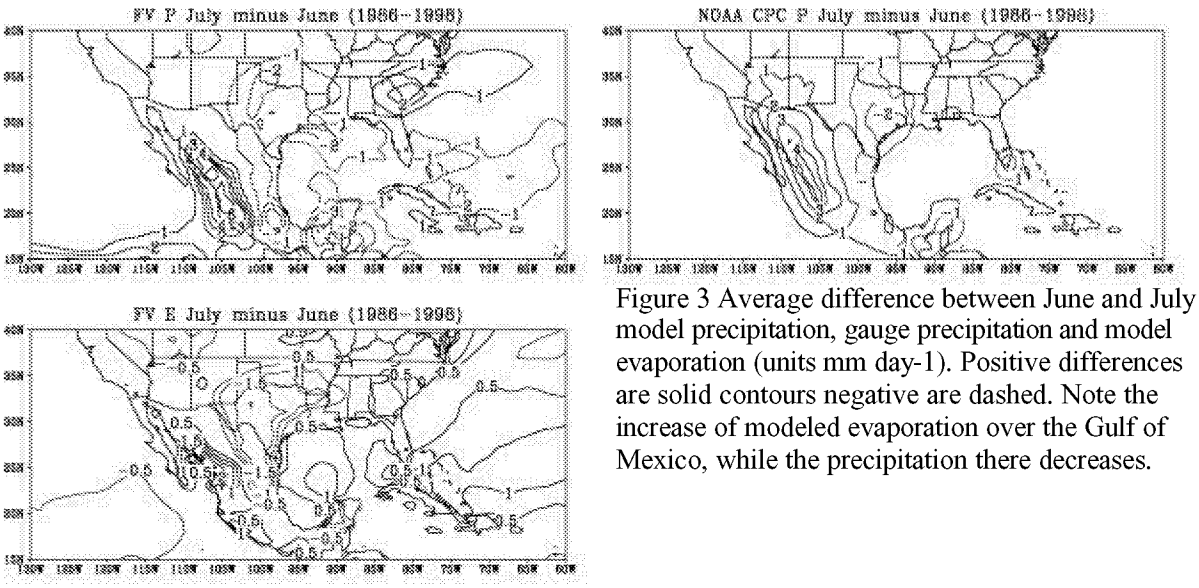

Figure 3 Average difference between June and July model precipitation, gauge precipitation and model evaporation (units mm day-1). Positive differences are solid contours negative are dashed. Note the increase of modeled evaporation over the Gulf of Mexico, while the precipitation there decreases.

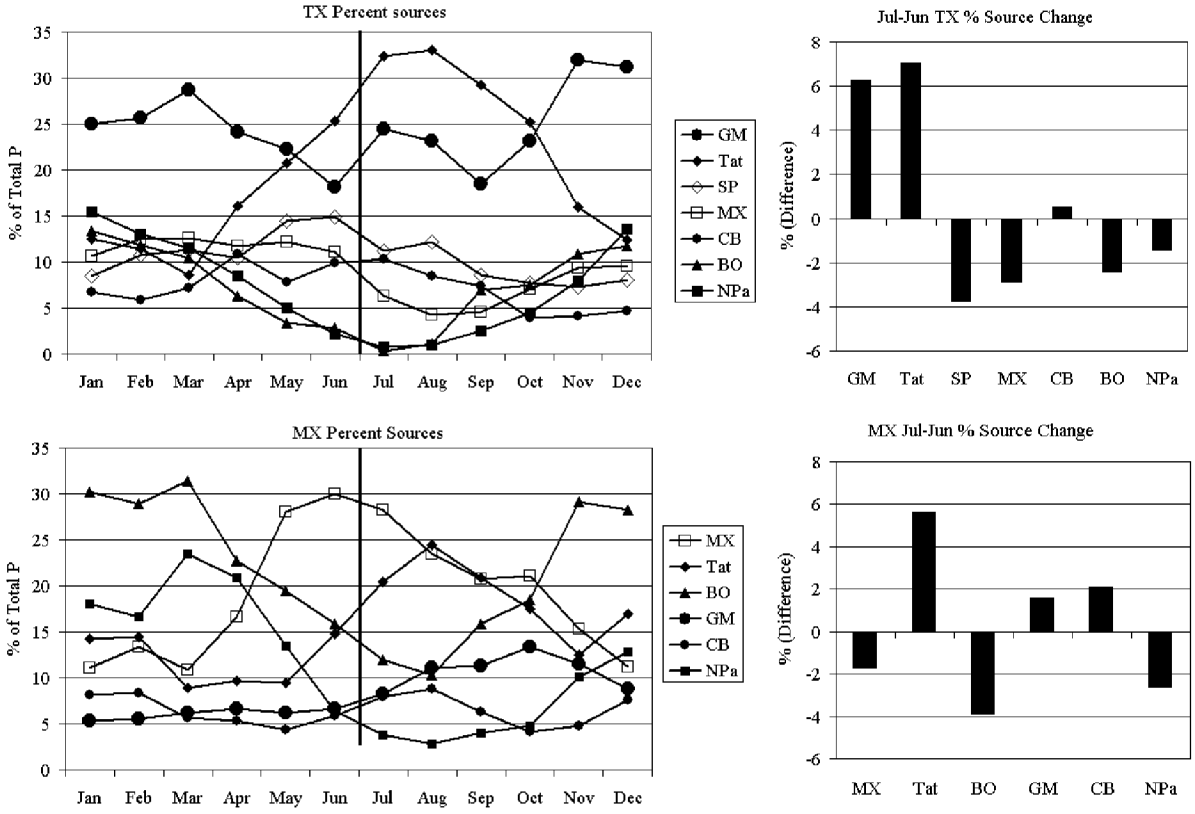

Figure 4 The mean annual cycle of the percent of precipitation that originated as evaporation from key source regions (Figure 1) for Texas (TX) and western Mexico (MX) precipitation. The bar charts show the July minus June difference of the percentages.

Session VI

Link Between Low Frequency and Weather/Regional Phenomena

Storm Track Prediction

Jeffrey S. Whitaker and Thomas M. Hamill
NOAA Climate Diagnostics Center

The transition between a 'climate' and a 'weather' forecast can be defined to occur at the point in the forecast when individual synoptic-scale, 'weather' producing systems can no longer be skillfully predicted. At this point, one must begin issuing forecasts of the statistics of synoptic-scale storms, i.e. the storm tracks, instead of forecasts of the synoptic-scale storms themselves. Storm tracks are predictable as long as the large-scale, low-frequency flow modulates the storm tracks and remains predictable.

In this study we have utilized an "MRF reforecast dataset" (http://www.cdc.noaa.gov/~jsw/refcst), consisting of 23 years of forecasts with a recent version of NCEP's medium range forecast model, to assess the predictability of storm tracks out to week three. Coherent, predictiable modes of storm track variability are identified, and used as a basis for for producing calibrated, quantitative precipitation probability forecasts (QPPF) in week two.

Storm tracks in the MRF reforecast dataset are defined in terms of accumulated precipitation, which in wintertime is primarily produced by synoptic-scale weather systems. Predictable storm track patterns are identified via a canonical correlation (CCA) analysis that uses model forecast precipitation as a predictor, and analyzed precipitation from the NCEP/NCAR reanalysis as a predictand. Figure 1 shows the most predictable DJF storm track pattern for (A) a day 10 forecast, (B) a week two forecast, and (C) an average over the first three weeks of the forecast.

The most predictable storm track pattern is an eastward shift of the climatological Pacific storm track for all three forecast ranges. This shift is associated with a "PNA-like" mode of variability of the tropospheric circulation. However, a similar analysis (not shown) that keys on the most predictable 500 mb height pattern identifies the classic PNA pattern as most predictable That pattern is slightly shifted to the north and east of the pattern shown in Fig. 1, and hence does not as effectively modulate the Pacific storm track.

Correlations between predicted and observed precipitation increase with increasing averaging time (Fig. 1), although the predictability of the associated 500 mb heights does not (not shown). This indicates that the predictability of storm-tracks inherently depends upon the averaging interval. The larger the separation between the averaging interval and the time-scale

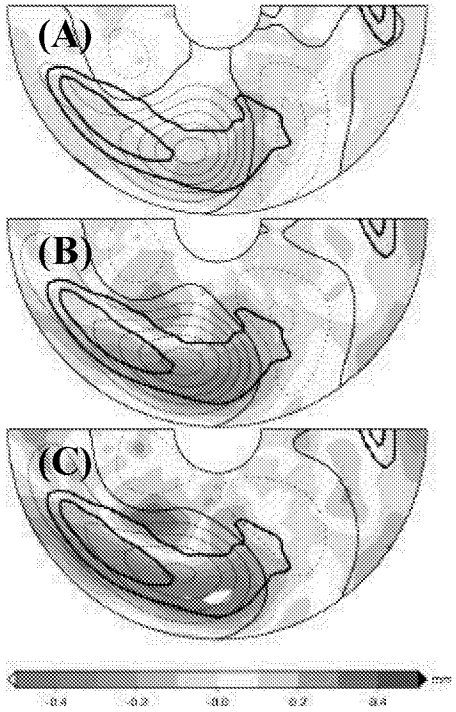

Figure 1: Climatological storm track (thick solid), 500 mb height regression (thin solid) and correlation between the CCA predictor index and analyzed precipitation for the most predictable storm track pattern in (A) 10 day forecasts, (B) week two forecasts and (C) an average over the first three weeks of the forecast.

of the synoptic-scale storms that make up the storm track, the higher the predictability. In the limit that the averaging interval goes to zero, (Fig. 1a) the "storm track" consists of a snapshot of an invidual storm, and predictability is expected only out to the boundary between a weather and a climate forecast (by our definition). Conversely, as the averaging interval becomes much greater than the lifetime of an individual storm, the predictability is determined by the underlying statistical/dynamical relationships between the large-scale flow and the storm tracks.

An experimental real-time 15 member ensemble has been run at CDC since December 2001 using the same model used to generate the "reforecast" dataset. The statistics of forecast

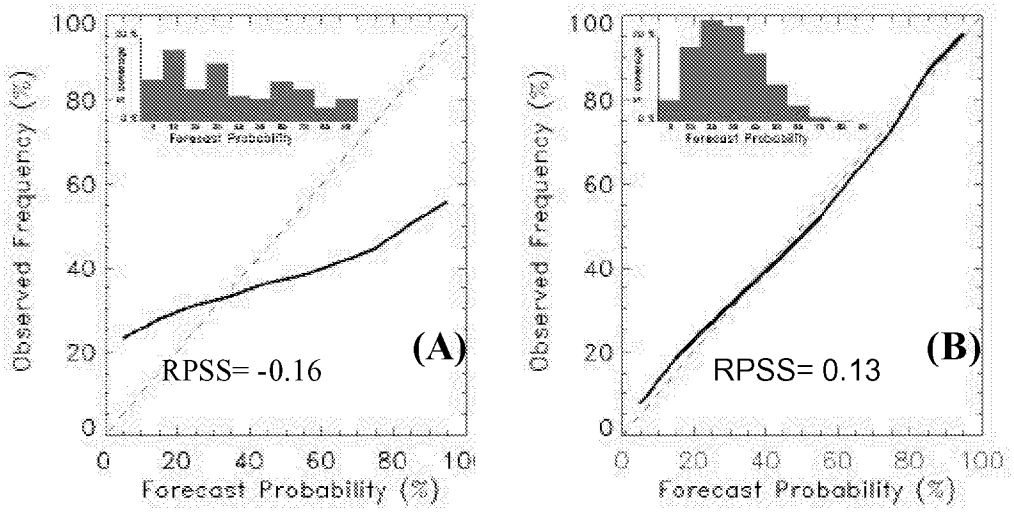

Figure 2: Reliability diagrams for experimental week two tercile probability forecasts for precipitation, derived from a 15 member ensemble for the 90 days starting on Dec 1, 2001. (A) is for probabilities derived from the raw ensemble (by counting the number of members that fall in each tercile, and (B) for probabilities derived using a statistical correction to the first and second moments of the forecast ensemble.

errors derived from this dataset allow for corrections to the first and second moments of the real-time ensemble. These corrections are essential for creating useful QPPF forecasts in week two that take advantage of the predictable storm track modes we have identified. Figure 2 shows reliability diagrams for tercile probability forecasts for week two precipitation over the PNA region computed with and without our statistical correction technique. Without corrections to the first and second moments the forecasts have virtually no reliability, and the ranked-probability skill score (RPSS) is actually worse than that of a climatological forecast. With the corrections derived from the 23-year history of forecast errors, the forecasts are very reliable, and the RPSS indicates that the errors are about 16% better than those of a climatological forecast. A more detailed description of the algorithm for generating the calibrated probabilities is available on our website (http://www.cdc.noaa.gov/~jsw/refcst). We expect that more sophisticated procedures can be used when our ultimate goal of an full 15-member 23 year ensemble reforecast dataset is achieved.

Extreme Weather Events and Their Relationship to Low Frequency Teleconnection Patterns

Yehui Chang: GEST, NASA/GSFC, ychang@dao.gsfc.nasa.gov
Siegfried Schubert: NASA/GSFC, schubert@dao.gsfc.nasa.gov

Introduction

A new method for identifying the structure and other characteristics of extreme weather events is introduced and applied to both model simulations and observations. The approach is based on a linear regression model that links daily extreme precipitation amounts for a particular point on the globe to precipitation and related quantities at all other points. We present here some initial results of our analysis of extreme precipitation events over the United States, including how they are influenced by ENSO and various large-scale teleconnection patterns such as the PNA.

The results are based on simulations made with the NASA/NCAR AGCM (Lin and Rood 1996). The quality of the simulated climate for the NASA/NCAR AGCM forced with observed SSTs is described in Chang et al. (2001). The runs analyzed here consist of three 20-year runs forced with idealized cold, neutral and warm ENSO SST anomalies (superimposed on the mean seasonal cycle of SST). The idealized warm or cold SST anomalies are fixed throughout each 20-year simulation and consist of the first EOF (+/- 3 standard deviations) of monthly SST data. Comparisons are made with the results obtained from a similar analysis that uses daily NOAA precipitation observations (Higgins et al. 1996) over the United States and NCEP/NCAR reanalysis data (Kalnay et al. 1996) for the period 1949-1998.

Method

We consider the simple linear regression model in which a variable Y is regressed against the daily precipitation extremes, X, at a base point o. The regression model has the form

$$Y(j,k) = a\,X(o) + e,$$

where j indicates the jth grid point, k is the time lag in days with respect to the time of the maximum in $X(o)$, and e is the error in the regression model. The regression links the daily extreme (maximum) precipitation for a particular point $X(o)$ with precipitation or other related quantities Y at all other points j, and time lags k. We carry out the analysis for each month of the year separately (e.g. all Januaries, all Februaries, etc.), allowing us to examine the seasonal dependence of the extremes. In the following, we show the composite average of Y over all times when $X(o)$ is an extreme event (the average conditions that occur when $X(o)$ is a maximum). We also show the regression coefficient a. These show the co-variability, or structure and time evolution of the extreme events.

Results

In the following we present some initial results of our analysis. Figure 1 shows, for example, a composite of the precipitation (shading), 300mb heights (contours) and 850mb wind (vectors) during extreme precipitation events for each month at the base grid point (77.5W, 40N). The upper figure shows the results based on 36 years (1949-1998) of daily NOAA precipitation observations and NCEP/NCAR reanalysis. The lower figure shows the results based on 60 years

(20 cold, 20 warm and 20 neutral years) of NASA/NCAR model simulations. The results show the expected large regional and seasonal changes in the structure and scales of the extreme precipitation events, with continental-scales and strong dynamical controls during the cold season, and highly localized events during the warm season. The NASA/NCAR AGCM does remarkably well in reproducing the basic structures of the extreme events. Figure 2 shows the regression coefficient *a* relating the precipitation extremes at the base point (77.5W,40N) to precipitation at other grid points and at different time lags relative to the maximum. The results show coherence in time with a sequence of patterns that is consistent (during the cold season) with the northeastward motion of cyclones along the East Coast.

In order to study the link between the extreme events and various low frequency modes of atmospheric variability we first identify the leading patterns of monthly variability using a rotated EOF analysis of the 300mb height. The top panel of Figure 3 shows, for example, the nine leading monthly EOFs for DJF for the GCM simulations. The first EOF is the ENSO response, the second resembles the Arctic Oscillation, while the third resembles the Pacific/North American (PNA) pattern. The bottom panel of Figure 3 shows scatter plots of the principal components of the monthly EOFs (here the daily height data have been projected onto the monthly EOFs) versus the amplitude of the linear regression pattern associated with the extreme precipitation events at base point (82W,27N). For the latter, all daily values of precipitation (not just the times with extreme values) are projected onto the regression patterns. The height pattern associated with the precipitation extremes at this point over Florida (not shown) consists of a storm system that apparently develops in the Gulf and moves up the east coast. The point was chosen because it illustrates a case where the extremes are strongly impacted by ENSO. This is evident from the top left panel of the bottom panel of Figure 3 where we find that the warm ENSO events are associated with more large daily precipitation amounts (positive values of PC 1 or red dots) compared with cold events (blue dots). We also see some impact from the PNA mode (top right panel of the lower panel of Figure 3), in that there is a tendency for the positive values of the PNA pattern to be associated with the largest daily precipitation amounts.

References

Chang, Y., and coauthors, 2001: The climate of the FVCCM-3 model. Technical Report Series on Global Modeling and Data Assimilation. NASA/TM-2001-104606, Vol. 20.

Higgins, R. W., J. E. Janowiak, and Y. Yao, 1996: A gridded hourly precipitation database for the United States (1963-1993). NCEP/Climate Prediction Center Atlas 1, 47pp.

Kalnay, E., and Coauthors, 1996: The NCEP/NCAR 40-year reanalysis project. Bull. Amer. Meteor. Soc., 77, 437-471.

Lin, S.-J., and R. B. Rood, 1996: Multidimensional flux form semi-lagrangian transport schemes. *Mon. Wea. Rev.,* 124, 2046 – 2070.

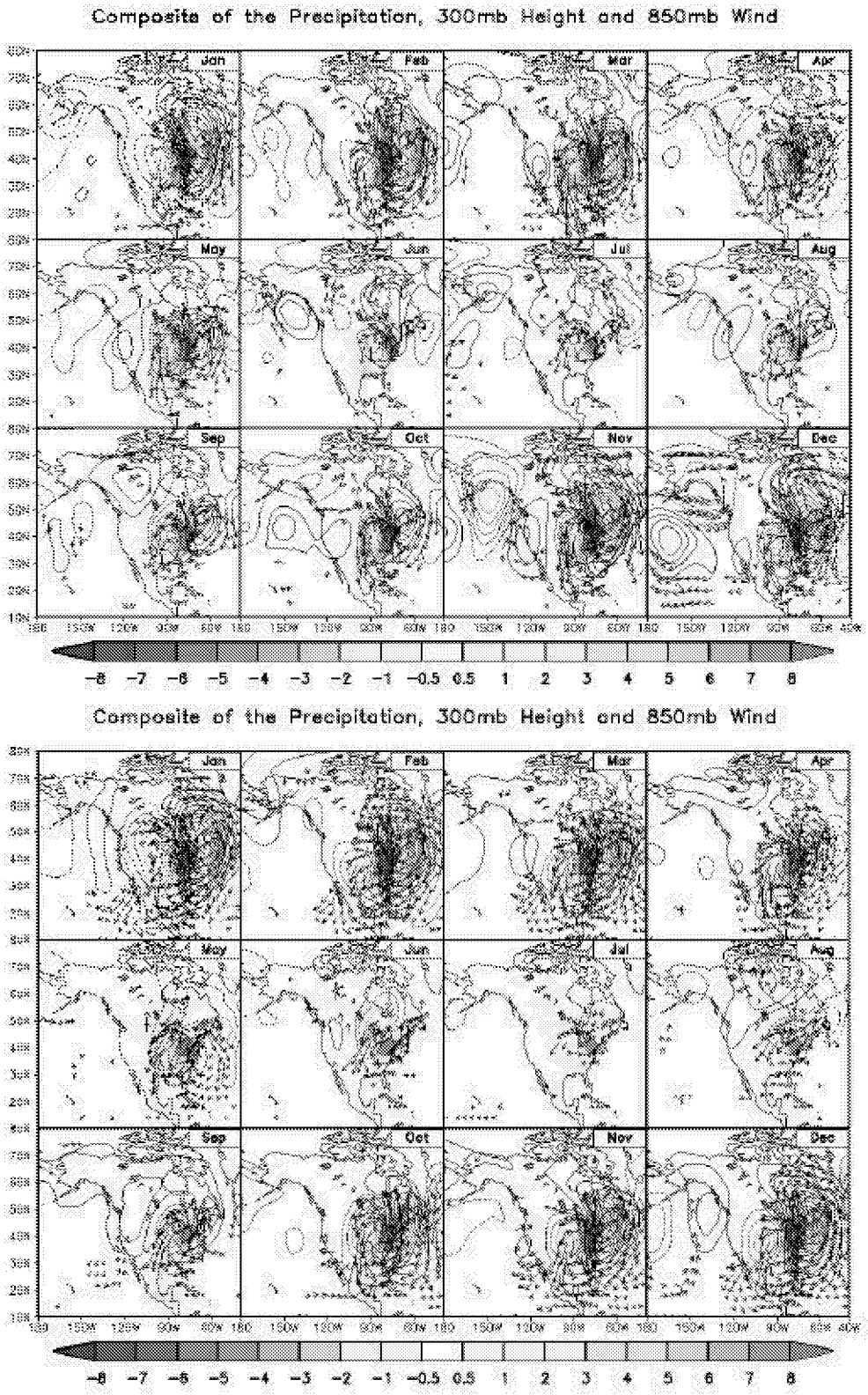

Figure 1. A composite of the precipitation (shading), 300mb heights (contours) and 850mb wind (vectors) during extreme precipitation events for each month at base grid point (77.5W, 40N). Upper figure: The results based on 36 years (1963-1998) of daily NOAA precipitation observations and NCEP/NCAR reanalysis. Lower figure: The results based on 60 years of NASA/NCAR model simulations. Precipitation has units of mm/day. Height contours are 20m. Colored contours are significant at the 5% level.

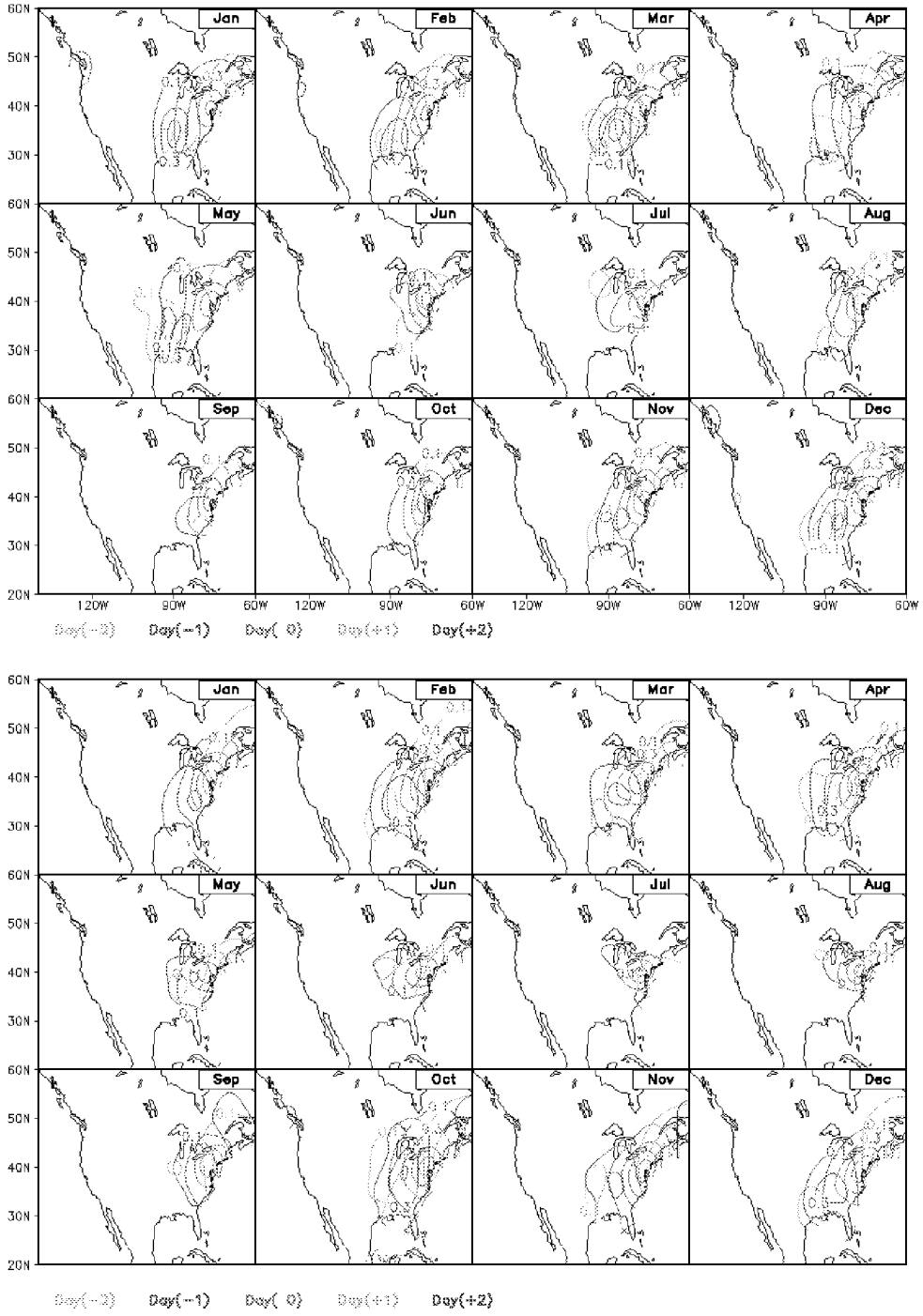

Figure 2. The regression coefficient ***a*** relating the precipitation extremes at the base point (77.5W,40N) to precipitation at other grid points and at different time lags relative to the maximum. Top panel is for the observations and bottom panel is for the model. The colors indicate the lag in days.

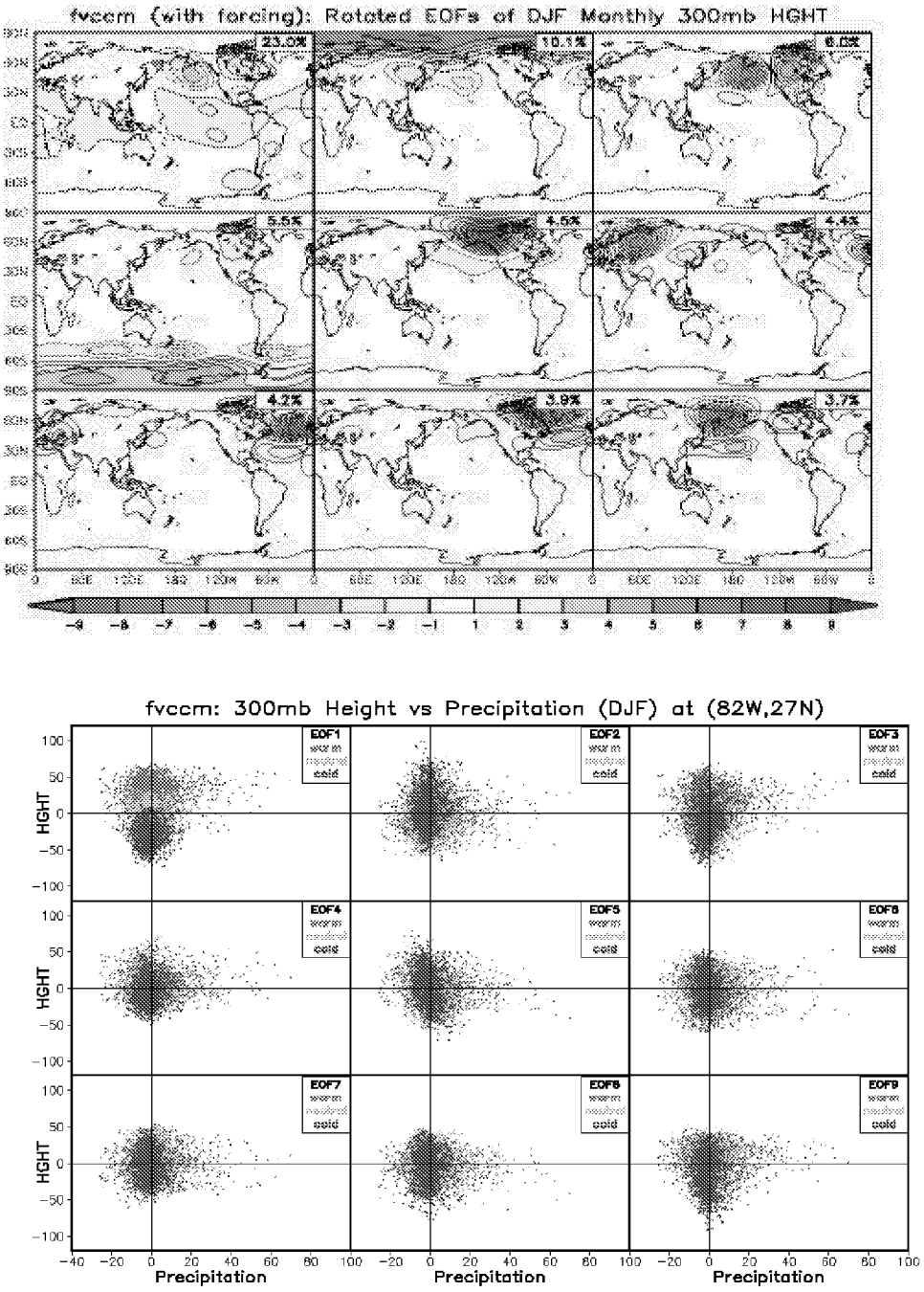

Figure 3. Upper panel: The nine leading EOFs of the monthly mean 300mb height during DJF from the 60 years of GCM simulations with idealized (20 warm, 20 neutral and 20 cold years) ENSO SST forcing. Lower panel: Scatter plots of the daily amplitude of the linear regression model based on extreme precipitation at grid point (82W,27N) versus the daily values of the principal component of the nine leading monthly EOFs of 300mb height shown above. The red, green and blue colors show the warm, neutral and cold ENSO SST cases respectively.

"The Relationship Between the Classic PNA Pattern and the ENSO-Forced Pattern on Time Scales From Daily to Seasonal"

David M. Straus and J. Shukla

From the perspective of seasonal mean predictability, one can distinguish between the SST-forced external response and chaotic internal variability. The former (latter) leads to predictable (unpredictable) components of seasonal mean fields. A large number of ensemble seasonal historical forecasts made with the COLA AGCM (forced by observed SSTs) for many winters are used to distinguish patterns of internal variability (including the PNA pattern of Wallace and Gutzler) from true forced response patterns, such as the dominant ENSO-forced pattern. The former can be identified from EOF analysis of the deviations of seasonal means about the ensemble means, and from long integrations using climatologically varying SSTs. The latter can be identified from EOF analysis of the ensemble means or from the pattern which optimizes the "signal to noise" ratio. A number of consistency checks are used to confirm the validity of these identifications.

The presence of internal variability patterns in seasonal means is thought to be due in large part to statistical residuals of shorter time episodes. Information on the strength and duration of these episodes can be gleaned from projections of daily and 5-day mean fields from individual integrations onto internal variability patterns. Comparison to similar projections onto the external patterns yields information on the shorter time scale manifestations of the forced response.

Internal variability can depend on the state of SST forcing, yielding probability shifts in for example the PNA pattern between warm and cold ENSO winters. In addition, changes in the nature of ENSO itself during the past 50 years have led to subtle changes in the forced patterns, and the degree to which they are distinguishable from internal variability. These issues will also be addressed using large numbers of COLA AGCM ensemble integrations.

ASSESSMENT OF MIDLATITUDE SUBSEASONAL VARIABILITY IN NASA/GSFC GENERAL CIRCULATION MODELS

Robert X. Black*
Dennis P. Robinson
Brent A. McDaniel
Georgia Institute of Technology
Atlanta, Georgia

1. Introduction

The success of short-term climate prediction efforts is critically dependent upon the veracity with which atmospheric general circulation models (GCMs) are able to simulate the atmospheric circulation. A minimum expectation is that GCMs employed are capable of realistically representing important aspects of the current climate. Regional climate is strongly influenced by second order atmospheric circulation features such as storm track variability and anomalous weather regimes, both of which are dynamically linked to the midlatitude jet stream and are associated with alterations in surface weather. A proper representation of the behavior of anomalous weather regimes and storm tracks is essential for reliable climate simulations. A detailed assessment of short-term climate variability thus provides an important benchmark for a climate model.

We perform an exploratory study of storm tracks and anomalous weather regimes in extended integrations of NASA/GSFC GCMs. This includes intercomparisons of the representation of these natural phenomena in AMIP-type simulations of NASA/NCAR (NASCAR) and Aries (NSIPP) models. Specifically, we employ the AMIP fvccm3-1.2.0 NASCAR run and the ens05 AMIP run of NSIPP 1. We diagnose their statistics, structure, and dynamical characteristics and contrast these results to parallel observational reanalyses (NCEP/NCAR) to isolate systematic errors. Long-term goals include (a) determining the extent to which the models are able to replicate observed characteristics of the phenomena and (b), in cases where a specific shortcoming is identified, performing targeted dynamical diagnoses aimed at deducing the underlying physical reasons for the systematic errors.

2. Intraseasonal eddy statistics

After removing long-term seasonal trend values, the intraseasonal eddy activity is then bandpass filtered into 2-10 day (synoptic) and 10-90 day (low frequency) period bands, respectively. The collective effect of the synoptic eddies is manifested as "storm tracks" while low frequency eddies are linked to large-scale anomalous weather regimes. These filters were applied to the daily NCEP/NCAR reanalyses and model simulation output for the winter months during the AMIP-2 time period.

A first order characterization of the intraseasonal eddy activity was obtained by calculating the upper tropospheric eddy kinetic energy (EKE) distribution for the entire intraseasonal eddy spectrum (synoptic plus low frequency) which is displayed in Figure 1. This analysis shows that, though energy magnitudes are comparatively weak in both NSIPP and NASCAR models, the regional EKE patterns are well represented. This result carries over to separate considerations of the synoptic and low frequency eddies (not shown) suggesting improvements over earlier models (e.g., Black and Dole 2000). The 300 hPa EKE magnitudes averaged over the Northern Hemisphere extratropics are summarized in Table 1. The total intraseasonal EKE is 20-30% weaker in the models than in observations. Considering the individual eddy components, the most striking difference is the 36% shortfall in synoptic EKE for NSIPP. Potential reasons for this characteristic are discussed later.

(20 – 90^{0}N)	Synoptic Eddies	Low Freq Eddies	Total Intraseasonal
NCEP/NCAR Reanalyses	75 $m^2 s^{-2}$	86 $m^2 s^{-2}$	161 $m^2 s^{-2}$
NSIPP	48 (64%)	65 (76%)	113 (70%)
NASCAR	60 (80%)	70 (81%)	130 (81%)

Table 1. The 300 hPa intraseasonal eddy kinetic energy averaged over 20-90^{0}N for observations (NCEP/NCAR) and the two model simulations. Model values expressed as absolute values and as percentage of observations.

The horizontal structure of transient eddies can be diagnosed by plotting eddy major axes which depict the orientation and amount of eddy anisotropy. Eddies are elongated along the eddy major axis with the axis length proportional to the degree of eddy anistotropy. The eddy major axis vanishes for circular (isotropic) eddies. We have applied this analysis to the model simulations (not shown). Both the NSIPP and NASCAR model faithfully represents the meridional elongation of synoptic eddies observed in the core of the primary jet streams as well as the east-west "bowing" that occurs north and south of the jet streams. Both models are also able to represent the general east-west orientation of low frequency eddies. The degree of anisotropy for the low frequency eddies is misrepresented in the models, however. This likely impacts local barotropic interactions between low frequency eddies and the climatological-mean flow. The structural characteristics are confirmed by ensemble analyses of anomalous weather regimes (not shown).

3. Dynamical diagnoses of eddy behavior

It is of scientific and practical interest to delineate dynamical reasons for existing model discrepancies in representing short-term climate behavior. We approach this by considering the main eddy forcing mechanisms. Synoptic eddies are strongly forced by baroclinic growth while barotropic deformation in the upper troposphere impacts both synoptic and low frequency eddies. To this end, we have performed preliminary diagnoses of the baroclinic and barotropic aspects of the model dynamics.

Regional values of the baroclinic growth parameter (not shown) are very well represented by both models. In fact, one of the few differences from observations is that in both model simulations the parameter is too strong over the Atlantic storm track region. This result is perhaps surprising given the aforementioned relative weakness in simulated synoptic EKE, particularly for NSIPP. This suggests that other dynamic processes are likely responsible for this model feature. For synoptic eddies, upper tropospheric barotropic deformation acts as an EKE sink in the jet exit regions where large-scale shearing and stretching processes tend to elongate the eddies along their major horizontal axis. Our analyses show that regional deformation magnitudes are generally overestimated by the NSIPP model. This suggests that the synoptic eddies are likely experiencing enhanced barotropic energy losses to the mean flow in the jet exit regions. This behavior is confirmed by analyzing local barotropic energy conversions (not shown) which show local synoptic EKE losses in the NSIPP model that are similar to, and in some cases exceed, observed values (noting that one would expect conversion values to be reduced by 30% or more as barotropic EKE conversions are proportional to the EKE, itself). Consistent with this argument, for the NASCAR simulation we find synoptic EKE levels and barotropic deformation magnitudes that are both closer to observed values.

To summarize: synoptic eddies in the NSIPP model encounter anomalously strong barotropic damping at upper levels while the background baroclinic forcing is closer to observations. The relative importance of barotropic and baroclinic forcing can be quantified by dividing the barotropic deformation magnitude by the baroclinic growth parameter. Regions where this ratio is low are more strongly influenced by baroclinic processes than barotropic processes and vice-versa. Fig. 2 displays this ratio for the models and observations and concisely shows that barotropic deformation likely plays a stronger role in the NSIPP simulation than in observations or the NASCAR simulation (i.e., smaller areas of dark shading in the storm track regions). This may help to explain the relative weakness of synoptic EKE in the NSIPP model compared to observations and NASCAR.

We note that the low frequency EKE is also under-represented by both models (though proportionally better than synoptic EKE). This is a puzzling result for NSIPP since it is reasonably well accepted in the literature that barotropic deformation acts as a *source* of EKE for low frequency eddies in the midlatitude atmosphere. Indeed, the NSIPP model actually provides a quantitatively good representation of the local barotropic energy conversions between the mean flow and low frequency eddies (not shown) which are positive in the jet exit regions. Here we speculate that existing deficiencies in low frequency EKE may be related to the scale interaction between the synoptic and low frequency eddies. First, individual synoptic eddies often act as the "seeds" for the onset of large-scale weather regimes. Secondly, synoptic eddies collectively provide positive dynamical feedbacks that help maintain anomalous weather regimes. In both cases, relatively weak synoptic eddies will likely result in anomalously weak low frequency eddies. This is clearly an avenue for further investigation.

Reference:

Black, R.X., and R.M. Dole, 2000: Storm tracks and barotropic deformation in climate models. *J.Climate,* **13,** 2712-2728.

Acknowledgments. This research is supported by the Global Modeling Program of NASA's Office of Earth Science under Grant NAG 5-10374.

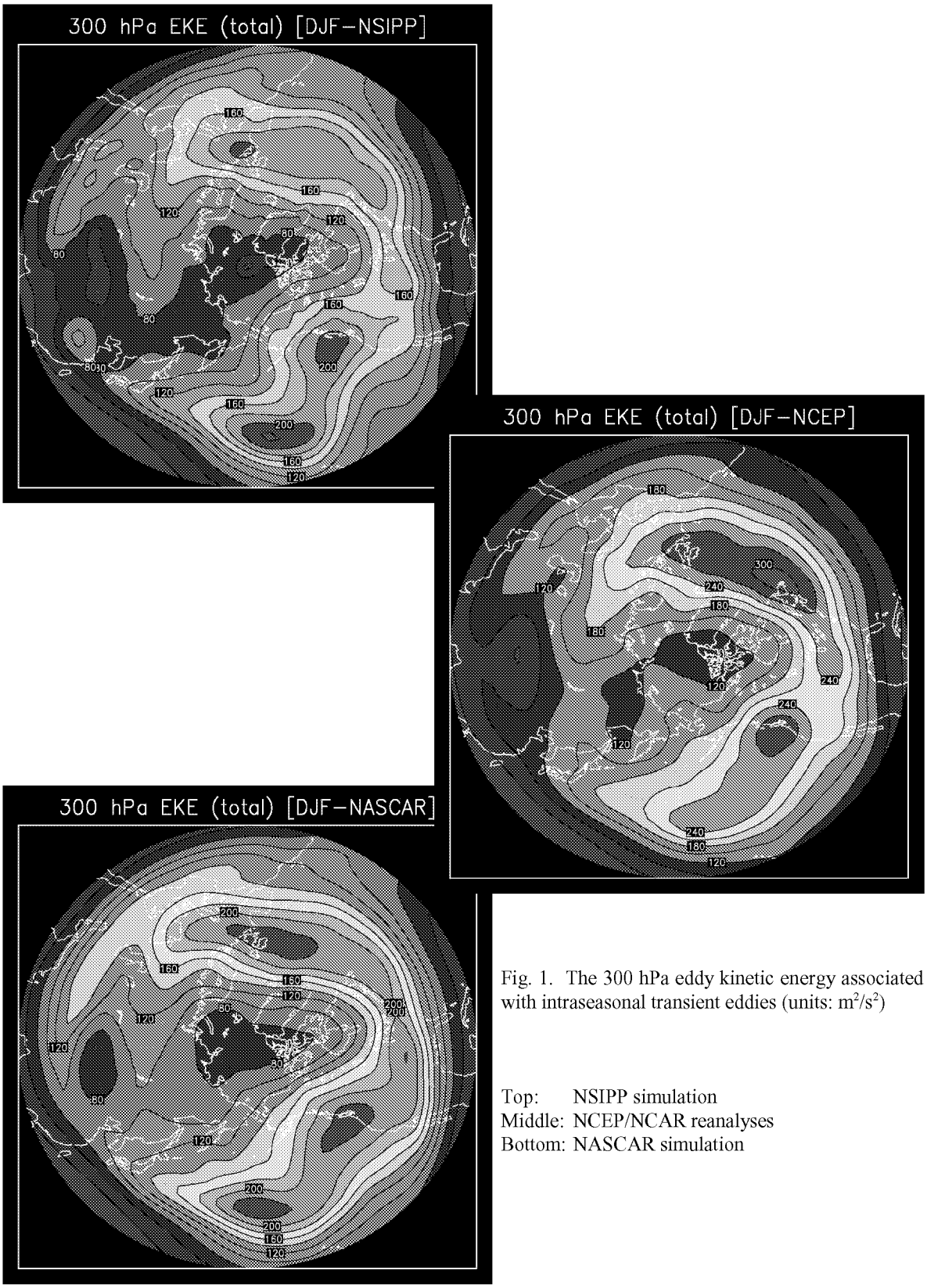

Fig. 1. The 300 hPa eddy kinetic energy associated with intraseasonal transient eddies (units: m^2/s^2)

Top: NSIPP simulation
Middle: NCEP/NCAR reanalyses
Bottom: NASCAR simulation

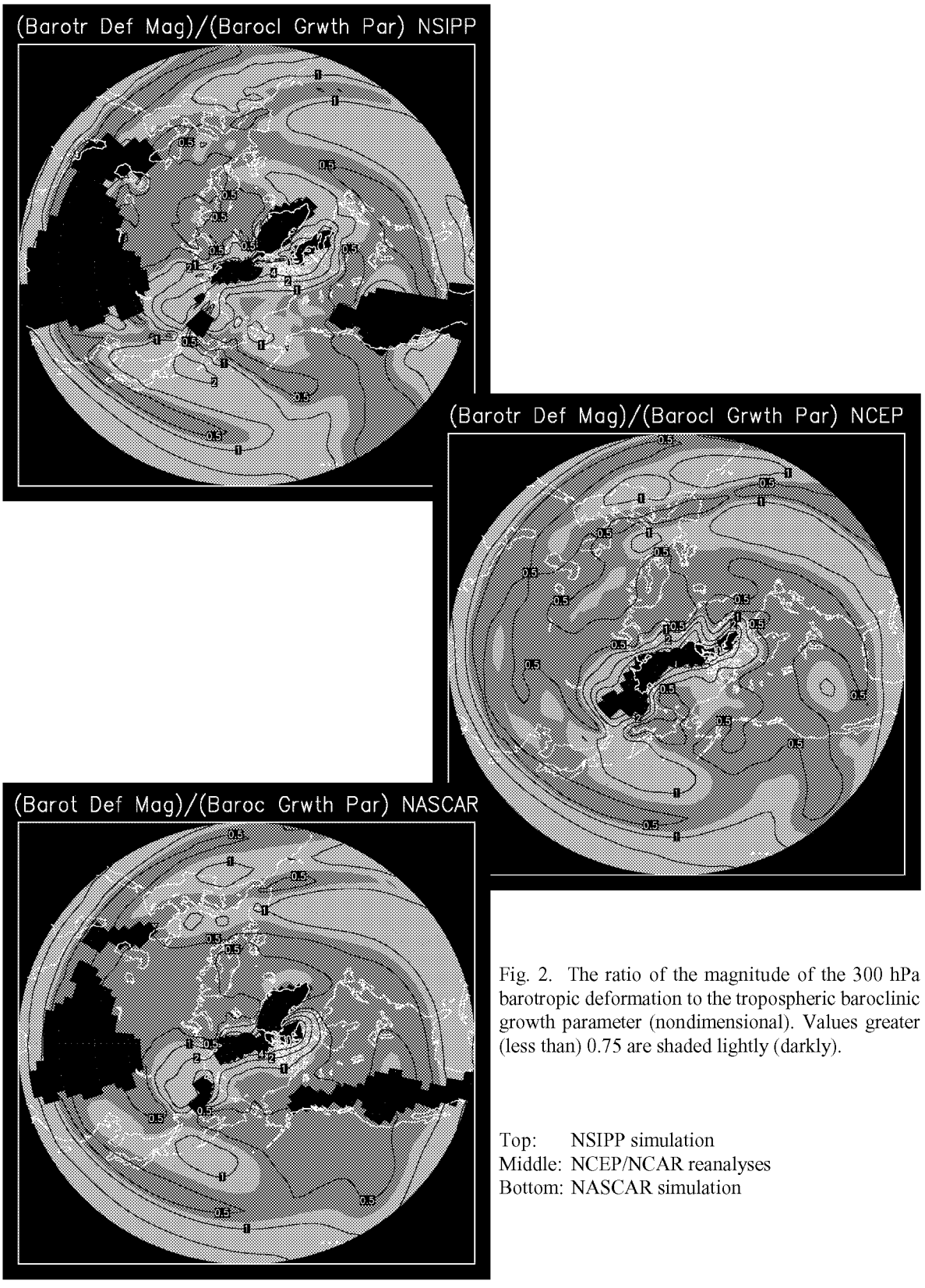

Fig. 2. The ratio of the magnitude of the 300 hPa barotropic deformation to the tropospheric baroclinic growth parameter (nondimensional). Values greater (less than) 0.75 are shaded lightly (darkly).

Top: NSIPP simulation
Middle: NCEP/NCAR reanalyses
Bottom: NASCAR simulation

Diagnostics of Climate Variability and Trend Using Potential Vorticity Maps

Ming Cai and Eugenia Kalnay
Department of Meteorology
University of Maryland, College Park, MD 20742
cai@atmos.umd.edu

Daily pressure fields on a constant potential vorticity (PV) surface (PV = 2.5 unit) are analyzed using NCEP/NCAR reanalysis II (1979-2000) dataset. Potential vorticity folding indexes (PVFI) are developed to measure the mean latitudinal position, area, and intensity of the polar front zone over the Northern Hemisphere. It is found that these indexes closely related to the interannual and decadal variability of the cold air temperature anomalies over the high latitudes (north of 40 degrees). In general, these indexes are negatively correlated with the cold air temperature anomalies near the surface. The interannual variability of these indexes has a strong QBO signal. These indexes also exhibit strong interdecadal variability. Between early 80s and early 90s, these indexes all exhibit a negative trend, accompanied with which is a warming trend in both cold/warm surface air temperature anomalies. During last 5 years of 90s, these indexes have a positive trend superimposed on a QBO-like interannual variability. Interestingly, the surface air temperature anomalies continuously exhibit a warm trend while their interannual variability follows the interannual variability of PVFI. This seems to suggest that we are beginning to observe a separation between the climate trend induced by change in circulation and that induced by other factors, such as anthropogenic factors.

Systematic Errors and Surface Fluxes in the NCEP Global Model

Glenn White
Environmental Modeling Center
National Centers for Environmental Prediction
NWS/NOAA/DOC
Camp Springs, MD
Glenn.White@noaa.gov

This paper reflects the following assumptions:

a) Improving the atmospheric analysis/forecast systems currently used for 0-15 day numerical weather prediction and coupling them to complex land and ocean analysis/forecast systems can significantly improve 15-60 day forecasts.
b) Improving either the 0-15 or 15-60 day forecasts will usually improve the other.
c) Investigating the shortcomings of the current forecast system is a key ingredient in improving forecasts.
d) More realistic physics and tropics are required for successful 15-60 day forecasts than for 0-7 day mid-latitude forecasts. We may well not know the physics in the actual atmosphere as well as we need to produce successful 15-60 day forecasts.
e) 15-60 day and seasonal forecasts need for model verification and diagnosis a reanalysis consistent with the forecast model.

The Global Modeling branch plans to implement a global ocean data assimilation system and coupled model for 15-60 day and seasonal forecasts within the next year, replacing the current operational system that is coupled to a tropical Pacific Ocean analysis/forecast system. The atmospheric portion of the system will be upgraded every 1 to 2 years based on changes to the medium-range model. Significant changes to the MRF will be tested for their effects on seasonal forecasts. If improvement is found, the new version will be frozen and tested extensively for seasonal forecast model upgrade. This will mean that the seasonal forecast model will lag the operational medium-range model by 1-2 years. A similar schedule will be applied to improvements to the ocean model.

During the late winter of 2001-2002, operational forecasts of 500 hPa height by the MRF reached 60% anomaly correlation (widely accepted as a measure of the limit of useful skill) at day 8 in the extra-tropical Northern Hemisphere, an improvement of 1 day from 10 years ago. Anomaly correlations for operational week-2 (day 8-14 mean) forecasts for the same period were 50% for the MRF and 55% for the MRF ensemble; for extended periods in the late winter the forecast skill for week-2 exceeded 60%. Such levels of skill reflect the efforts of many skilled scientists; however, the results also suggest that new approaches may be needed to extend forecast skill to 15-60 days.

Fig. 1 compares time-mean errors in zonal mean temperature in one and fifteen-day operational MRF forecasts for Dec. 2001-Feb. 2002 with the error in zonal mean temperature from an integration with observed SST of the operational model at T170 resolution from mid-December 2000. Both are verified against operational analyses. The patterns are quite similar, although differences can be seen near the poles in the troposphere. The magnitudes of errors are comparable in the troposphere, but the longer run shows considerable larger errors in the

stratosphere. The tropospheric cold bias is saturated by day 15, but the stratospheric bias continues to grow beyond day 15.

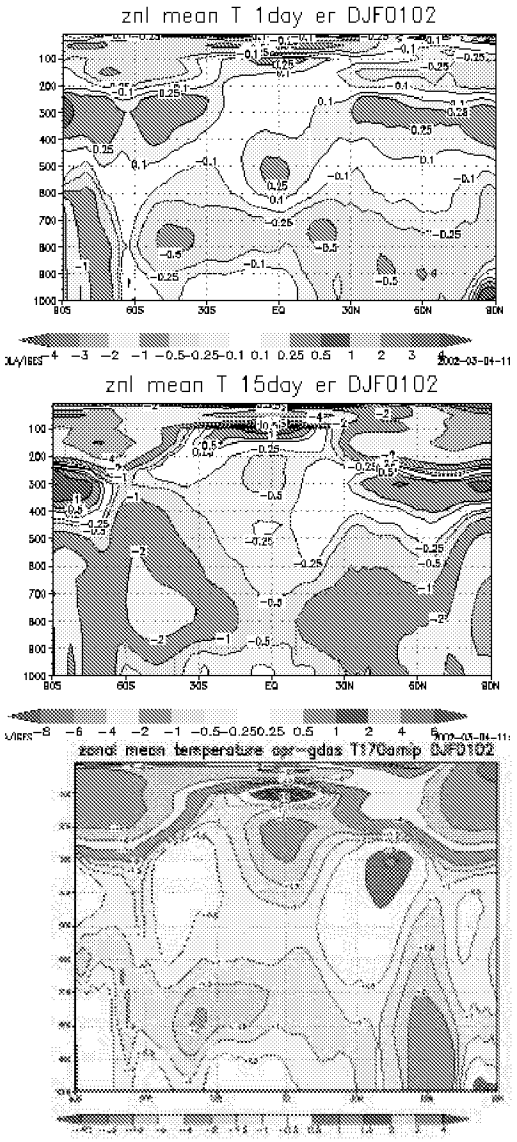

Fig. 1 Zonal mean error in temperature for (top) 1 day forecasts (middle) 15 day forecasts and (bottom) integration from mid-Dec. 2000 verified against analyses for Dec. 2001-Feb.2002.

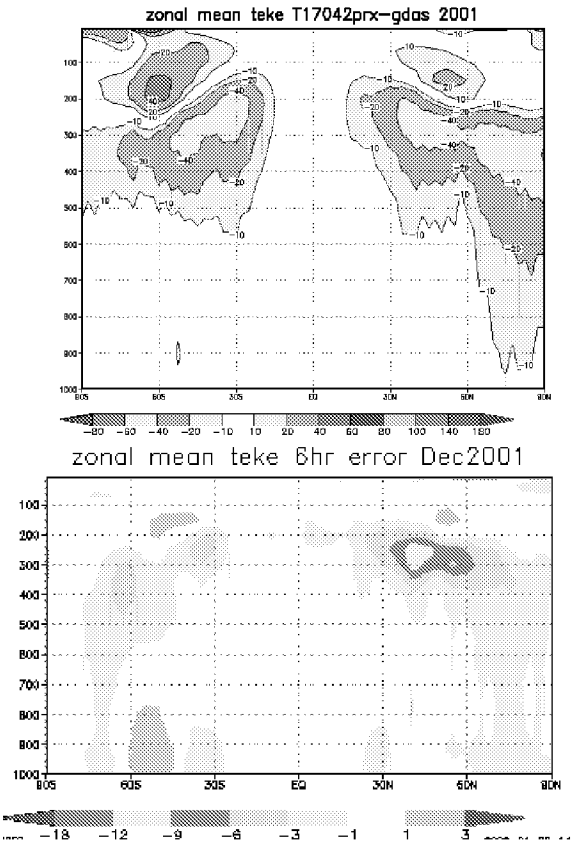

Fig. 2 Zonal mean error in transient eddy kinetic energy from (top) integration from mid-Dec. 2000 for all of 2001 and (bottom) 6 hour forecasts for Dec. 2001 verified against operational analyses.

Fig. 2 compares the zonal mean error in transient eddy kinetic energy in the T170m integration, averaged over 2001, and the same field in 6-hour forecasts for December 2001. Both are verified against zonal mean transient eddy kinetic energy in operational analyses. The patterns are quite similar and indicate that the model's under-forecast of eddy activity reflects problems that begin in the first 6 hours of integration. Figures 1 and 2 show that problems that develop in long integrations of the NCEP global model clearly can be seen in short-term operational medium-range forecasts and suggest that reducing such errors in short-term forecasts will improve 15-60 day and seasonal forecasts.

Realistic air-sea fluxes are essential for useful coupled model forecasts. Several groups are currently studying air-sea fluxes. The WGNE/SCOR Working Group on Air-Fluxes (http: //www.soc.soton.ac.uk/JRD/MET/WGASF) has recently published a report on validation of air-sea fluxes (Taylor, ed., 2000) and held a workshop on air-sea fluxes (White, ed., 2001). The GEWEX SEAFLUX (http://paos.colorado.edu/~curryja/ocean) working group is comparing estimates of air-sea fluxes and emphasizes the use of satellite observations in determining air-sea fluxes. Peter Gleckler and Jan Polcher (Gleckler and Polcher, 2002) are developing SURFA, an ongoing project to collect surface fluxes from operation NWP analysis/forecast systems and verify them against high-quality in-situ observations over both land and ocean.

Global Mean Balances

	2001			
	CDAS	GDAS	Kiehl and Trenberth	Range
P (mm/d)	2.84	2.97	2.69	2.69-3.1
E	2.86	3.1	2.69	
P-E	-.02	-.13		
Sens.heat (W/m^2)	15.59	9.31	24	16-27
Latent heat	83.06	89.97	78	78-90
Sfc dsw	205.91	201.13	198	
Usw	45.11	29.01	30	
NSW	160.8	172.12	168	142-174
Dlw	336.17	333.6	324	
Ulw	396.81	397.69	390	
NLW	60.64	64.09	66	40-72
net rad	100.16	108.03	102	99-119
NHF	+1.5	8.76	0	

Table 1 Global mean surface water and energy balance in the CDAS and GDAS for 2001 and from a climatology by Kiehl and Trenberth (1997). Range displays the range of independent estimates considered by Kiehl and Trenberth (1997).

Table 1 compares global mean surface fluxes averaged over 2001 from CDAS (done with the 1995 NCEP operational global data assimilation system) and the currently operational GDAS to climatological estimates by Kiehl and Trenberth (1997) and the range of estimates they considered. The large range of estimates is one measure of the uncertainty in our knowledge of air-sea fluxes. The hydrological cycle is more intense in the NCEP analyses than in the climatological estimate, but its magnitude lies within the range of independent estimates. Sensible heat flux in the current system is lower than other estimates and may reflect the introduction of a new boundary layer parameterization in the late 1990s. CDAS had too high an oceanic surface albedo; short wave radiation in the current GDAS is closer to the estimates of Kiehl and Trenberth. The current GDAS however has a larger imbalance at the surface than CDAS.

Table 2 compares the global mean water and surface energy balance over the oceans from CDAS and GDAS for 2001 to climatological estimates from da Silva et al. (1994), based on COADS observations for 1981-1992, and from the Surface Radiation Budget (Darnell *et al.*, 1992; Gupta *et al.*, 1992), based on retrievals of surface radiation fields from top of the atmosphere satellite observations and ISCCP clouds. The COADS-based estimate produces a large imbalance, indicating a large uncertainty in our knowledge of air-sea fluxes. The SRB net long wave is lower than other estimates (Kiehl and Trenberth, 1997).

Global Mean Balances
2001 Ocean

	CDAS	GDAS	COADS	SRB
P mm/day	3.08	3.24		
E	3.35	3.64		
P-E	-.27	-.40		
Sensible heat W/m^2	11.41	5.65	10.1	
Latent heat	97.01	105.47	88	
Sfc dsw	198.66	201.56		
Usw	34.85	18.47		
Nsw	163.81	183.09	170.4	173.4
Dlw	353.21	347.35		
Ulw	408.4	409.05		
Nlw	55.19	61.7	49.2	41.9
net rad	108.62	121.39	121.1	131.5
NHF	0.2	10.27	23.3	

Table 2 Global mean surface water and energy balance over the ocean in the CDAS and GDAS for 2001 and from climatologies by da Silva et al. (1994) and from the Surface Radiation Budget.

Fig. 3(upper panel) compares surface stress along the equator from 12-year climatologies from the NCEP/NCAR reanalysis and from COADS. The reanalysis had too weak zonal surface stress. Fig. 3 (lower panel) shows zonal surface stress along the equator for 2001 from CDAS (the NCEP/NCAR reanalysis), GDAS (the operational analysis), and 3 integrations from mid-Dec. 2000 with observed SSTs. GDAS and the parallel X (PRX) give reasonable zonal surface stress in the east Pacific; two other versions of the model, including the operational seasonal forecast model (SFM) and a different convection (RAS) have too strong stress in the East Pacific.

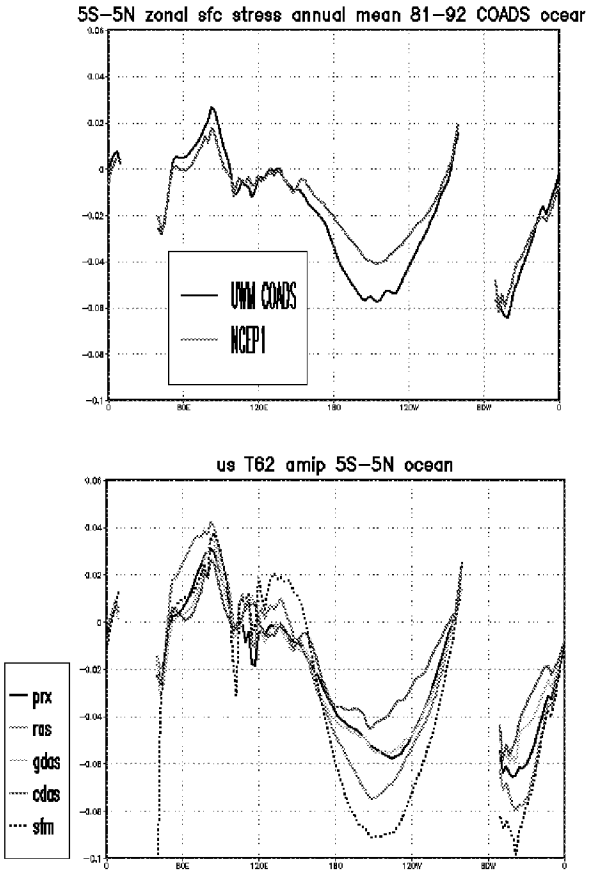

Fig. 3 Annual mean zonal surface stress over the ocean averaged from 5S-5N for (upper) the NCEP/NCAR reanalysis and COADS (da Silva et al., 1994) for 1981-92 and (lower) GDAS, CDAS and 3 integrations from mid-Dec. 2000 for 2001.

Considerable work is needed to improve both the forecast system's air-sea fluxes and our knowledge of air-sea fluxes. Considerable differences exist between different estimates of air-sea fluxes; our current knowledge of air-sea fluxes is insufficient to close the surface energy budget. Current global forecast systems have problems with cloudiness

that produce inaccurate short wave fluxes and problems with moisture that affect long wave fluxes. Low-level oceanic stratus clouds are difficult for current systems to model correctly.

References

da Silva, A., C.C. Young, and S. Levitus, 1994: *Atlas of Surface Marine Data 1994. Vol. 1: Algorithms and Procedures. NOAA Atlas NESDIS 6,* U.S. Dept. of Commerce, Washington, D.C., 83 pp.

Darnell, W.L., W.F. Staylor, S.K. Gupta, N.A. Richey, and A.C. Wilber, 1992: Seasonal variation of surface radiation budget derived from International Satellite Cloud Climatology Project C1 Data. *J. Geophys. Res., 97,* 15741-15760.

Gleckler, P., and J. Polcher, 2002: Project SURFA: A WGNE Pilot Study. *WCRP/SCOR Workshop on Inter-comparison and validation of ocean-atmosphere flux field.*. Bolger Center, Potomac, MD, USA, 21-24 May 2001, WCRP-115, WMO/TD-No. 1083, 6-7.

Gupta, S., W. Darnell, and A. Wilber, 1992: A parameterization of long wave surface radiation from satellite data: Recent improvements. *J. Appl. Meteor., 31*, 1361-1367.
Kiehl, J. T., and K.E. Trenberth, 1997: Earth's annual global mean energy budget. *Bull. Amer. Meteor. Soc., 78*, 197-208.

Taylor, P.K., Ed., 2001: *Inter-comparison and validation of ocean-atmosphere energy flux fields. Joint WCRP/SCOR Working Group on Air-Sea Fluxes Final Rep.*, WCRP-112, WMO/TD-No. 1036, 306 pp.

White, G., Ed., 2002: *WCRP/SCOR Workshop on Inter-comparison and validation of ocean-atmosphere flux field.*. Bolger Center, Potomac, MD, USA, 21-24 May 2001, WCRP-115, WMO/TD-No. 1083, 362 pp.

Configuration and Intraseasonal Duration of Interannual Anomalies of the Great Plains Low-Level Jet

H. M. Helfand
Data Assimilation Office, Laboratory for Atmospheres
NASA/Goddard Space Flight Center, Greenbelt, Maryland

Despite the fact that the low-level jet of the southern Great Plains (the GPLLJ) of the U. S. is primarily a nocturnal phenomenon that virtually vanishes during the daylight hours, it is one of the most persistent and stable climatological features of the low-level continental flow during the warm-season months, May through August. We have used significant-level data to validate the skill of the GEOS-1 Data Assimilation System (DAS) in realistically detecting this jet and inferring its structure and evolution. We have then carried out a 15-year reanalysis with the GEOS-1 DAS to determine its climatology and mean diurnal cycle and to study its interannual variability.

Interannual anomalies of the meridional flow associated with the GPLLJ are much smaller than the mean diurnal fluctuations, than random intraseasonal anomalies, and than the mean wind itself. There are three maxima of low-level meridional flow variance over the Great Plains and the Gulf of Mexico: a 1.2 m2 s-2 peak over the southeast Texas, to the east and south of the mean velocity peak, a 1.0 m2 s-2 peak over the western Gulf of Mexico, and a .8 m2 s-2 peak over the upper Great Plains (UGP), near the Nebraska/South Dakota border. Each of the three variance maxima corresponds to a spatially coherent, jet-like pattern of low-level flow interannual variability. There are also three dominant modes of interannual variability corresponding to the three variance maxima, but not in a simple one-to-one relationship.

Cross-sectional profiles of mean southerly wind over Texas remain relatively stable and recognizable from year to year with only its eastward flank showing significant variability. This variability, however, exhibits a distinct, biennial oscillation during the first six to seven years of the reanalysis period and only then. This intermittent biennial oscillation (IBO, one of the three modes discussed in the previous paragraph) in the low-level flow is restricted to the region surrounding eastern Texas and is also evident in the NCEP/NCAR reanalysis data set from about 1978 to 1985 or 1986 and again from 1995 to 2000. It is evident as well in surface pressure in both the GEOS-1 and NCEP/NCAR sets.

The interannual anomalies do not necessarily persist uniformly throughout an entire season, but can fluctuate from one part of the season to the next. To estimate the characteristic subseasonal time scales for coherence of these fluctuations, we have taken the weekly anomaly of low-level wind at each point of the domain from the climatological average for that given point and that given week of the season and

computed the covariance of its fluctuations over all weeks and over all years with the weekly climatological anomaly of the meridional wind at each of the three reference points discussed above. The typical duration of a coherent interannual anomaly within a given warm season increases with decreasing latitude from 2 to 3 weeks over the UGP, to 6 to 7 weeks over eastern Texas. Coherence over the western Gulf of Mexico is intermediate between the two with a typical duration of 4 to 5 weeks. There appears to be evidence that the interannual anomalies over Texas the Gulf propagate to the UGP after a week and those over the Gulf propagate there after 2 to 3 weeks. There also appears to be some reverse propagation of interannual anomalies over the UGP to Texas and to the Gulf after a period of about one week.

The interannual anomalies in southerly flow over eastern Texas seem to correlate well with interannual anomalies of surface temperature and (negative) ground wetness and over western Texas.

REPORT DOCUMENTATION PAGE

Form Approved
OMB No. 0704-0188

1. AGENCY USE ONLY *(Leave blank)*	2. REPORT DATE	3. REPORT TYPE AND DATES COVERED
	November 2002	Technical Memorandum

4. TITLE AND SUBTITLE
Technical Report Series on Global Modeling and Data AssimilationVol. 23—Prospects for Improved Forecasts of weather and Short-Term Climate Variability on Subseasonal (2 week to 2 month) Time Scales

5. FUNDING NUMBERS
Code 971

6. AUTHOR(S)
Siegfried Schubert, Randall Dole, Max Suarez,Huug van den Dool, and Duane Waliser

7. PERFORMING ORGANIZATION NAME(S) AND ADDRESS (ES)
Goddard Space Flight Center
Greenbelt, Maryland 20771

8. PEFORMING ORGANIZATION REPORT NUMBER
2002–00538-0

9. SPONSORING / MONITORING AGENCY NAME(S) AND ADDRESS (ES)
National Aeronautics and Space Administration
Washington, DC 20546-0001

10. SPONSORING / MONITORING AGENCY REPORT NUMBER
TM–2002–104606, Vol. 23

11. SUPPLEMENTARY NOTES
S. Schubert, M. Suarez, GSFC, Greenbelt, MD
R. Dole, NOAA, Boulder, CO, H. van den Dool, NOAA, Institute of Terrestrial and Planetary Atmospheres Stony Brook, NY

12a. DISTRIBUTION / AVAILABILITY STATEMENT
Unclassified–Unlimited
Subject Category: 46
Report available from the NASA Center for AeroSpace Information,
7121 Standard Drive, Hanover, MD 21076-1320. (301) 621-0390.

12b. DISTRIBUTION CODE

13. ABSTRACT *(Maximum 200 words)*

This workshop, held in April 2002, brought together various Earth Sciences experts to focus on the subseasonal prediction problem. While substantial advances have occurred over the last few decades in both weather and seasonal prediction, progress in improving predictions on these intermediate time scales (time scales ranging from about 2 weeks to 2 months) has been slow. The goals of the workshop were to get an assessment of the "state of the art" in predictive skill on these time scales, to determine the potential sources of "untapped" predictive skill, and to make recommendations for a course of action that will accelerate progress in this area.

One of the key conclusions of the workshop was that there is compelling evidence for predictability at forecast lead times substantially longer than 2 weeks. Tropical diabatic heating and soil wetness were singled out as particularly important processes affecting predictability on these time scales. Predictability was also linked to various low-frequency atmospheric "phenomena" such as the annular modes in high latitudes (including their connections to the stratosphere), the Pacific/North American (PNA) pattern, and the Madden Julian Oscillation (MJO). The latter, in particular, was highlighted as a key source of untapped predictability in the tropics and subtropics, including the Asian and Australian monsoon regions.

14. SUBJECT TERMS
weather, forecasts, climate variability

15. NUMBER OF PAGES
171

16. PRICE CODE

17. SECURITY CLASSIFICATION OF REPORT	18. SECURITY CLASSIFICATION OF THIS PAGE	19. SECURITY CLASSIFICATION OF ABSTRACT	20. LIMITATION OF ABSTRACT
Unclassified	Unclassified	Unclassified	UL